From Visionary Tale to Application The Bright and Dark Side of Photo-Biocatalysis

Höfler, Georg

DOI
10.4233/uuid:39e7cf46-5d0e-49b0-8718-e8adac9cb8bb

Publication date
2020

Document Version
Final published version

Citation (APA)
Höfler, G. (2020). *From Visionary Tale to Application The Bright and Dark Side of Photo-Biocatalysis*. [Dissertation (TU Delft), Delft University of Technology]. https://doi.org/10.4233/uuid:39e7cf46-5d0e-49b0-8718-e8adac9cb8bb

From Visionary Tale to Application

The Bright and Dark Side of Photo-Biocatalysis

Dissertation

for the purpose of obtaining the degree of doctor
at Delft University of Technology
by the authority of the Rector Magnificus Prof. Dr. Ir. T.H.J.J van der Hagen
chair of the Board for Doctorates
to be defended publicly on
Friday 10th, July 2020 at 12:30 o'clock

by

Georg Theo HÖFLER

Master of Science in Molecular and Applied Biotechnology,
Rheinisch-Westfälische Technische Hochschule Aachen, Germany
born in Friedrichshafen, Germany

This dissertation has been approved by the promotors:

Composition of the doctoral committee:

Rector Magnificus,	chairperson
Prof. Dr. F. Hollmann	TU Delft, promotor
Prof. Dr. I.W.C.E. Arends	Universiteit Utrecht, promotor
Dr. C.E. Paul	TU Delft, copromotor

Independent members:

Prof. Dr. U. Hanefeld	TU Delft
Prof. Dr. J. Deska	Aalto University, Finland
Dr. F. Mutti	University of Amsterdam
Dr. S. Schmidt	Rijksuniversiteit Groningen
Prof. Dr. W. R. Hagen	TU Delft, reserve member

Funding: This research is supported by the European Research Council (ERC Consolidator Grant No. 648026).

Keywords: photo-biocatalysis, chloroperoxidase, NADH regeneration

Printed by: Gildeprint, Enschede

Cover by: Georg Höfler

ISBN: 978-94-6384-143-6

Für meine Familie und Freunde

Alla mia famiglia e ai miei amici

Aan mijn familie en vrienden

À ma famille et à mes amis

मेरे परिवार और दोस्तों के लिए

Pentru familia și prietenii mei

A mi familia y amigos

To my family and friends

Table of Contents

Summary

Redox biocatalysis is a promising approach to carry out redox reactions in industry. The chemical nature of redox reactions requires a stoichiometric supply of redox equivalents. The outstanding class of enzymes “Oxidoreductases” require specific redox equivalents for their function. We envision more environmentally friendly sources for these redox equivalents, in order to promote the application of various sorts of oxidoreductases.

Redox equivalents can originate from cost-effective and abundant sacrificial electron donors, such as formate and water through the use of photocatalysis. This research aimed to identify the critical factors necessary to design effective combinations of redox biocatalysis with photocatalysis that can supply redox equivalents to the enzymes. For this, two different approaches were investigated in the first two research chapters.

The investigations in **Chapter 2** show that the combination of 5-deazariboflavin (dRf) and putidaredoxin reductase (PDR) from *Pseudomonas putida* is active under lab-scale conditions for the photoenzymatic NADH regeneration. For these experiments EDTA was applied as the sacrificial electron donor together with blue light (450 nm) illumination. The total turnover number for NAD^+ of 21 is reasonable compared with other light-driven NADH regeneration systems performing in a range of single digit to hundred turnovers of NADH. However, the regeneration rate is rather low, approx. $9 \times 10^{-4}\ s^{-1}$, compared to currently applied systems that reach turnover rates of $2\ s^{-1}$. The limited activity of the system was ascribed to the photodegradation of the flavin prosthetic group in PDR. In a strictly anaerobic reaction setup with 50 mM Tris-HCl buffer (pH 8), 20 mM EDTA, 0.25 mM methyl viologen (MV^{2+}), 60 μM dRf, 0.2 mM NAD^+, 5 μM PDR, 0.115 μM ADH-A and 10 mM ethyl acetoacetate at 25 °C with illumination at 450 nm for 24 h we reached up to 72, 21, 17, 868, and 37700 turnovers for dRf, NAD^+, MV^{2+}, PDR, and ADH-A, respectively.

Overall, the system is characterised by low total turnovers of enzyme and cofactor due to their poor photostability and the interference of photocatalytic side reactions.

Following the result of this study that reveals the importance of enzyme stability under photocatalytic conditions, the study of extraordinarily stable enzymes was pursued. For this purpose, the thermostable vanadium-dependent chloroperoxidase from *Curvularia inaequalis* (*Ci*VCPO), known for its robustness, was investigated in **Chapter 3** and photocatalytically supplied with redox equivalents. The graphitic carbon nitride (g-C_3N_4-25K), a heterogeneous photocatalyst, was chosen for the photocatalytic formation of hydrogen peroxide. g-C_3N_4-25K enables the use of more atom efficient electron donors such as formate or even water. Our studies show that *Ci*VCPO is also inactivated rapidly when in direct contact with the photocatalyst. To circumvent this, a reaction set-up was tested in which the heterogeneous photocatalyst was physically separated from the biocatalyst. Indeed, in this way the inactivation and side reactions caused by the photocatalyst itself could be prevented. Under optimised conditions, applying 20 mg g-C_3N_4-25K, 250 mM formate with a flowrate of 0.5mL/h and a second feed of 0.5 mL/h containing 40 mM 4-pentenoic acid and 80 mM KBr, the reaction was stable and formed 165.6 µmol bromolactone in 44 h resulting in a TTN of 1180 for the immobilised *Ci*VCPO.

The results of the first chapters indicate that biocatalysts are more strongly influenced by the photocatalysts than anticipated. To validate that the limitation of the photo-enzymatic approach derives from the photocatalysis, the chemoenzymatic halocyclisation of 4-pentenoic acid catalysed by *Ci*VCPO was upscaled in **Chapter 4**. The *in-situ* formation of hypobromite necessary for the reaction by *Ci*VCPO is a practical, safer and advantageous alternative to the established chemical methods. Unexpectedly, *Ci*VCPO was inhibited by high concentrations of the 4-pentenoic acid as well as competitively inhibited by KBr. To enable high product concentrations despite inhibitions and strong pH shift during the reaction, a fed-batch strategy with a pH stat was chosen. By feeding the reactants, inhibitions could be circumvented and the cosubstrate hydrogen peroxide was used more efficiently. Additionally, use of a biphasic system proved to be beneficial to allow for highly concentrated feeds. Overall, 1.8 mmol of *Ci*VCPO were added, corresponding to a total turnover number of the enzyme of more than 715000 [$mol_{product} \times mol^{-1}_{CiVCPO}$] or more than 770 $g_{product} \times g^{-1}_{CiVCPO}$. In total, 81.4 g of bromolactone were obtained with an

E^+-factor of 354 $kg_{waste} \times kg^{-1}_{product}$ for the overall process. These results pave the way towards upscaled biocatalytic halogenation.

In the final chapter, all findings in this thesis were evaluated. We conclude that biocatalytic oxidations suffer from severe limitations under direct illumination and side-reactions in combination with photocatalysts. Emphasis was placed on the importance of process innovations for already established biocatalytic oxidation systems.

Samenvatting

Redox biokatalyse is voor de chemische industrie een veelbelovende manier om redox reacties uit te voren. Chemische kenmerken van redox reacties maakt dan een stoichiometrische hoeveelheid redox equivalenten nodig is voor deze reacties. De uitstekende klas enzymen “de oxidoreductases” hebben specifieke redox equivalenten nodig om te kunnen functioneren. Wij voorzien het gebruik van milieuvriendelijkere bronnen voor deze redox equivalenten, om zo verschillende applicaties voor oxidoreductases mogelijk te maken.
De redox equivalenten zouden kunnen komen van voordelige en voldoende beschikbare elektron donoren, zoals methaanzuur en water, met behulp van fotokatalyse. Dit onderzoek richtte zich op de identificatie van kritieke factoren die belangrijk zijn in het ontwerp van effectieve combinaties van biokatalyse en fotokatalyse, om zo de enzymen van de redox equivalenten te voorzien. Om dit te bewerkstelligen zijn in de eerste twee hoofdstukken twee verschillende mogelijkheden onderzocht.

Het onderzoek in **Hoofdstuk 2** laat zien dat de combinatie van 5-deazariboflavine (dRf) en putidaredoxin reductase (PDR) van *Pseudomonas putida* activiteit laat zien in de foto-enzymatische regeneratie van NADH op lab schaal. Voor deze experimenten werd EDTA gebruikt als elektron donor, samen met blauw licht (450 nm). Het totaal aantal omzettingen voor NAD^+ bedroeg 21, wat redelijk vergelijkbaar is met andere licht-aangedreven NADH regeneratie systemen, die enkele tot aan honderden omzettingen kunnen halen. De regeneratie snelheid is echter traag, met slechts $9 \times 10^{-4}\ s^{-1}$, in vergelijking tot de huidige gebruikte systemen, die snelheden tot 2 s^{-1} halen. De limieten van het systeem werden toegeschreven aan fotodegradatie van de flavine in een prothetische groep van de PDR. Onder anaerobe condities in een 50 mM Tris-HCl buffer (pH 8) met 20 mM EDTA, 0.25 mM methyl viologeen (MV^{2+}), 60 μM dRf, 0.2 mM NAD^+, 5 μM PDR, 0.115 μM ADH-A en 10 mM ethyl acetoacetaat bij 25 °C beschenen met licht van

450 nm voor 24 uur haalden we tot aan 72, 21, 17, 868, en 37700 omzettingen voor dRf, NAD^+, MV^{2+}, PDR, en ADH-A, respectievelijk.

Over het algemeen werd het systeem gekenmerkt door lage totale omzettingen voor het enzym en de cofactor vanwege hun lage fotostabiliteit en interactie van foto-katalytische zijreacties.

Aangezien de resultaten van deze studie wezen op het belang van enzym stabiliteit onder foto-katalytische condities, richtten wij ons vervolgens op uitzonderlijk stabiele enzymen. Om deze reden werd in **Hoofdstuk 3** de thermostabiele, van vanadium afhankelijke, chloroperoxidase van *Curvularia inaequalis* (*Ci*VCPO), welk bekent staat om zijn robuustheid, onderzocht en werden de redox equivalenten foto-katalytisch gegenereerd. Grafiet carbonitride (g-C_3N_4-25K), een heterogene foto-katalysator, werd verkozen voor de foto-katalytische generatie van waterstof peroxide. Dit maakte het gebruik van atoom efficiënte elektron donoren, zoals methaanzuur en zelfs water, mogelijk. Ons onderzoek laat echter zien dat ook *Ci*VCPO snel gedeactiveerd raakt, wanneer in direct contact met de foto-katalysator. Om dit te voorkomen werd er een reactie ontwerp getest waarbij de fotokatalysator en de biokatalysator fysiek van elkaar gescheiden waren. Zoals verwacht konden op deze manier het deactiveren van het enzym en andere zijreacties voorkomen worden. Onder geoptimaliseerde condities, met het gebruik van 20 mg g-C_3N_4-25K, 250 mM methaanzuur met een debiet van 0.5 mL per uur en een tweede stroom van 0.5 mL per uur met daarin 40 mM 4-penteen zuur en 80 mM KBr, werd een stabiele reactie verkregen waar 165.6 µmol bromolactone werd gevormd in 44 uur. Dit resulteerde in een totaal aantal omzettingen van 1880 voor de geïmmobiliseerde CiVCPO.

De resultaten in de eerste hoofdstukken laten zien dat de biokatalysator sterker worden beïnvloed door de fotokatalysator van verwacht. Om te valideren dat de foto-enzymatische processen inderdaad werden gelimiteerd door de fotokatalyse, werd een chemo-enzymatische reactie, de halogeen-cyclisering van 4 penteenzuur door CiVCPO, opgeschaald in **Hoofdstuk 4**. Het *in situ* vormen van de benodigde

hypobromide door CiVCPO is een praktische en veilige manier in vergelijking met andere chemische reacties. Onverwachts bleek *Ci*VCPO echter deels geïnhibeerd door hoge concentraties 4-penteenzuur en zelfs volledig geïnhibeert door KBr. Om, ondanks deze inhibities en een verschuiving in pH, toch hoge product concentraties te behalen, werd er een fed-batch strategie met pH controle toegepast. Door de reactanten te voeden werden inhibities omzeild en kon het cosubstraat H_2O_2 efficiënter worden gebruikt. Daarnaast maakte een twee-fasen systeem de voeding van hoge concentraties mogelijk. Uiteindelijk werd er 1.8 mmol *Ci*VCPO toegevoegd, wat resulteerde in een totaal aantal omzettingen van meer dan 715000 [$mol_{product} \times mol^{-1}_{CiVCPO}$], oftewel meer dan 770 $g_{product} \times g^{-1}_{CiVCPO}$. In totaal werd 81.4 g bromolactone verkregen met een E-factor van 354 $kg_{waste} \times kg^{-1}_{product}$ over het gehele proces. Deze resultaten maken de weg vrij voor de opschaling van biokatalytische halogenaties.

In het laatste hoofdstuk worden alle behaalde resultaten van dit proefschrift geëvalueerd. We concluderen dat biokatalytische oxidaties zeer worden gelimiteerd indien met licht beschenen en dat er verscheidene zij-reacties kunnen plaatsvinden in combinatie met fotokatalyse. We leggen de nadruk op het belang van proces innovaties voor reeds bestaande biokatalytische systemen.

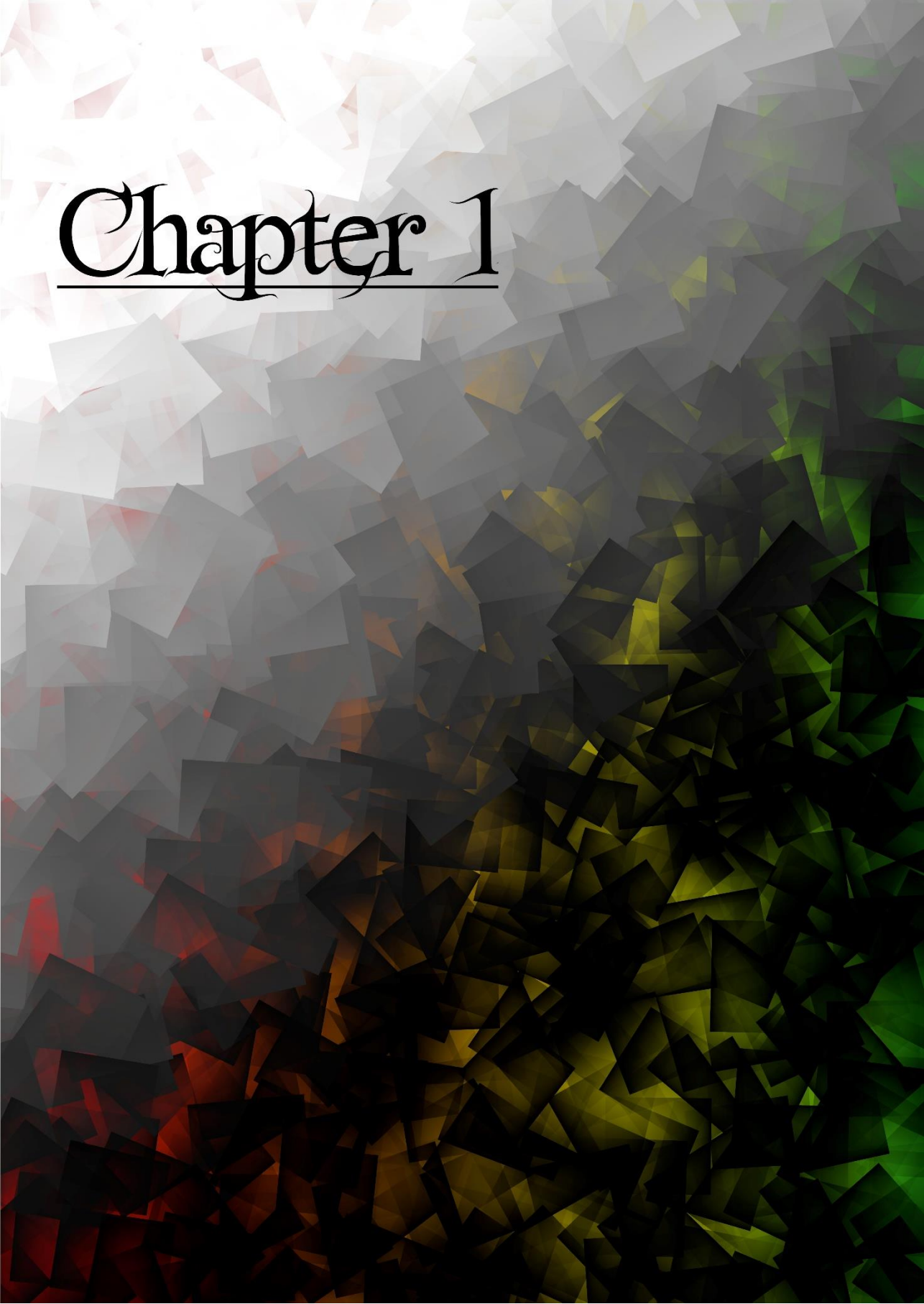
Chapter 1

Chapter 1: General introduction

Georg T. Höfler, Frank Hollmann, Caroline E. Paul, Marine C. R. Rauch, Morten M. C. H. van Schie, Sébastien J. Willot; Andrada But

Based on

“The autotrophic biorefinery: Organisms and enabling technologies.”; 2020; book chapter in preparation

and

Org. Biomol. Chem. 2019, 17, 9267-9274

Introduction of biocatalysis

The chemical industry is a keystone of human development, but with an increasing population, we now face a situation where we must use more sustainable raw materials if it is to survive.[1-2] The turn of phrase “engineering a better world without chemistry” is not the solution: a new, more sustainable, efficient and greener chemistry is necessary.[3] Switching the resource base for chemical production from fossil feedstocks to renewable raw materials provides exciting possibilities for the use of industrial biotechnology-based processes.[4]

Biocatalysis provides many attractive features in the context of green chemistry: mild reaction conditions (physiological pH and temperature), an environmentally compatible catalyst (an enzyme) and solvent (often water) combined with high activities and chemo-, regio- and stereoselectivities in multifunctional molecules.[5] The foundation of biocatalysis are proteins with a catalytic property, known as enzymes. They reduce the activation energy of the catalysed reaction by stabilising the transition state and thereby facilitating the reaction in milder conditions.

The basis of a protein is a long chain of amino acids interacting and folding into a three-dimensional structure. This 3D structure harbours a catalytic active unit in its so-called active site, creating a unique chiral coordination room for the reaction. Therefrom derives the above-mentioned superb selectivity of enzymes. The catalytic active units are typically amino acids, coordinated metals or cofactors bound in the active site. They allow for chemoselectivity catalysing the transformation of certain functional moieties, circumventing the need for functional group activation and avoiding protection and deprotection steps required in traditional organic syntheses.[5] The unique shape of the active site allows for a high specificity towards certain substrates also known as the lock and key principle. Furthermore, the complex but flexible structure can undergo conformational changes upon interaction with the substrate, increasing the force holding the substrate enzyme complex together, also known as Koshland’s induced fit model.[6] The unique selectivity makes these catalysts attractive for the synthesis of fine chemicals with the potential

of high product purity, fast reactions, mild reaction conditions while generating less waste. These properties make for a more attractive route compared to conventional routes regarding environmental and economic benefits. Biocatalytic processes can be divided into three groups depending on the format of the biocatalyst used for the conversion: (a) resting whole-cell biocatalysis, (b) isolated enzyme biocatalysis, and (c) immobilized-enzyme biocatalysis.[7] The focus here is on isolated enzymes. A widespread application of biocatalysis in industrial organic synthesis is imminent and according to a recent estimate more than 130 processes have been commercialised.[5, 8]

Nevertheless, this relatively young branch of chemistry also encounters some problems. The specificity of enzymes toward certain substrates can become an issue if nature doesn't provide an enzyme active on the desired substrate. Furthermore, in many cases enzymes show a poor stability compared to conventional catalysts. Nowadays, advances in protein engineering have made tailoring the catalyst properties to the need of a specific reaction possible. Improving the enzyme regarding promiscuity (the ability of an enzyme to catalyse a side reaction in addition to its main reaction), the cofactor dependency and the substrate scope are common examples. Further manipulating the enzyme's tolerance against solvents, temperature and pH profile is possible.[9] Additionally, the development of effective immobilisation techniques has paved the way for optimising the performance and recovery and recycling of enzymes.[5] The unique properties and potential evolution of enzymes promote biocatalysis to one of the best choices for a more sustainable and efficient synthesis.

Nowadays, a large number of enzymes is already known and have been categorised into EC numbers according to the type of reaction they catalyse (Figure 1).[10]
EC 1: Oxidoreductases: Catalyse oxidation/reduction reactions.
EC 2: Transferases: Transfer of a functional group from one compound to another.
EC 3: Hydrolases: Hydrolyse one substrate to two products.
EC 4: Lyases: Add or remove functional groups from substrates non-hydrolytically.
EC 5: Isomerases: Rearrange, e. g. isomerise, atoms within a single molecule.
EC 6: Ligases: Join two molecules by synthesis of new C-O, C-S, C-N or C-C bonds with simultaneous breakdown of ATP.
EC 7: Translocases: Move or separate ions or molecules across or within membranes.

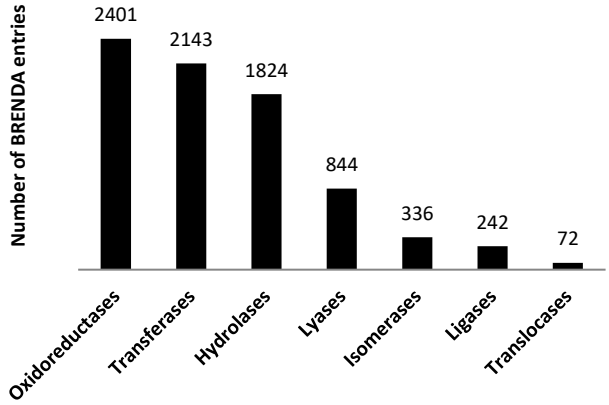

Figure 1. Division of enzymes registered in BRENDA according to their EC classes.

In addition, the number of enzymes interesting for biocatalysis is increasing due to the field's rapid development state with important tools such as:
1. Metagenomics: the analysis of genetic material from the environment to identify new enzymes from the vast diversity provided by nature;
2. Protein engineering: the evolution of enzymes to accept non-natural substrates and to be tolerant of conditions outside of natural conditions, such as organic co-solvents, high substrate concentrations, higher temperatures, and wider pH ranges;

3. High-throughput screening and analysis: the ability to quickly screen vast numbers of reactions to determine the best enzymes and conditions for a desired transformation."[11]

4. Bioinformatics: the ability to use computing power to mine large enzyme databases and identify useful candidates for a particular transformation;

5. Biodiversity: the isolation of new microorganisms and their enzymes especially from unconventional environments.

In industry, enzymes are generally divided into three major sectors: technical, food and animal feed enzymes.[12] The main fraction of commercialised industrial enzymes are the technical enzymes, being applied in numerous industries, including the detergent, textile, paper, fuel, and alcohol industries. The second largest group, food enzymes, includes enzymes found in the dairy, brewing, wine, juice, fat and oil, and baking industries. The third type of industrial enzymes is used in the animal feed industry adding value to the feedstock.[13]

A new branch of technical applied enzymes is used for organic synthesis purposes. In particular lipases are widely applied from pharma to bulk industry. One important example is the resolution of chiral compounds. In addition, transferases and oxidoreductases are encountered in a significant number of applications such as: resolution of racemic amines and direct chiral synthesis (transaminases) and reduction of the carbonyl functionality of aromatic ketones (ketoreductases and alcohol dehydrogenases).[13]

The above-mentioned class of oxidoreductases is a prominent class. These redox enzymes catalyse the reduction or oxidation of their substrate and can offer resource-efficient solutions to long-standing chemical problems.[14] Oxidoreductases constitute approximately 30% of all the BRaunschweig ENzyme Database (BRENDA) enzymatic activities, among which around 50% use nicotinamide adenine dinucleotide NADH/NAD^+ and/or NADPH/$NADP^+$ as a cofactor (Figure 1).[15] NAD(P)H-dependent oxidoreductases are able to oxidise a substrate by transferring a hydride (H^-) group to a nicotinamide adenine dinucleotide cofactor (either NAD^+ or $NADP^+$), resulting in the reduced form NADH or NADPH. There are over 150000 different sequences annotated as or predicted to be NAD(P)H-dependent oxidoreductases.[16]

Nevertheless, industrial application of NAD(P)H-dependent oxidoreductases is limited by their dependence on these expensive, complex cofactors. To overcome this drawback of cofactor dependency we are in need of atom efficient, cheap and more sustainable regeneration systems to circumvent stoichiometric use of cofactors.

A more detailed and exemplified introduction regarding requirements and evaluation of industrial biocatalysis will be given in the next section. Furthermore, the state of the art in cofactor regeneration, including new approaches using photocatalysis as well as enzymes relevant for this thesis, namely putidaredoxin reductase and vanadium-dependent chloroperoxidase, will be discussed in the following section.

Industrial application of enzymes

Biocatalysis is successfully employed from gram to ton scale. The global enzyme market accounts for $7 billion and is predicted to increase to $10 billion by 2024.[17] Nonetheless, the application of biocatalysis on industrial scale experiences several challenges. For the application of KREDs for instance, realistic process requirements were defined by Codexis as the following:

- >95% conversion of substrate to product
- >99.5% *ee* in a 24-hour reaction
- substrate loadings exceeding 100 g/L
- a substrate-to-enzyme ratio of >50
- an NADP concentration lower than <0.5 g/L[18]
- straightforward and clean product isolation[19-20]

These requirements can be challenging. Enzymes often show low tolerance towards high concentrations of reactants, since they have been optimised by nature to perform with very low concentrations. In addition, the standard solvent, water, does not allow for high concentrations of insoluble organic compounds. To tackle this issue, the use of co-solvents, or even the use of enzymes in pure solvents, are

becoming more frequent strategies. Directed evolution is also employed to increase the tolerance of enzymes towards reactants and solvents.[17]

Depending on the product, another challenge for industrial viability is the relative high cost contribution of the enzyme to the product due to its low stability and high cost. In order to reduce the enzyme cost contribution, their activity, stability and recyclability has to be improved. This can be achieved by protein engineering and/or immobilisation of the enzyme.[17] Furthermore, the expression levels of desired enzymes need to be improved, ideally in common host organisms, thereby reducing the cost of the enzyme production.[21] The costs are strongly increased by enzyme purification. Either the enzyme should be usable without purification or efficient purification methods need to be developed.[14]

Lastly, the rapid discovery of a suitable enzyme for a reaction and its implementation on a larger scale is essential to push the application of biocatalysis further.[21] Therefore, we require high throughput screening (HTS) methods that are close to the industry parameters. Moreover, knowledge of fundamental process engineering parameters, and how they scale to increase the speed of upscaling from laboratory to pilot scale, is crucial.[22]

In general, methods available to promote biocatalysis in industrial scale are:[7, 22]

- biocatalyst modification
- medium engineering (non-conventional reaction media)
- substrate feeding
- reactor engineering
- *in situ* product removal
- process monitoring and control

In addition, enzymes dependent on cofactors need either an economic supply or a cofactor regeneration system discussed in the following section.[14]

One of the historically most frequently employed biocatalysts on industrial scale are ketoreductases (KREDs), which catalyse the transfer of a hydride from NAD(P)H to ketones and aldehydes.[14] Current research on KREDs is focused on important advancements, such as widening the substrate scope; improving the activity;

minimizing the loading of the expensive cofactor; increasing the overall robustness by using higher substrate concentrations and a wider temperature range and improving the compatibility with organic solvents; gaining efficiency through immobilization; and applying KREDs for dynamic kinetic resolutions (DKRs) to set two contiguous chiral centres.[11] Promising examples of industrially applicable KRED processes are listed in Table 1.

One of the most successful examples of application of KREDs is the synthesis of a chiral intermediate for atorvastatin, which is carried out on a multi-ton scale by Codexis.[7, 32] In the first step of the three-enzyme two-step process (Scheme 1), a KRED catalyses the asymmetric reduction of an α-chloroketone to the corresponding chlorohydrin. Simultaneously the regeneration the cofactor NADPH is driven by a glucose dehydrogenase GDH. In a second step the chlorohydrin is converted to a cyanohydrin by a halohydrin dehalogenase (HHDH). The KRED catalysed chlorohydrin product was obtained with 85% yield and >99.5% *ee*. However, the activities were too low for commercial application and the required high enzyme loadings caused formation of an emulsion, thus resulting in a problematic downstream process.[33] Additionally, the enzymes showed poor stability under operating conditions. To allow a practical large-scale process, the three enzymes were optimized by *in vitro* enzyme evolution.[32] The resulting improvements are shown in Table 2.

Table 1. Examples of industrially applicable KRED processes.[11]

Product	Substrate loading [g/L]	Yield [%]	*ee* [%]	Conditions	Ref.
	400	94	99.8	pH 7.0; 30 °C; no co-solvent; natural KRED's	[23]
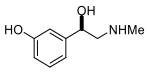	130	91	>99	pH 7.0; 30 °C; 50% 2-PrOH co-solvent; 0.05 g/L $NADP^+$; 50 g scale	[24]
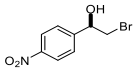	125	97	99.9	pH 7.2; 30 °C; biphasic 3:1 phosphate buffer: *n*-heptane; 0.125 g/L NAD^+; 1.25 g/L KRED; 1.25 g/L GDH; 100 g scale	[25]
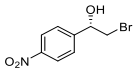	250	96	>99	pH 6.5-7.7; 30 °C; 3:1 phosphate buffer: 2-PrOH; 0.5 g/L $NADP^+$; 1.25 g/L KRED; 100 g scale	[25]
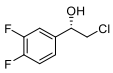	135	80	99.5	pH 7.0; 30 °C; 7:3 tris buffer: 2-PrOH; 7.5 g/L KRED; 1.35 kg scale	[26]
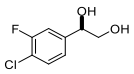	75	100	99.5	pH 6.5-7.0; 29-31 °C; water/heptane/PEG6000 biphasic solvent mixture; 0.8 g/L NAD^+; 0.8 g/L KRED; 0.8 g/L GDH; 30 kg scale	[27]
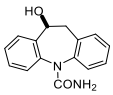	100	96	99.9	55 °C; 60% 2-PrOH co-solvent; 1g/L KRED	[28]
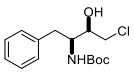	195	81	>99.9 de	pH 9.0; 45 °C; triethanolamine buffer; 9% v/v 2-PrOH; 0.65 g/L NAD^+; 1.3 g/L KRED; 90 g scale	[29]
	250	97	99.9	pH 6.3; 5:3 buffer: 2-PrOH; 19 g/L KRED; 4 kg scale	[30]
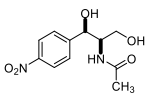	100	100	>99 dr>98:2	pH 6.5; 30 °C; 0.1 g/L $NADP^+$; 2 g/L KRED; 2 g/L GDH;	[31]

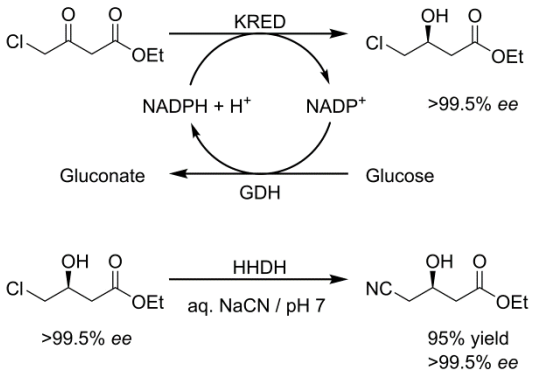

Scheme 1. Synthesis of a chiral intermediate for atorvastatin.

Table 2. Evolution of KRED/GDH catalyst for synthesis of atorvastatin intermediate.[33]

Parameter	Wild-type	Best variant
TTN catalyst	3000	>100000
TTN $NADP^+$	4000	>20000
STY [g/L/day]	80	600
Yield [%]	80	>95
ee [%]	99.8	>99.9
Enzyme [g/L]	100	
Substrate [g/L]	80	200
Reaction time [h]	24	10
Phase separation	>1 h	*ca.* 1 min
Work-up	Complex	Very simple

An example of successful practical application of enzymes in pharmaceutical industry is the synthesis of simvastatin, a cholesterol-lowering drug. This drug was originally developed by Merck, being their best-selling drug and the second most sold statin in the world (more than $3 million only in USA).[34-35] Simvastatin was chemically synthesised starting with the hydrolysis of the natural product lovastatin to give monacolin J, which can be converted to simvastatin by the lactonisation of the acid.[17] The overall process requires six steps, which are technically and economically demanding.[32] The biocatalytic approach, on the other hand, requires just two steps for the synthesis of simvastatin. Employing a whole cell acyltransferase LovD, which enables the regioselective acylation of the C-8 hydroxyl

group of monacolin J with α-dimethylbutyryl-*S*-*N*-acetylcysteamine (DMB-S-NAC), simvastatin can be synthesised directly.[36]

After the discovery of LovD, Codexis improved not only the enzyme but also process chemistry to enable a large-scale simvastatin manufacturing process, by carrying out nine iterations of *in vitro* evolution, creating 216 libraries and screening 61779 variants to develop a LovD variant with improved activity, in-process stability, and tolerance to product inhibition. The new process with the approximately 1000-fold improved enzyme allows full conversion at high substrate loading. Additionally, the amounts of acyl donor and of solvents for extraction could be minimised and facilitated easy product separation. This process combines many advantageous characteristics demanded by Green Chemistry nowadays:

- The enzyme is produced efficiently from renewable feedstock.
- The use of toxic and hazardous substances like *tert*-butyl dimethyl silane chloride, methyl iodide, and *n*-butyl lithium is reduced.
- The reaction is carried out at ambient temperature and at near atmospheric pressure.
- The reaction conditions are aqueous and solvent use is reduced.
- The only by-product (methyl 3-mercaptopropionic acid) is recycled.
- The major waste streams generated are biodegradable.
- Codexis' process can produce simvastatin with yields of 97%, significant when compared with <70% with alternative manufacturing routes.[32]

Furthermore, the evaluation of the environmental impact of bio-based products with respect to their entire life cycle is important and the choice of the raw material often turns out to be an important parameter influencing the life cycle performance.[4]

The two oldest green metrics are the *E*-factor and Trost's atom economy (AE), first proposed in 1991.[37] Atom economy is the conversion efficiency of a chemical process in terms of all atoms involved in the production of the desired products.[38] Atom economy can be described with:

$$AE = \frac{Molecular\ weight\ of\ desired\ product}{\sum Molecular\ weight\ of\ reactants} \frac{[g/mol]}{[g/mol]} * 100$$

It is calculated by dividing the molecular weight of the product by the total sum of the molecular weights of all educts considering the stoichiometry of the reaction.[37] Maximising the atom economy is to increase the incorporation of starting materials or reagents into the final product. It is in essence the prevention of pollution at the molecular level.[39]

The second important metric is the *E*-factor (*E* for environmental), which provides a simple and reliable measure to estimate the resource intensity of a given process or reaction and the wastes generated.[37, 40] In contrast to AE, the *E*-factor can easily be applied to a multi-step process thereby facilitating an assessment of a complete process.[37] The *E*-factor can be described with:

$$E = \frac{\sum m(waste)}{m(product)} \frac{[kg]}{[kg]}$$

A higher *E*-factor means more waste, indicating more extensive consumption of resources and results in a greater negative environmental impact. The ideal *E*-factor is zero, implying no waste was produced.[37] There is an ongoing debate on whether to include the amount of water used in the *E*-factor.[40] However, the current trend in the pharmaceutical industry is to include water in the *E*-factor.[37, 41] The typical scope of *E*-factors in the chemical industry are shown in Table 3.

Table 3. *E*-factors in the chemical industry.[37]

Industry segment	*Tonnes per annum*	*E-factor (kg waste per kg product)*
Oil refining	106–108	<0.1
Bulk chemicals	104–106	<1 – 5
Fine chemicals	102–104	5 – 50
Pharmaceuticals	10–103	25 – >100

Furthermore, the ‘classical’ *E*-factor does not take the energy consumption (heating, cooling, stirring, pumping etc.) of a reaction into account.[40] Today’s energy is provided by electricity, which is still mostly obtained from burning fossil fuels (gas, oil, coal), resulting in emission of CO_2 into the atmosphere and therefore should be taken into account as waste. The E^+-factor can be described with:

$$E^{+} = \frac{\sum m(waste)}{m(product)}\frac{[kg]}{[kg]} + \frac{W * CI}{m(product)}\frac{[kWh * \frac{kg(\mathrm{CO2})}{kWh}]}{[kg]}$$

W: electrical power used; CI: carbon intensity, i.e. the local average CO_2 emissions caused for the generation of electricity.[40]

This extension of the *E*-factor is an important improvement to assess the environmental viability of a process, but in general these assessments need to be addressed with caution. As already mentioned, the opinions on what to include as waste into the calculation of the *E*-factor differ and the true environmental impact of different wastes vary strongly. These *E*-factors can be a useful tool to identify major contributors to the negative environmental impact of a process and thereby help to improve it. But as long as we are generating unrecyclable waste, we cannot claim a truly green and sustainable process.

Photocatalytic NAD(P)H regeneration

Many of the above introduced oxidoreductases are dependent on cofactors for their function. The regeneration of these cofactors is an ongoing issue. In this section general and novel photocatalytic regeneration systems will be introduced.

Regeneration of cofactors in general

As mentioned, NAD(H) and NADP(H) are the natural cofactors, supplying redox equivalents to enzymes (Scheme 2). The central role of NAD(P) as electron donor and acceptor in biocatalytic redox reactions has motivated researchers to develop *in situ* regeneration systems to allow the use of these costly cofactors in catalytic amounts and thereby reduce their cost contribution to the desired product.[42]

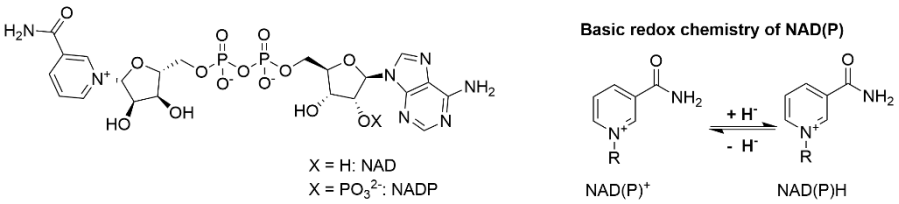

Scheme 2. Structure and basic chemistry of the nicotinamide cofactors.

Nowadays, various approaches combing biocatalysis with electrochemistry, photochemistry and cascade regenerations are investigated. In industrial processes applying oxidoreductases, as already presented with the example of atorvastatin synthesis in the previous section, the issue of redox equivalent supply is solved by a second enzyme reaction (cascade regeneration), converting NAD^+ or NADH to the respective counterpart.
This method has proven itself to reach very high total turnover numbers (TTN) of the cofactors with a range of 10^3-10^5 being economically sufficient.[43] Further benefits are the inherent compatibility with the enzymatic production systems and the ease of application. Nevertheless, this mostly works at the expense of a very poor atom efficiency depending on the cosubstrate (sacrificial electron donor). The cosubstrate often has to be used in large excess, in order to push the equilibrium of the reaction favourably. The most common cascade regeneration systems are shown in Table 4.

Another reason for the dominance of enzymatic regeneration systems lies in their intrinsic regioselectivity. The reduction of $NAD(P)^+$ to NAD(P)H can principally lead to three different regioisomers of NAD(P)H, whereas only the 1,4-NAD(P)H can be used by the production enzyme. Hence, a successful NAD(P)H regeneration system must be highly selective, otherwise loss of the costly nicotinamide cofactor due to formation of inactive regioisomers will make the approach economically unattractive.[44]

Table 4. Selection of common enzymatic NAD(P)H regeneration systems.

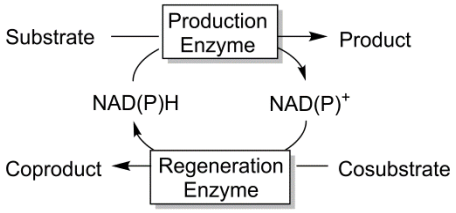

Regeneration enzyme	Cosubstrate	Coproduct
Formate dehydrogenase (FDH)	HCO_2H	CO_2
Alcohol dehydrogenase (ADH)		
Glucose dehydrogenase (GDH)	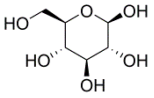	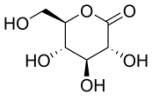
Phosphite dehydrogenase (PDH)	H_3PO_3	H_3PO_4
Hydrogenase (HAse)	H_2	-

The oxidative regeneration of cofactors has also been reported using a variety of enzymatic and chemical methods.[45-46] In general, the oxidation of the cofactor is easier, because there is no selectivity issue and the oxidised cofactors are more stable. The focus here is on novel ways for reductive regeneration of cofactors.

Photocatalysis

In photocatalysis, coloured compounds, called photosensitisers or photocatalysts, absorb light and thereby get excited to a higher energy state, enabling reactions impossible in their ground state. Photobiocatalysis using isolated enzymes can be divided into (1) photocatalytic regeneration cascades, (2) 'true' photoenzymatic cascades and (3) photoenzymatic reactions. In photoenzymatic cascades, redox enzymes are supplied with redox equivalents needed for their catalytic cycles, i.e. photocatalytic regeneration of redox enzymes. 'True' photoenzymatic cascades combine a biocatalytic transformation with a photocatalytic generation of the enzyme's starting material or a follow-up step of the enzymatic product. 'Photoenzymes' catalysing photoenzymatic reactions need light to be functional.
The focus here is on photocatalytic regeneration cascades. In more detail, reductive regeneration of redox enzymes can be achieved either directly, i.e. by direct reduction of the enzymes' active sites or indirectly, i.e. involving the nicotinamide cofactors. A selection of photochemical NAD(P)H regeneration systems used to promote biocatalytic reduction reactions is summarised in Table 5.

Although various photocatalysts and relay systems have been reported in the past ten years, the overall NAD(P) turnover numbers and the product concentrations achieved are far away from being applicable. Compared to the multiple thousands (even millions) reported for enzymatic regeneration systems the current performance falls back by orders of magnitude. Significant improvements will be necessary in the nearer future to make photochemical NAD(P)H regeneration systems a viable alternative (rather than a lab curiosity) to existing enzymatic systems.

Table 5. Selection of indirect photochemical NAD(P)H regeneration systems.

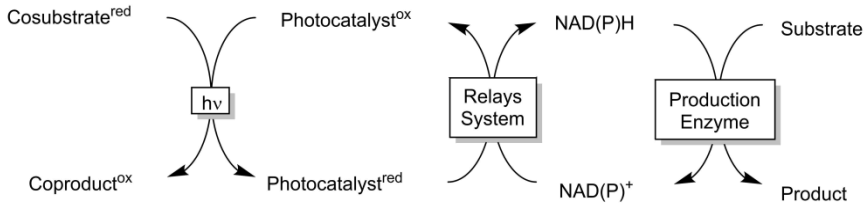

Cosubstrate	Photocatalyst	Production enzyme / Product (final con. [mM])	TN (NAD(P))	TN (Catalysts)	Ref.
[Cp*Rh(bpy)(H_2O)]$^{2+}$ as relay system [47]					
TEOA	CNR	GluDH / Glutamate (10)	10	Rh: 20 CNR: n.d. GluDH: n.d.	[48]
TEOA	mCNS	LacDH / Lactate (5)	5	Rh: 20 mCNS: n.d. LacDH: n.d.	[49]
TEOA	Eosin Y	GluDH / Glutamate (10)	200	Rh: 40 Eosin Y: 500 GluDH: n.d.	[50-51]
TEOA	$[Ru(bpy)_3]^{2+}$	GluDH / Glutamate (5)	5		[52]
H_2O	$[Co_4(H_2O)_2(PW_9O_{34})_2]^{10-}$	GluDH / Glutamate (5)	1.5		[52]
TEOA	Chemically converted graphene	*Lb*ADH / Various alcohols (<10)	15	Rh: 30	[53-54]
TEOA	Chemically converted graphene	FDH / HCO_2H	116	Rh: 232	[55-57]
	Hydrogen-Terminated Silicon Nanowires	GluDH / Glutamate (5)	4	Rh: 20	[58]
NAD(P)H:Flavin oxidoreductases as relay system					
Ascorbic acid	Quantum dots	*Tb*ADH / Isobutanol	8	FNR: 3167	[59]
EDTA	DRf	ADH-A / Chiral alcohols (<5)	21	PDR: 870 DRf: 72 MV: 17	[ch. 2]

TEOA: triethanolamine; CNR: graphitic carbonitride nanorods; mCNS: mesoporous carbonitride spheres; LacDH: lactate dehydrogenase; GluDH: glutamate dehydrogenase; FDH: formate dehydrogenase; DRf: 5-deazariboflavin; MV: methyl viologen.

The majority of photocatalysts follow a so-called ECE (electron transfer-chemical-electron transfer) mechanism resulting in two major issues for the selective formation

of 1,4-NAD(P)H. First, the intermediate NAD-radical can dimerise (comprising yet another pathway to inactivate the nicotinamide cofactor). Second, the chemical protonation step is rarely regioselective leading to the formation of the undesired NAD(P)H isomers (Scheme 3).[60]

To circumvent (or at least alleviate) the loss of enzyme-active 1,4-NAD(P)H due to direct single electron reduction by the reduced photocatalyst, generally a relay system is applied to convert the ECE-steps into a regioselective hydride transfer step. The organometallic complex $[Cp^*Rh(bpy)(H_2O)]^{2+}$ proposed by Steckhan[61-66] or NAD(P)H:Flavin oxidoreductases[59, 67-70] are the most frequently used catalysts for this purpose. The oxidoreductase, putidaredoxin reductase, used in this thesis will be described in the following section.

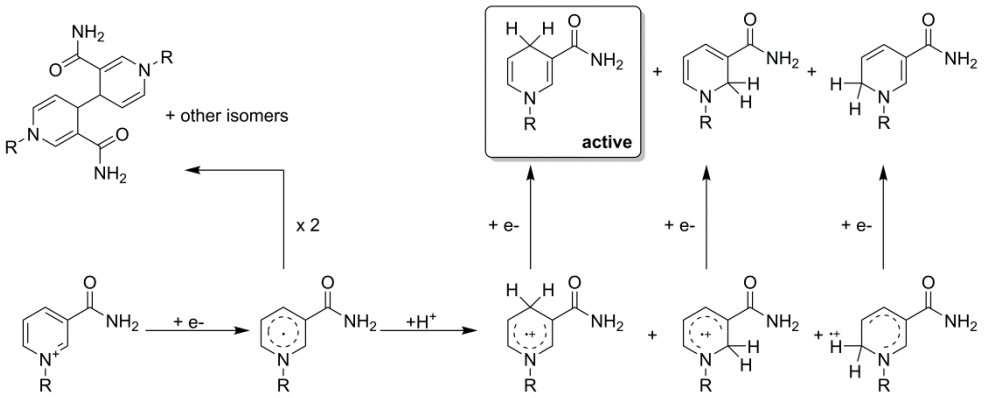

Scheme 3. ECE mechanism of NAD(P)$^+$ reduction and its consequences for the formation of NAD(P)-dimers and NAD(P)H isomers.

Noteworthy, for photocatalytic cofactor regeneration, it is mostly reduction reactions that have been reported with few exceptions on monooxygenases.[71-72] A plausible explanation for this is the so-called *Oxygen Dilemma*.[73] Since most photochemical redox reactions follow single electron transfer mechanisms, radicals are involved in the NAD(P)H regeneration step. Radicals, however, react very fast (diffusion-controlled) with molecular oxygen thereby diverging the electron flow away from NAD(P)$^+$ (or the relay catalysts) to O_2.[74] As a consequence strict anaerobic conditions are necessary for the application of these relay systems.

In this thesis, photochemical regeneration of oxidoreductases has been explored in two very different examples: (1) the putidaredoxin reductase-catalysed *in situ* regeneration of reduced nicotinamide cofactors and (2) the chloroperoxidase-catalysed formation of hypohalites (photochemical generation of the H_2O_2 cosubstrate).

Putidaredoxin reductase

This enzyme finds its origin in the well-studied cytochrome P450 systems, which work with the aid of ferredoxin and ferredoxin reductase. These reductases have been previously studied as relay systems for photocatalytic regeneration. Found in *Pseudomonas putida,* the putidaredoxin reductase (PDR, 46 kDa, E.C. 1.18.1.3) is the first subunit of its cytochrome P450cam*,* responsible of carrying redox equivalents towards the P450 from NADH *via* putidaredoxin. This enzyme belongs to the flavin oxidoreductase class with a flavin adenine dinucleotide (FAD) covalently bound in its active site. Uniquely, the redox potential of FAD bound in PDR can vary strongly depending on the presence of NAD^+. Binding of small amounts of NAD^+ decreases the redox potential substantially (by 60-80 mV) to a midpoint potential of -369 mV.[75] Additionally, the strong reducing power of PDR might be connected to the S-H groups found its active site. To enable the reduction of NAD^+ to NADH, the redox potential needs to be lower than -330 mV. PDR is a bifunctional enzyme, which in addition to catalyzing electron transfer to putidaredoxin, also functions as a NAD(H):dithiol/disulfide oxidoreductase. PDR seems unique in this class of enzymes due to the lack of the traditional disulfide redox centers.[76] These unique properties of PDR make it an interesting candidate for a relay system in a photocatalytic regeneration cascade (see Chapter 2).

Haloperoxidases as promising redox catalysts

To circumvent the regeneration of cofactors, hydrogen peroxide can be applied as cosubstrate in combination with peroxidases or peroxygenases. A class of enzymes where the use of hydrogen peroxide is coupled to halogenation are the haloperoxidases. Enzymatic halogenation is a promising, more sustainable transformation method, because it can directly use halogen salts as substrates, and circumvents the intermediate production of gaseous chlorine and bromine or hypohalites. Within this class of haloperoxidases, vanadium-dependent haloperoxidases take a special position due to their inherent stability. In this section we will discuss haloperoxidases in general and focus on the vanadium-dependent chloroperoxidase from *Curvularia inaequalis* due to its outstanding activity and stability.

Haloperoxidases are classified by the most electronegative halide ion they can oxidise. A chloroperoxidase can, for example, oxidise Cl^-, Br^- and I^-, while a bromoperoxidase can oxidise Br^- and I^- but not Cl^-. A fluoroperoxidase has not been identified yet and is rather unlikely ever to be found due to the high electronegativity and oxidation potential of F^-. Today, two kinds of haloperoxidases are known: the heme-dependent haloperoxidases[77] and the vanadium-dependent haloperoxidases.[78-81] As suggested by their names, they differ with respect to the prosthetic group and consequently in their catalytic mechanisms. The heme-dependent haloperoxidases utilise an Fe^{IV}-porphyrin$^+$ (compound I) species formed from the heme resting state and H_2O_2 to oxidise halides. The vanadium-dependent haloperoxidases on the other hand use a peroxo-vanadate species (formed by the reaction with H_2O_2) for the same transformation (Scheme 5). In both classes of haloperoxidases, the hypohalites after formation diffuse out of the enzyme active site.[82] Hence any oxidative transformation taking place is not supported by the (chiral) enzyme environment and the selectivity of the transformation is controlled by the reactivity of the starting material rather than by the enzyme. Some exceptions (haloperoxidases of bacterial origin) to this rule have been reported.[83-84][85-87] Indeed, selective halogenations would be of great interest for synthetic organic

synthesis, especially if performed by highly active and stable enzymes. As of today, however, the molecular basis for the assumed selectivity remains unclear and the number of examples is yet too little. Hopefully, future engineered haloperoxidases will indeed combine the best of all: H_2O_2-dependent reactions, high robustness, catalytic activity and selectivity.

Heme-dependent haloperoxidases excel by their high catalytic activity (in the range of several dozen to hundreds per second) but are hampered by their poor robustness toward H_2O_2. Although this issue in principle can be overcome by slow dosing of H_2O_2 or *in situ* generation of H_2O_2,[88] such measures usually complicate the reaction schemes. In contrast to the limited number of heme-dependent haloperoxidases, a rich variety of vanadium-dependent haloperoxidases are mainly available from marine organisms,[89-95] but also from other sources such as lichens[85-86, 95-96] and terrestrial fungi.[97] The rich microbiology and biochemistry of haloperoxidases has been reviewed by Wever and coworkers.[79-81, 98-99]

One of the most striking differences of vanadium-dependent haloperoxidases to their heme-counterparts is the robustness against H_2O_2. In particular, the chloroperoxidase from *Curvularia inaequalis* (*Ci*VCPO) excels in this respect as it can be stored in the presence of at least 100 mM H_2O_2 for days without noticeable loss in catalytic activity.[100] The same is true for the general stability of *Ci*VCPO at elevated temperatures (up to 70 °C) and in the presence of organic cosolvents (ethanol, ethyl acetate, acetone). From a practical point of view, it is, however, advisable to control the H_2O_2 concentration in the reaction mixture due to the spontaneous reaction between hypohalites and H_2O_2 yielding singlet oxygen ($^1O_2$) and halides (Scheme 4), which is well-documented for various haloperoxidases.[89, 101-104]

To control the H_2O_2 concentration, a range of *in situ* H_2O_2 generation methods are available.[88] Some of them have been evaluated in combination with haloperoxidases. Though the above-mentioned $^1O_2$ formation does not significantly impair the robustness of the enzyme, it lowers the yield in H_2O_2 and therefore is less attractive from an economical point-of-view. On the other hand, the primarily formed $^1O_2$ is very reactive and this ‘dark reaction’ for its *in situ* generation may find some

preparative applications, such as the transformation of β-citronellol to Rose oxide.[105] Wever and coworkers also pointed out that the enzymatic $^1O_2$ synthesis reaction is more efficient than chemically catalysed reaction by order of magnitudes.[103] For example, Na_2MoO_4[106] or $La(NO_3)_3/NaOH_{0.5}$,[107] as catalysts exhibit turnover frequencies in the range of several dozen per hour, while the enzyme shows turnover frequencies of dozens to thousands per second.

Haloperoxidases have been applied to a broad range of different oxidation and halogenation reactions. Among them halogenation of electron-rich aromatic compounds, halohydroxylation of C=C-double bonds, heteroatom oxidation, oxidative decarboxylation and more. Starting from γ,δ-unsaturated acids the corresponding halogenated butyrolactones are accessible.[108] Thus, this particular enzyme has significant synthetic potential. Coupled with *in situ* generation of H_2O_2, the applicability of this enzyme can increase, because oxygen instead of hydrogen peroxide would then be the final oxidant.

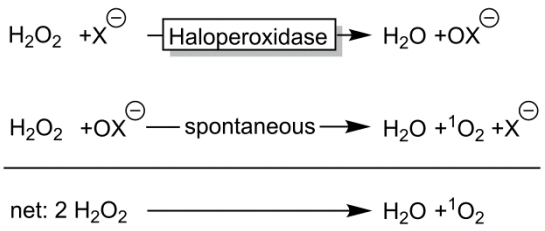

Scheme 4. Hypohalite-dependent disproportionation of H_2O_2.

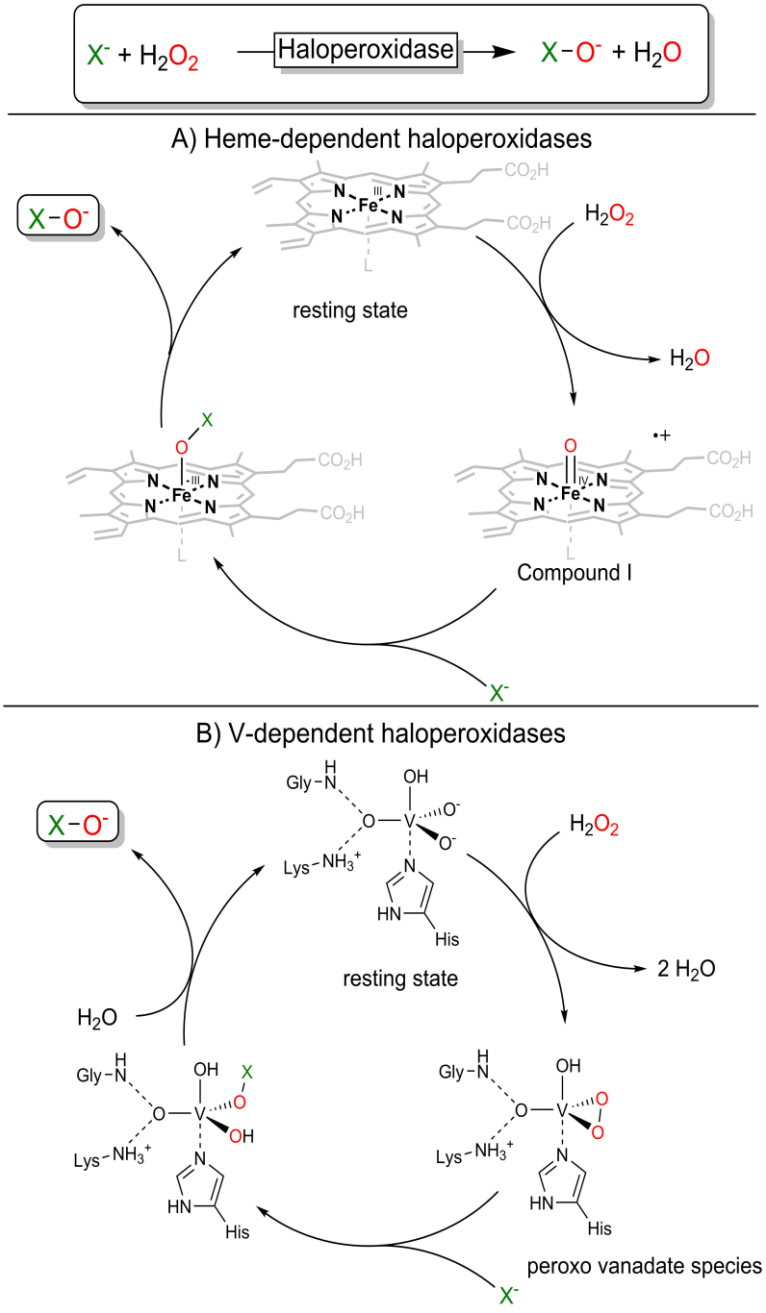

Scheme 5. Simplified halide oxidation mechanisms of haloperoxidases.

Content of this thesis

With this thesis, we want to contribute to the field of redox biocatalysis, by expanding our knowledge on photocatalytic cofactor re- and generation as well as demonstrating the scalability of a haloperoxidase reaction. The scope and limitations of the photocatalytic approach to solve the cofactor issue will be presented. Furthermore, we believe haloperoxidases bear great promise for application at a larger scale. To show the potential of these enzymes the *Ci*VCPO, as an outstanding example of oxidoreductases, has been chosen for upscaling of a reaction to an industrially more relatable scale.

Chapter 2 investigates a photoenzymatic NADH regeneration system using photocatalysis in combination with an enzyme-based relay system, putidaredoxin reductase, to drive a NADH-dependent ketoreduction.

Chapter 3 concerns the photocatalytic generation of H_2O_2 to fuel a haloperoxidase. In this heterologous photocatalysis approach the *Ci*VCPO has been chosen as model enzyme due to its outstanding performance.

Chapter 4 describes the use of *Ci*VCPO for a scalable and greener halogenation reaction to investigate the scalability of this interesting class of enzyme.

Finally, **Chapter 5** provides a general discussion and conclusion of the most important discoveries in this thesis.

References

[1] Y. Gaber, Hydrolases as Catalysts for Green Chemistry and Industrial Applications - Esterase, Lipase and Phytase, Lund University, Biotechnology Department, **2012**.
[2] C. Okkerse, H. van Bekkum, *Green Chem.* **1999**, *1*, 107-114.
[3] R. A. Sheldon, *J. Environ. Monitor* **2008**, *10*, 406-407.
[4] R. Hatti-Kaul, U. Törnvall, L. Gustafsson, P. Börjesson, *Trends Biotechnol.* **2007**, *25*, 119-124.
[5] R. A. Sheldon, I. Arends, U. Hanefeld, *Green chemistry and catalysis*, John Wiley & Sons, New York City, United States, **2007**.
[6] D. E. Koshland, *Angew. Chem. Int. Edit.* **1994**, *33*, 2375-2378.
[7] R. A. Sheldon, J. M. Woodley, *Chem. Rev.* **2018**, *118*, 801-838.
[8] A. J. J. Straathof, S. Panke, A. Schmid, *Curr. Opin. Biotech.* **2002**, *13*, 548-556.
[9] K. A. Powell, S. W. Ramer, S. B. del Cardayre, W. P. C. Stemmer, M. B. Tobin, P. F. Longchamp, G. W. Huisman, *Angew. Chem. Int. Edit.* **2001**, *40*, 3948-3959.
[10] E. C. Webb, Enzyme nomenclature 1992. Recommendations of the Nomenclature Committee of the International Union of Biochemistry and Molecular Biology on the Nomenclature and Classification of Enzymes, Academic Press, London, England, **1992**.
[11] D. L. Hughes, *Org. Process. Res. Dev.* **2018**, *22*, 1063-1080.
[12] J. R. Cherry, A. L. Fidantsef, *Curr. Opin. Biotech.* **2003**, *14*, 438-443.
[13] S. Jemli, D. Ayadi-Zouari, H. B. Hlima, S. Bejar, *Crit. Rev. Biotechnol.* **2016**, *36*, 246-258.
[14] C. K. Prier, B. Kosjek, *Curr. Opin. Chem. Biol.* **2019**, *49*, 105-112.
[15] L. S. Vidal, C. L. Kelly, P. M. Mordaka, J. T. Heap, *Bba-Proteins Proteom.* **2018**, *1866*, 327-347.
[16] J. D. Stewart, in *Future Directions in Biocatalysis* (Ed.: T. Matsuda), Elsevier Science B.V., Amsterdam, The Netherlands, **2007**, pp. 293-304.
[17] E. M. M. Abdelraheem, H. Busch, U. Hanefeld, F. Tonin, *React. Chem. Eng.* **2019**.
[18] G. W. Huisman, J. Liang, A. Krebber, *Curr. Opin. Chem. Biol.* **2010**, *14*, 122-129.
[19] J. M. Woodley, *Curr. Opin. Chem. Biol.* **2013**, *17*, 310-316.
[20] P. Tufvesson, J. Lima-Ramos, N. Al Haque, K. V. Gernaey, J. M. Woodley, *Org. Process. Res. Dev.* **2013**, *17*, 1233-1238.
[21] J. P. Adams, M. J. B. Brown, A. Diaz-Rodriguez, R. C. Lloyd, G. D. Roiban, *Adv. Synth. Catal.* **2019**, *361*, 2421-2432.
[22] G. J. Lye, P. A. Dalby, J. M. Woodley, *Org. Process. Res. Dev.* **2002**, *6*, 434-440.
[23] J. Liang, S. J. Jenne, E. Mundorff, C. Ching, J. M. Gruber, A. Krebber, G. W. Huisman, *Ketoreductase polypeptides for the reduction of acetophenones*, U.S. Patent Application 2017/0067032 A1, **2014-03-09**.
[24] O. Alvizo, S. J. Collier, J. Hennemann, S. H. Oh, W. Zha, *Ketoreductase polypeptides for the preparation of phenylephrine*, U.S. Patent 9,834,758 B2, **2017-12-05**.
[25] R. Trussardi, H. Iding, *Process for the preparation of chiral 2-aryl morpholines*, U.S. Patent Application 2016/0289718 A1, **2016-10-06**.
[26] S. L. Zhou, D.; Wang, R.; Zhang, S.; Chen, Z. , *Method for Preparing Chiral 2-Chloro-2,3-difluorophenethyl Alcohol*, Chinese Patent Application CN 106520849, **2017-03-22**.
[27] J. C. Lin, A.; Gu, W.; Iding, H.; Li, J.; Xin, L.; Meier, C. S. P.; Sha, J.; Wang, Y.; Zhang, H.; Zhang, J.; Zhang, T., *Process for the Manufacturing of Medicaments*, U.S. Patent Application 2017/0022183 A, **2017-01-26**.
[28] A. S. Gohel, D. J.; Wong, B.; Sukumaran, J.; Yeo, W., S. J. N. L.; Collier, S., *Biocatalytic Process for Preparing Eslicarbazepine and Analogs Thereof*, U.S. Patent Application 2017/0159028 A1, **2017-06-08**.
[29] Y. K. V. Bong, M.; Collier, S. J.; Mitchell, V.; Mavinahalli, J., *Ketoreductase-mediated Stereoselective Route to Alpha Chloroalcohols*, U.S. Patent Application 2016/0160187 A1, **2016-06-09**.
[30] W. W. Zhu, B.; Wu, H., *Enzymatic Preparation Method of (S)-N-tert-Butoxycarbonyl-3-hydroxypiperidine*, Chinese Patent Application CN 106520856, **2017-03-22**.
[31] X. H. Xie, X.; Zhang, J.; Zhang, R., *Preparation Method of Chloramphenicol Compounds*, Chinese Patent Application CN 106566851, **2019-11-11**.
[32] P. Hoyos, V. Pace, A. R. Alcantara, *Catalysts* **2019**, *9*.
[33] R. A. Sheldon, P. C. Pereira, *Chem. Soc. Rev.* **2017**, *46*, 2678-2691.

[34] E. A. Stein, *Clin. Cardiol.* **2003**, *26*, 25-31.
[35] M. Bifulco, A. Endo, *Pharmacol. Res.* **2014**, *88*, 1-2.
[36] X. K. Xie, K. Watanabe, W. A. Wojcicki, C. C. C. Wang, Y. Tang, *Chem. Biol.* **2006**, *13*, 1161-1169.
[37] R. A. Sheldon, *Green Chem.* **2017**, *19*, 18-43.
[38] B. M. Trost, *Science* **1991**, *254*, 1471-1477.
[39] K. E. Parent*, Vol. 2019*, Green Chemistry Institute American Chemical Society, Washington, https://www.acs.org/content/dam/acsorg/greenchemistry/education/resources/cleaning-up-with-atom-economy.pdf, **accessed on 2019-12-16**.
[40] F. Tieves, S. J. Willot, M. van Schie, M. C. R. Rauch, S. H. H. Younes, W. Zhang, J. Dong, P. Gomez de Santos, J. M. Robbins, B. Bommarius, M. Alcalde, A. S. Bommarius, F. Hollmann, *Angew. Chem. Int. Ed. Engl.* **2019**, *58*, 7873-7877.
[41] S. K. Ma, J. Gruber, C. Davis, L. Newman, D. Gray, A. Wang, J. Grate, G. W. Huisman, R. A. Sheldon, *Green Chem.* **2010**, *12*, 81-86.
[42] H. K. Chenault, G. M. Whitesides, *Appl. Biochem. Biotech.* **1987**, *14*, 147-197.
[43] W. A. van der Donk, H. M. Zhao, *Cur.r Opin. Biotech.* **2003**, *14*, 421-426.
[44] E. Steckhan, *Electrochemistry III*, Springer-Verlag Berlin and Heidelberg, Germany, **1998**.
[45] F. Hollmann, I. W. C. E. Arends, K. Buehler, *Chemcatchem* **2010**, *2*, 762-782.
[46] A. Weckbecker, H. Groger, W. Hummel, *Adv. Biochem. Eng. Biot.* **2010**, *120*, 195-242.
[47] S. H. Lee, H. J. Lee, K. Won, C. B. Park, *Chem-Eur. J.* **2012**, *18*, 5490-5495.
[48] J. Liu, J. Huang, H. Zhou, M. Antonietti, *ACS appl. mater. inter.* **2014**, *6*, 8434-8440.
[49] J. H. Huang, M. Antonietti, J. Liu, *J. Mater. Chem. A* **2014**, *2*, 7686-7693.
[50] S. H. Lee, D. H. Nam, C. B. Park, *Adv. Synth. Catal.* **2009**, *351*, 2589-2594.
[51] S. H. Lee, D. H. Nam, J. H. Kim, J. O. Baeg, C. B. Park, *Chembiochem* **2009**, *10*, 1621-1624.
[52] J. Ryu, D. H. Nam, S. H. Lee, C. B. Park, *Chem-Eur. J.* **2014**, *20*, 12020-12025.
[53] S. Choudhury, J. O. Baeg, N. J. Park, R. K. Yadav, *Green Chem.* **2014**, *16*, 4389-4400.
[54] S. Choudhury, J. O. Baeg, N. J. Park, R. K. Yadav, *Angew. Chem. Int. Ed.* **2012**, *51*, 11624-11628.
[55] R. K. Yadav, J. O. Baeg, A. Kumar, K. J. Kong, G. H. Oh, N. J. Park, *J. Mater. Chem. A* **2014**, *2*, 5068-5076.
[56] R. K. Yadav, G. H. Oh, N. J. Park, A. Kumar, K. J. Kong, J. O. Baeg, *J. Am. Chem. Soc.* **2014**, *136*, 16728-16731.
[57] R. K. Yadav, J. O. Baeg, G. H. Oh, N. J. Park, K. J. Kong, J. Kim, D. W. Hwang, S. K. Biswas, *J. Am. Chem. Soc.* **2012**, *134*, 11455-11461.
[58] H. Y. Lee, J. Ryu, J. H. Kim, S. H. Lee, C. B. Park, *Chemsuschem* **2012**, *5*, 2129-2132.
[59] K. A. Brown, M. B. Wilker, M. Boehm, H. Hamby, G. Dukovic, P. W. King, *ACS Catal.* **2016**, *6*, 2201-2204.
[60] F. Hollmann, A. Schmid, *Biocatal. Biotransfor.* **2004**, *22*, 63-88.
[61] E. Steckhan, S. Herrmann, R. Ruppert, J. Thommes, C. Wandrey, *Angew. Chem. Int. Edit.* **1990**, *29*, 388-390.
[62] R. Ruppert, S. Herrmann, E. Steckhan, *J. Chem. Soc. Chem. Comm.* **1988**, 1150-1151.
[63] S. Grammenudi, M. Franke, F. Vögtle, E. J. J. o. i. p. Steckhan, *J. Inclusion. Phenom.* **1987**, *5*, 695-707.
[64] R. Wienkamp, E. Steckhan, *Angew. Chem. Int. Edit.* **1983**, *22*, 497-497.
[65] E. Steckhan, *Angew. Chem. Int. Edit.* **1986**, *25*, 683-701.
[66] F. Hollmann, B. Witholt, A. Schmid, *J. Mol. Catal. B-Enzym* **2002**, *19*, 167-176.
[67] G. T. Hofler, E. Fernandez-Fueyo, M. Pesic, S. H. Younes, E. G. Choi, Y. H. Kim, V. B. Urlacher, I. W. C. E. Arends, F. Hollmann, *Chembiochem* **2018**, *19*, 2344-2347.
[68] L. Wan, C. F. Megarity, B. Siritanaratkul, F. A. Armstrong, *Chem. Commun.* **2018**, *54*, 972-975.
[69] H. Asada, T. Itoh, Y. Kodera, A. Matsushima, M. Hiroto, H. Nishimura, Y. Inada, *Biotechnol. Bioeng.* **2001**, *76*, 86-90.
[70] J. J. Pueyo, C. Gomezmoreno, *Enzyme Microb. Technol.* **1992**, *14*, 8-12.
[71] S. H. Lee, Y. C. Kwon, D. M. Kim, C. B. Park, *Biotechnol. Bioeng.* **2013**, *110*, 383-390.
[72] J. H. Lee, D. H. Nam, S. H. Lee, J. H. Park, C. B. Park, K. J. Jeong, *J. Ind. Eng. Chem.* **2016**, *33*, 28-32.
[73] D. Holtmann, F. Hollmann, *Chembiochem* **2016**, *17*, 1391-1398.
[74] M. M. C. H. van Schie, S. H. H. Younes, M. C. R. Rauch, M. Pesic, C. E. Paul, I. W. C. E. Arends, F. Hollmann, *Mol. Catal.* **2018**, *452*, 277-283.
[75] V. Reipa, M. J. Holden, V. L. Vilker, *Biochemistry-Us* **2007**, *46*, 13235-13244.
[76] I. F. Sevrioukova, T. L. Poulos, *J. Biol. Chem.* **2002**, *277*, 25831-25839.

[77] M. Hofrichter, R. Ullrich, *Appl. Microbiol. Biotechnol.* **2006**, *71*, 276-288.
[78] C. Leblanc, H. Vilter, J. B. Fournier, L. Delage, P. Potin, E. Rebuffet, G. Michel, P. L. Solari, M. C. Feiters, M. Czjzek, *Coordin. Chem. Rev.* **2015**, *301*, 134-146.
[79] R. Wever, M. A. van der Horst, *Dalton T.* **2013**, *42*, 11778-11786.
[80] R. Wever, Springer, New York, United states, **2012**.
[81] R. Wever, Peroxidases and catalases: biochemistry, biophysics, biotechnology and physiology, John Wiley & Sons, New York, United States, **2010**.
[82] J. W. P. M. Vanschijndel, P. Barnett, J. Roelse, E. G. M. Vollenbroek, R. Wever, *Eur. J. Biochem.* **1994**, *225*, 151-157.
[83] J. N. Carter-Franklin, J. D. Parrish, R. A. Tschirret-Guth, R. D. Little, A. Butler, *J. Am. Chem. Soc.* **2003**, *125*, 3688-3689.
[84] J. Latham, E. Brandenburger, S. A. Shepherd, B. R. K. Menon, J. Micklefield, *Chem. Rev.* **2018**, *118*, 232-269.
[85] P. Bernhardt, T. Okino, J. M. Winter, A. Miyanaga, B. S. Moore, *J. Am. Chem. Soc.* **2011**, *133*, 4268-4270.
[86] L. Kaysser, P. Bernhardt, S. J. Nam, S. Loesgen, J. G. Ruby, P. Skewes-Cox, P. R. Jensen, W. Fenical, B. S. Moore, *J. Am. Chem. Soc.* **2012**, *134*, 11988-11991.
[87] Z. D. Miles, S. Diethelm, H. P. Pepper, D. M. Huang, J. H. George, B. S. Moore, *Nat. Chem.* **2017**, *9*, 1235-1242.
[88] B. O. Burek, S. Bormann, F. Hollmann, J. Z. Bloh, D. Holtmann, *Green Chem.* **2019**, *21*, 3232-3249.
[89] H. S. Soedjak, A. Butler, *Biochemistry-Us* **1990**, *29*, 7974-7981.
[90] J. N. Carter-Franklin, A. Butler, *J. Am. Chem. Soc.* **2004**, *126*, 15060-15066.
[91] M. Sandy, J. N. Carter-Franklin, J. D. Martin, A. Butler, *Chem. Commun.* **2011**, *47*, 12086-12088.
[92] E. E. Coupe, M. G. Smyth, A. Fosberry, R. M. Hall, J. A. Littlechild, *Protein. Expres. Purif.* **2007**, *52*, 265-272.
[93] H. Vilter, *Phytochemistry* **1984**, *23*, 1387-1390.
[94] N. Itoh, Y. Izumi, H. Yamada, *J. Biol. Chem.* **1986**, *261*, 5194-5200.
[95] A. Frank, C. J. Seel, M. Groll, T. Gulder, *Chembiochem* **2016**, *17*, 2028-2032.
[96] H. Plat, B. E. Krenn, R. Wever, *Biochem. J.* **1987**, *248*, 277-279.
[97] J. W. P. M. Vanschijndel, E. G. M. Vollenbroek, R. Wever, *Biochim. Biophys. Acta* **1993**, *1161*, 249-256.
[98] R. R. Wever, R.,, Peroxidases and catalases: biochemistry, biophysics, biotechnology and physiology, John Wiley & Sons, New York, United States, **2010**.
[99] R. Wever, B. E. Krenn, R. Renirie, in *Methods Enzymol., Vol. 605* (Ed.: B. S. Moore), Academic Press, London, England, **2018**, pp. 141-201.
[100] E. Fernandez-Fueyo, M. van Wingerden, R. Renirie, R. Wever, Y. Ni, D. Holtmann, F. Hollmann, *Chemcatchem* **2015**, *7*, 4035-4038.
[101] D. R. Morris, L. P. J. J. o. B. C. Hager, *J. Biol. Chem.* **1966**, *241*, 1763-1768.
[102] R. Renirie, C. Pierlot, R. Wever, J. M. Aubry, *J. Mol. Catal. B-Enzym* **2009**, *56*, 259-264.
[103] R. Renirie, C. Pierlot, J. M. Aubry, A. F. Hartog, H. E. Schoemaker, P. L. Alsters, R. Wever, *Adv. Synth. Catal.* **2003**, *345*, 849-858.
[104] E. Deboer, R. Wever, *J. Biol. Chem.* **1988**, *263*, 12326-12332.
[105] P. L. Alsters, W. Jary, V. Nardello-Rataj, J. M. Aubry, *Org. Process. Res. Dev.* **2010**, *14*, 259-262.
[106] V. Nardello, J. Marko, G. Vermeersch, J. M. Aubry, *Inorg. Chem.* **1995**, *34*, 4950-4957.
[107] V. Nardello, J. Barbillat, J. Marko, P. T. Witte, P. L. Alsters, J. M. Aubry, *Chem-Eur. J.* **2003**, *9*, 435-441.
[108] F. Tieves, S. J. P. Willot, M. M. C. H. van Schie, M. C. R. Rauch, S. H. H. Younes, W. Y. Zhang, J. J. Dong, P. G. de Santos, J. M. Robbins, B. Bommarius, M. Alcalde, A. S. Bommarius, F. Hollmann, *Angew. Chem. Int. Edit.* **2019**, *58*, 7873-7877.

Chapter 2

Chapter 2: A photoenzymatic NADH regeneration system

Georg T. Höfler, Elena Fernández-Fueyo, Milja Pesic, Sabry Younes, Eun-Gyu Choi, Yong H. Kim, Vlada B. Urlacher, Isabel W.C.E. Arends and Frank Hollmann

Based on ChemBioChem 2018, 19(22), 2344–2347

Summary

A photoenzymatic NADH regeneration system was established. The combination of deazariboflavin as a photocatalyst with putidaredoxin reductase enabled the selective reduction of NAD^+ into the enzyme-active 1,4-NADH to promote an alcohol dehydrogenase-catalysed stereospecific reduction reaction. The catalytic turnover of all the reaction components was demonstrated. Factors influencing the efficiency of the overall system were identified.

Introduction

Biocatalytic redox reactions are receiving increasing attention in preparative organic synthesis.[1] Specifically, stereospecific ketoreductions and reductive aminations are now well established, especially in the pharmaceutical industry.[2-3] Being reductive by nature, these reactions need to be constantly supplied with reducing equivalents in the form of the reduced nicotinamide adenine dinucleotide cofactors NAD(P)H. (Cost-)efficient reaction schemes inevitably involve sub-stoichiometric amounts of the NAD(P)H cofactors and their *in situ* regeneration.[4-5] Having been stated decades ago,[6] it is not astonishing that a broad range of catalytic methods for the

in situ regeneration of reduced nicotinamide cofactors have been developed.[4-5] All of them exhibit specific advantages and disadvantages, and it appears unlikely that a universal regeneration system will ever be found. In the 1970s, Willner and co-workers pioneered the use of visible light as a driving force to promote *in situ* NADPH regeneration.[7] Despite the promise of sunlight-driven cofactor regeneration, this approach was pursued in very few studies.[8] One reason is that photochemical redox reactions comprise single electron transfer steps, which makes their direct application to NAD(P)$^+$ reduction impractical. This is due to the formation of enzyme-inactive NADH isomers and dimers.[9] A relay system to transform two successive single-electron steps into a (selective) hydride transfer step is required. So far, the flavin adenine dinucleotide (FAD)-containing ferredoxin–NADP$^+$ reductase (FNR, E.C. 1.18.1.2) is the most widely used catalyst for this purpose.[10-13] FNR, however, is highly selective for the phosphorylated nicotinamide cofactor (NADP$^+$/NADPH) and is not applicable for the regeneration of the reduced, non-phosphorylated cofactor (NADH). We therefore evaluated the NAD-dependent putidaredoxin reductase (PDR) from *Pseudomonas putida* (E.C.1.18.1.5)[14] as a relay system. Striving for simple reaction setups, we evaluated flavins as photocatalysts.[8, 15-16] Overall, we aimed at establishing a photoenzymatic NADH regeneration system applicable to NADH-dependent, stereospecific reduction reactions (Scheme 1).

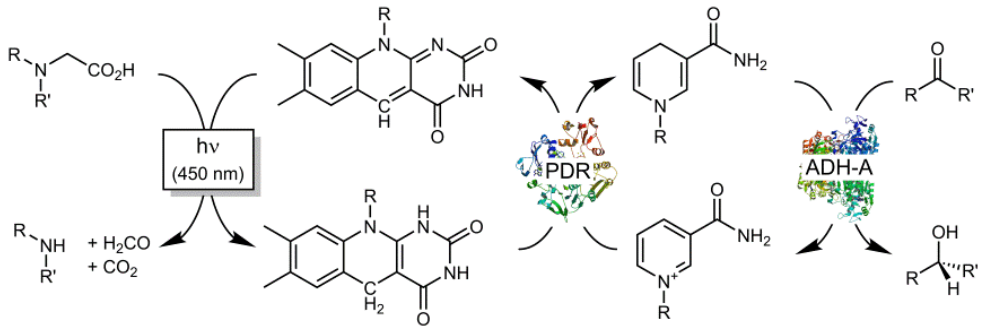

Scheme 1. Photoenzymatic reduction of NAD$^+$ to promote alcohol dehydrogenase (ADH)-catalysed stereospecific reduction of ketones. A photocatalyst, deazariboflavin, promotes the light-driven oxidation of a sacrificial electron donor (e.g., ethylenediaminetetraacetic acid, EDTA) and delivers the reducing equivalents to the NADH-regeneration catalyst (putidaredoxin reductase, PDR). NADH is productively used by an alcohol dehydrogenase for the specific reduction of ketones to alcohols.

Results and Discussion

In a first set of experiments we evaluated some commercially available flavins as well as chemically synthesised deazariboflavin (dRf) as photocatalysts to promote the reduction of NAD^+. Significant NAD^+ reduction was observed only with dRf as the photocatalyst (Figure 1). Most likely, this can be attributed to the fact that the redox potential of the dRf/dRfH2 couple (-0.273V vs. standard hydrogen electrode, SHE) is more negative than that of flavin mononucleotide (FMN)/ $FMNH_2$ or FAD/$FADH_2$ (-0.199 V vs. SHE),[17] which shifts the PDR redox equilibrium more to the reduced state. Strict exclusion of molecular oxygen from these reactions was crucial.

Figure 1 compares the time courses of the photochemical NADH-formation reactions under semi-anaerobic conditions (N_2 atmosphere, Figure 1A) and under glove box conditions (Figure 1B). Note that the apparent NADH concentration was estimated spectrophotometrically at 340 nm by using a molar extinction coefficient of ε_{340}= 6.22 mM^{-1} cm^{-1}. This method does not distinguish between enzymatically active 1,4-NADH and its (enzyme inactive) regioisomers. Noteworthy, the apparent NADH concentration in the first case peaked after approximately 6 h, whereas steady NADH accumulation was observed under strict anaerobic conditions. Apparently, even a trace amount of molecular oxygen (entering the sample in the first case) irreversibly inhibits the photochemical NAD^+ reduction reaction. Notably, in the absence of PDR, very significant reduction of NAD^+ (as judged spectrophotometrically) was also observed. This chemical reduction may be expected to yield significant amounts of non-enzyme-active NADH isomers such as 1,2-NADH, 1,6-NADH and/or NAD dimers (Scheme 2, photochemical),[18-19] whereas the PDR-mediated reduction of NAD^+ exclusively yields enzyme-active 1,4-NADH (Scheme 2, photoenzymatic).

Therefore, we further investigated the influence of the PDR concentration on the relative amount of 1,4-NADH formed (Figure 3). To assess the concentration of the latter, we used NADH-dependent ketoreduction reaction catalysed by the alcohol dehydrogenase (ADH) from *Rhodococcus ruber* (i.e., ADH-A; Figure 3).[20-23] Quite expectedly, the use of a high molar surplus of the dRf photocatalyst resulted in poor

selectivity of the NAD^+ reduction, and approximately one third of the overall reduced nicotinamide cofactor was the enzyme-active 1,4-NADH isomer.

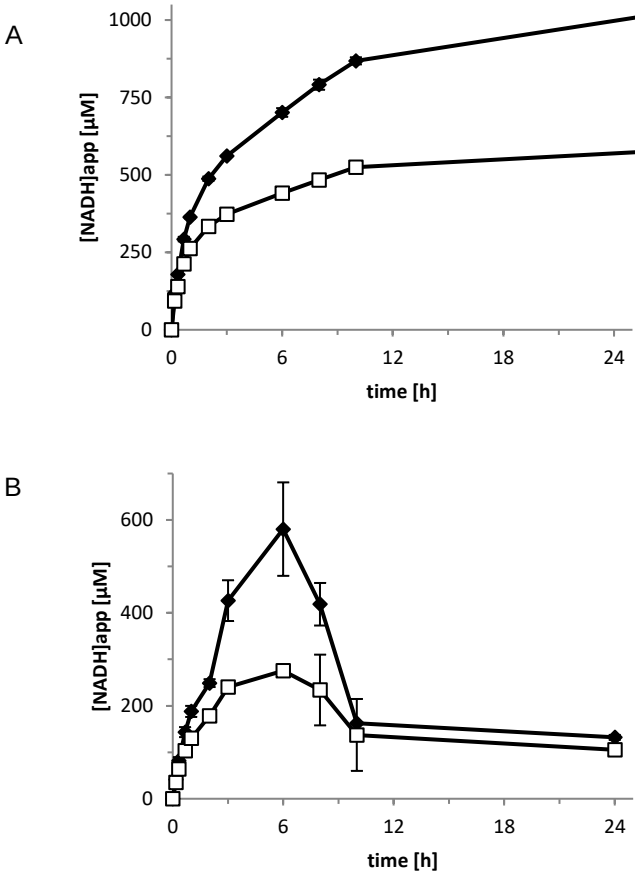

Figure 1. Photoenzymatic reduction of NAD^+ in the presence (◆) and absence (□) of PDR. A) Results obtained under 'anaerobic' conditions (using N_2-flushed reaction vessels under otherwise ambient atmosphere). B) The same experiments were entirely performed in a glovebox. General conditions: 50 mM Tris-HCl buffer (pH 8); [NAD^+] = 2 mM; [EDTA] = 20 mM; [dRf] = 60 µM, T = 25 °C; λ = 450 nm. Sampling: at intervals, samples were withdrawn, diluted in 50 mM Tris-HCl buffer (pH 8) and analysed spectrophotometrically. For calculation of the apparent NADH concentration a molar extinction coefficient of 6.22 M^{-1} cm^{-1} was used. Please note that this method does not distinguish between 1,2-, 1,4-, 1,6-NADH or NADH-dimers. Exemplary UV/Vis spectra are shown in Figure 2.

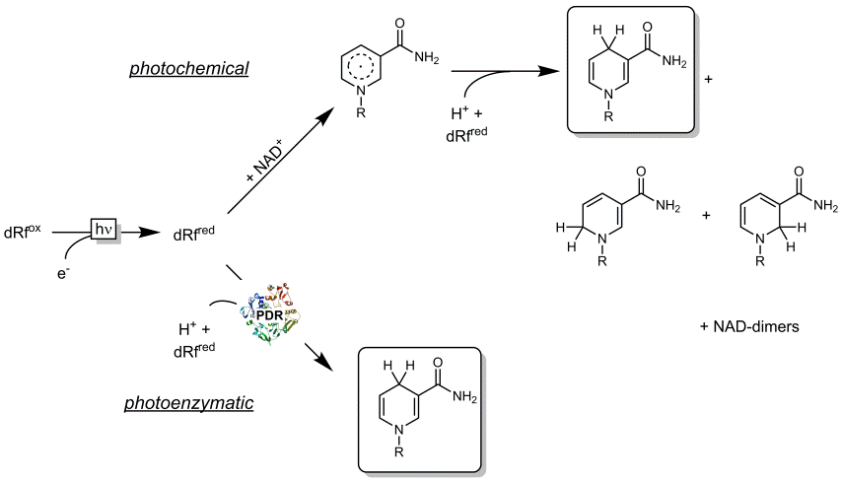

Scheme 2. Simplified representation of the two reactions competing for the photochemically formed, reduced deazariboflavin (dRfred). dRfred undergoes direct electron transfer to NAD^+ (photochemical reaction). The resulting NAD radical can either be protonated and reduced a second time leading to all NAD isomers possible or it can dimerise (for reasons of clarity, the different NAD dimers are not shown). Alternatively, dRfred reduces PDR (as two successive single electron transfer reactions), which in its reduced form exclusively yields enzyme-active 1,4-NADH.

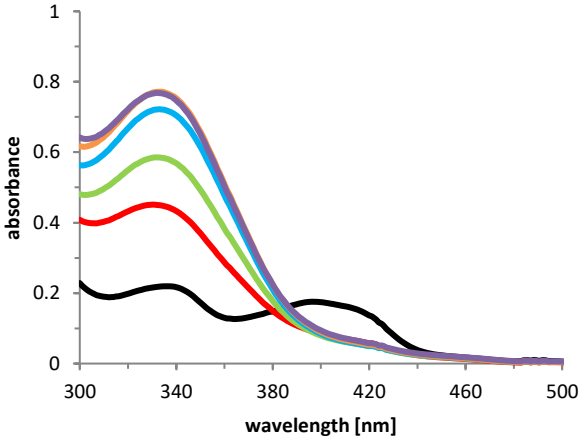

Figure 2. Exemplary UV/Vis traces of the photochemical and photoenzymatic reduction of NAD^+. Black 0 h; red 0.5 h; green 1 h; blue 2 h; orange 3 h; violet 4 h; General conditions: 50 mM Tris-HCl buffer (pH 8); [NAD^+] = 2 mM; [EDTA] = 20 mM; [dRf] = 60 µM; [PDR] = 3.8 µM; [ethyl acetoacetate] = 10 mM; T = 30 °C; λ = 450 nm; semi-anaerobic.

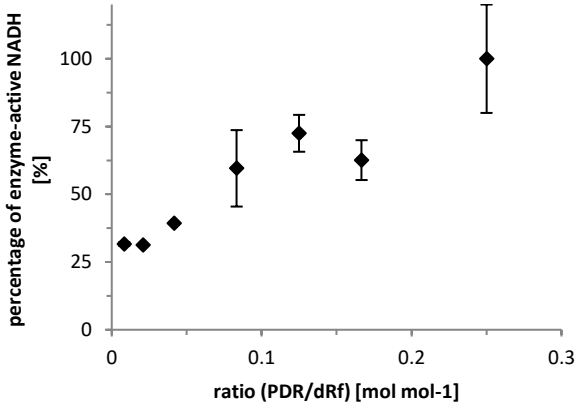

Figure 3. Influence of the ratio dRf to PDR on the selectivity of the photoenzymatic reduction of NAD^+. General conditions: the experiments were performed in a two-step, two-pot manner, that is, in a first step, the photoenzymatic reduction of NAD^+ was conducted at varying concentrations of dRf and PDR. 50 mM Tris-HCl buffer (pH 8); [NAD^+] = 2 mM; [EDTA] = 20 mM; [ethyl acetoacetate] = 10 mM; T = 30 °C; λ= 450 nm; semi-anaerobic. After 0.5-2.5 h the reactions were stopped, the apparent NADH concentration was determined spectrophotometrically (λ = 340 nm) and the mixtures were supplemented with ADH-A (0.143 µM final), incubated for 15 min and analysed by gas chromatography.

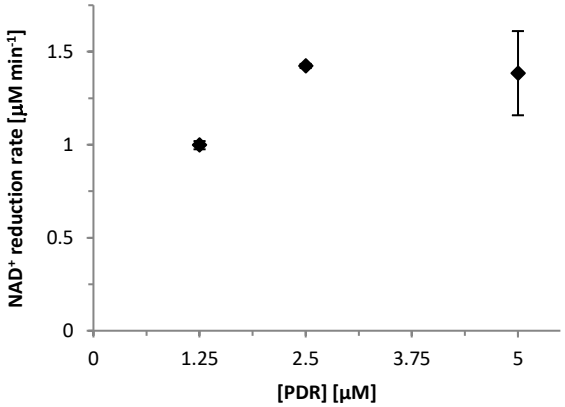

Figure 4. Influence of the PDR concentration on the NAD^+ reduction rate. General conditions: 50 mM Tris-HCl buffer (pH 8); [NAD^+] = 0.4 mM; [EDTA] = 10 mM; [dRf] = 5 µM; T = 25 °C; λ = 450 nm; anaerobic.

Nevertheless, at higher PDR concentrations, almost exclusive regioselectivity (i.e., fully enzyme-active NADH) was observed. Further characterisation of the photoenzymatic NAD^+ reduction system revealed that the overall rate (i.e., the rate

of NADH formation) was largely independent of the PDR concentration applied (Figure 4). The photocatalyst concentration, however, directly influenced the rate of the overall NADH generation reaction (Figure 5, □) and the rate of the PDR reduction (Figure 5, ◆). Comparing both concentration dependencies, it becomes obvious that both were linearly dependent on the photocatalyst (dRf) concentration. The reduction of PDR was roughly two times faster than the overall NAD^+ reduction, which suggested that the hydride transfer rate from PDR–$FADH_2$ to NAD^+ was overall rate limiting. This is in line with the thermodynamically uphill character of this reaction.

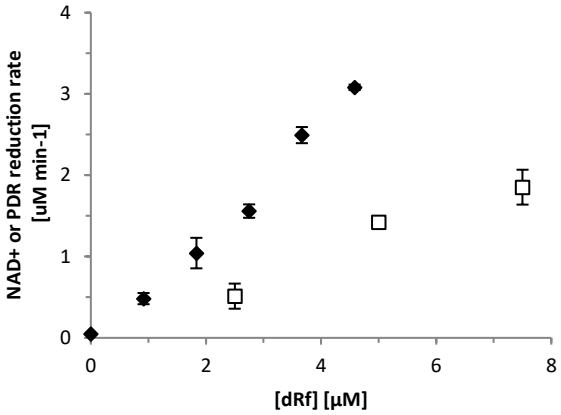

Figure 5. Rate-dependency of the photoenzymatic reduction of NAD^+ (□) and the PDR (◆) on the dRf concentration applied. General conditions: 50 mM Tris-HCl buffer (pH 8); [NAD^+] = 0.4 mM; [EDTA] = 10 mM; [PDR] = 2.5 µM (□) or 20 µM (◆); T = 25 °C; λ = 450 nm; anaerobic.

The reduction state of PDR (i.e., [PDR_{red}]/[PDR_{ox}]) is positively influenced by increasing *in situ* concentrations of dRf_{red}, which thereby also shifts the NAD^+/NADH equilibrium. This, however, may also come at the expense of an increased non-enzymatic reduction (i.e., non-selective reduction of NAD^+). To assess the principal feasibility of the proposed photoenzymatic NADH regeneration scheme, we directly applied it to promote the ADH-A-catalysed reduction of ethyl acetoacetate in a one-pot, one-step reaction (Figure 6).

Pleasingly, enantioselective reduction was feasible and multiple turnovers for the nicotinamide cofactor were observed. Similar to the previous observation, a significant difference was observed between experiments performed under semi-anaerobic conditions (Figure 6, ▲ and △) and under strictly anaerobic conditions (i.e., in a glove box) (Figure 6, ■ and □).

In the first case, product formation again ceased after approximately 5 h, whereas in the latter case, more robust product accumulation for at least 24 h was observed. The apparent small decrease in the product concentration is most likely due to hydrolysis of the ethyl ester product, which could not be determined with the gas chromatography (GC) method used. In the past, methyl viologen (MV^{2+}) has been used as a mediator for the ferredoxin-$NADP^+$-reductase-catalysed regeneration of NADPH.[7, 12]

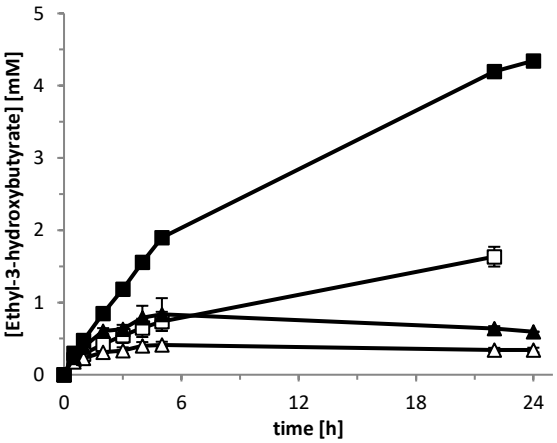

Figure 6. Photoenzymatic reduction of ethyl acetoacetate to (*S*)-ethyl-3-hydroxybutyrate using the plain regeneration system (Scheme 1, white-filled symbols) and in the presence of methyl viologen as co-catalyst (black symbols). Experiments were conducted under strictly anaerobic conditions (glove box, squares) or under semi-anaerobic reaction conditions (N_2 atmosphere, triangles). General conditions: 50 mM Tris-HCl buffer (pH 8); [EDTA] = 20 mM; [dRf] = 60 μM; [NAD^+] = 0.2 mM; [PDR] = 5 μM; [ADH-A] = 0.115 μM; [ethyl acetoacetate] = 10 mM; T = 25 °C; λ = 450 nm; anaerobic; [MV^{2+}] = 0 (□,△) or 0.25 mM (■,▲).

We therefore also evaluated MV^{2+} in our reaction system (Figure 6, ■ and ▲). Notably, upon using MV^{2+}, all catalytic components were also necessary to achieve reduction of ethyl acetoacetate. Performing the photoenzymatic reduction of ethyl

acetoacetate in the presence of 0.25 mm MV^{2+} increased the product formation rate approximately three- to fourfold. Most probably, MV^{2+} served as a co-catalyst for the reduction of PDR and thereby favourably shifted its reduction state and shifted the NADH/NAD^+ ratio. Unfortunately, spectrophotometric investigation of this hypothesis was not straightforward owing to the overlapping absorption spectra of PDR and MV^{2+}. Qualitatively, however, we observed electron transfer from dRf_{red} to MV^{2+} (Figure 7).

Figure 7. **Methyl viologen before (left) and after photocatalytic reduction (right).** General conditions: 50 mM Tris-HCl buffer (pH 8); [EDTA] = 10 mM; [dRf] = 20 μM; [MV] = 20 μM; T = 25 °C; λ = 450 nm; anaerobic.

The accelerating effect of MV^{2+} was also observed during our preliminary exploration of the substrate scope of the photoenzymatic reduction system (Table 1). Pleasingly, the stereochemical outcome of the ADH-A-catalysed ketoreduction reaction was not impaired by the artificial regeneration system. This also excludes any direct reduction of the carbonyl starting materials by any other reactant. Up to 72, 21, 17, 868, and 37700 turnovers were determined for dRf, NAD^+, MV^{2+}, PDR, and ADH-A, respectively.

Admittedly, relative to the productivity of the stoichiometric use of NADH, that of the current system falls back significantly. It should be kept in mind that no efforts for optimising the photoenzymatic reaction system have so far been undertaken. Especially, the robustness of the PDR under the current reaction conditions needs to be improved, as it was inactivated upon illumination with blue light (Figures 8 and 9). Most probably, the photoexcited enzyme-bound flavin cofactor is prone to photodegradation.[24]

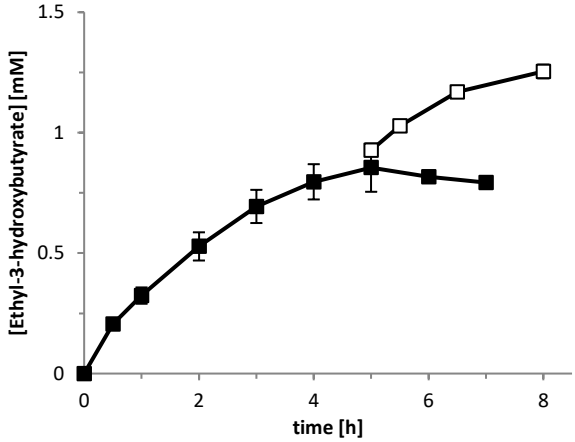

Figure 8. PDR spiking experiment. General conditions: 50 mM Tris-HCl buffer (pH 8), [EDTA] = 20 mM, [dRf] = 60 μM, [NAD^+] = 0.2 mM; [PDR] = 5 μM (◆) and 5 μM re-added after 5 h (□); [ADH-A] = 0.115 μM; [ethyl acetoacetate] = 10 mM; T = 30 °C ; λ = 450 nm; semi-anaerobic.

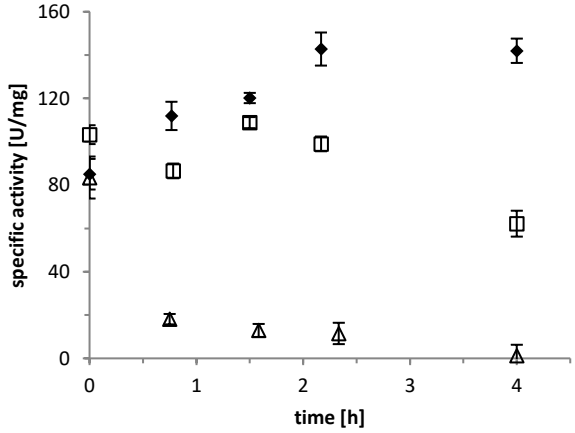

Figure 9. PDR stability in dark and illuminated. General conditions: 5 μM PdR in 50 mM Tris-HCl buffer (pH 8.0); T = 30 °C; λ = 450 nm; semi-anaerobic dark (◆); illuminated (□); [EDTA] = 20 mM; [dRf] = 200 μM; illuminated (△).

Hence, changing the photoexcitation wavelength appears to be of utmost importance to achieve robust photoenzymatic reaction schemes. Very promising preliminary results were obtained by changing the photocatalyst from dRf to safranin O

(photoexcitation at λ= 519 nm, Figure 10), and continuous product formation for at least 5 days was shown.

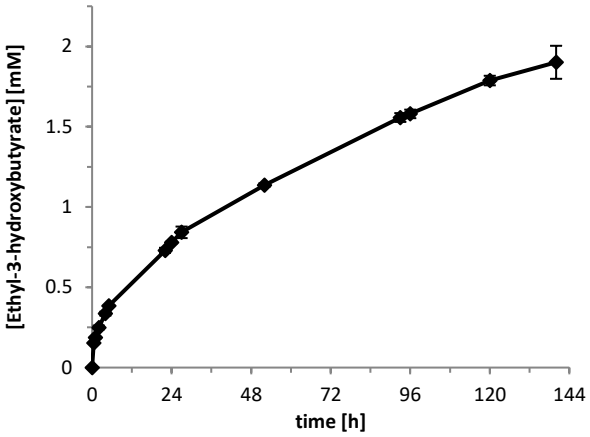

Figure 10. Preliminary green light-driven NADH regeneration system. General conditions: 50 mM MOPS buffer (pH 8); [safranin O] = 50 μM; [MV^{2+}] = 1.25 mM; [NAD+] = 0.2 mM; [MeFDH] = 5 μM; [ADH-A] = 0.115 μM; [ethyl acetoacetate] = 10 mM; T = 25 °C; λ = 514 nm; anaerobic.

Table 1. Photoenzymatic reduction of various ketones. [a]

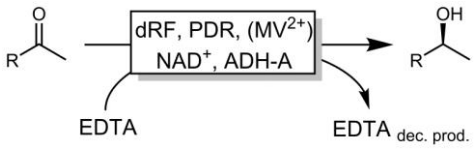

Product	c [mM] without MV^{2+}	*ee* [%]	c [mM] with MV^{2+}	*ee* [%]	c [mM] control[b]
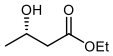	0.86 ± 0.09	99	3.11 ± 0.07	99	8.47
	0.41 ± 0.01	99	1.6 ± 0.07	99	4.18
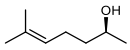	0.21 ± 0.06	95	0.58 ± 0.15	96	2.86
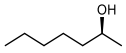	0.22 ± 0.05	99	0.65 ± 0.05	99	1.91

[a] general conditions: 50 mM Tris-HCl buffer (pH 8); [EDTA] = 20 mM; [dRf] = 60 μM; [NAD^+] = 0.2 mM; [PDR] = 5 μM; [ADH-A] = 0.115 μM; [ethyl acetoacetate] = 10 mM; T = 30 °C; t = 5 h; λ = 450 nm; anaerobic; [MV^{2+}] = 0 or 0.25 mM;
[b] using NADH (10 mM) as stoichiometric reductant.

Conclusion

Overall, with this contribution, we demonstrated that photoenzymatic regeneration of NADH was feasible by using the PDR from *Pseudomonas putida*. Potential pitfalls such as the undesired direct reduction of NAD^+ (leading to enzyme-inactive NAD isomers) and the photodegradation of the flavin prosthetic group were identified together with some promising solutions. The next steps will concentrate at further optimising the reaction setup to improve the NADH regeneration rate and therewith the practical feasibility of the approach.

Material and methods

Materials

Chemicals were purchased from Sigma-Aldrich, Fluka, Acros or Alfa-Aesar with the highest purity available and used as received.

Preparation of the biocatalysts

Putidaredoxin reductase (PDR)

Bacterial strains and plasmids

The plasmid pETM6 containing the gene encoding putidaredoxin reductase (PDR) was transformed into *E. coli* C43(DE3) by electroporation method using 40 µL competent cells and approximately 100 ng plasmid (1.6 kV; 200 Ω; 25 µF). Transformed cells were grown for 1 h at 37 °C in LB without antibiotics. 100 µL were plated out on a LB plate containing ampicillin and incubated overnight at 37 °C. A colony was picked and a pre-culture was grown over night at 37 °C. Glycerol stocks C43(DE3)-PDR containing 15% glycerol were prepared from the pre-culture.

Cultivation conditions

LB (Lysogeny broth) supplied with the appropriate antibiotic (ampicillin) was inoculated with 1%(v/v) of *E. coli* C43(DE3)-PDR (glycerol stock). Cells were grown for 3 h at 37 °C and subsequently induced with 0.2 mM isopropyl-β-D-thiogalactopyranoside (IPTG). After induction cultivation was continued for 24 h at 25 °C. Cells were harvested by centrifugation at 10000 × *g* for 10 min at 4 °C.

PDR purification

Bacteria were resuspended in 100 mL buffer (50 mM phosphate pH 7.4), supplemented with lysozyme (2mg/mL) and DNAseI. After 0.5 hour of incubation, cells were sonicated and debris was removed by centrifugation at 10000 × *g* for 0.5 hours. PDR was purified in one single step using a HPLC system. The separation was performed on a Q Sepharose FF 30-mL cartridge at a flow rate of 5 mL min^{-1}. After 90 mL, the retained proteins were eluted with a 0–25% NaCl gradient in 150 mL and 100% NaCl in 90 mL. The appropriate fractions were pooled, concentrated and dialysed against 50 mM phosphate (pH 7.4). The purification of the PDR was confirmed by sodium dodecyl sulfate (SDS)–PAGE in 12% gels stained with Coomassie brilliant blue R-250 (Sigma). The protein quantification was based on the absorbance at 378 nm (ε_{378}: 9.7 $mM^{-1}cm^{-1}$), 454 nm (ε_{454}: 10.0 $mM^{-1}cm^{-1}$) and 480 nm (ε_{480}: 8.5 $mM^{-1}cm^{-1}$).

PDR activity

Activity was measured with the 2,6-dichlorophenol-indophenol (DCIP) assay. The decrease of absorbance at 600 nm (ε_{600}= 21.0 mM^{-1} cm^{-1}) was followed and the initial linear change in absorption was used to calculate the activity. The assay was performed in 50 mM Tris-HCl buffer (pH 8) at 25 °C with the final concentration of 0.097 mM DCIP, 0.8 mM NADH and 0.01 µM PDR in 1 mL plastic cuvettes.

Alcohol dehydrogenase (ADH-A)

Bacterial strains and plasmids

The expression construct, pET15b-ADH-A, was transformed into chemically competent *E. coli* BL21(DE3). 50 µL competent cells and approximately 100 ng plasmid used. Transformed cells were grown for 1 h at 37 °C in LB without antibiotics. 100 µL were plated out on a LB plate containing ampicillin and incubated overnight at 37 °C. A colony was picked and a pre-culture was grown over night at 37 °C. Glycerol stocks *E. coli* BL21(DE3)-ADH-A containing 15% glycerol were prepared from the pre-culture.

Cultivation conditions

Expression was carried out in 2x YT media (1.6% (w/v) tryptone, 1.0% (w/v) yeast extract, 0.5% (w/v) NaCl) containing 50 µg/mL ampicillin, cells were incubated at 30 °C until an OD_{600} of 0.4 was reached. Expressions of the ADH-A was induced by addition of 1 mM IPTG. The culture was incubated for additional 5 h at 30 °C. Cells were harvested by centrifugation at 10000 × *g* for 10 min at 4°C.

ADH-A purification

Bacteria were resuspended in 20 mL Binding Buffer (20 mM sodium phosphate, 20 mM imidazole, 500 mM NaCl, 0.02% sodium azide, pH 7.5) fortified with protease inhibitors, lysozyme (2mg/mL) and DNaseI. Cells were lysed using a Cell disruptor and debris was removed by centrifugation at 30000 × *g* for 1 h at 4 °C. Protein was purified using a Ni^{2+} column, being eluted in the presence of 20 mM sodium phosphate, 500 mM imidazole, 500 mM NaCl, 0.02% sodium azide, pH 7.5.

ADH-A activity

The consumption of NADH was followed at 340 nm (ε_{340}= 6.22 mM^{-1} cm^{-1}) and the initial linear change in absorption was used to calculate the activity. The assay was performed in 50 mM Tris-HCl buffer (pH 8) at 25 °C with the final concentration of 5 mM ethyl acetoacetate, 0.2 mM NADH and 0.03 µM ADH-A in 1 mL plastic cuvettes.

Synthesis of deazariboflavin (dRf)

The synthesis of 5-deazariboflavin was carried out following and adapting the procedure established by Voss Jr. and co-workers.[25]

*Synthesis of 3,4-dimethyl-N-D-ribitylaniline (**2**):*

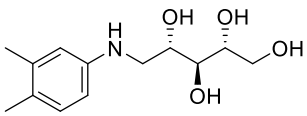

3,4-Dimethylaniline **1** (3.14 g, 26 mmol) was dissolved in anhydrous methanol (150 mL), sodium cyanoborohydride ($NaCNBH_3$) (3.11 g, 2 equiv.), followed by addition of D-ribose (11.2 g, 74.3 mmol) under stirring. The reaction mixture was further stirred under reflux for 48 h. The solvent was removed under reduced pressure, the residue was re-dissolved in 1 M HCl (50 mL), swirled until gas evolution caused. The solution was carefully neutralised with a saturated solution of sodium bicarbonate, extracted with ethyl acetate (6 × 50 mL), washed with brine, dried with $MgSO_4$, and the solvent was removed under reduced pressure. Recrystallization of the solid product from absolute ethanol gave *N*-ribitylaniline as a white crystalline solid. (6.17 g, 97%)

^{1}H NMR (400 MHz, MeOH-d_4) δ 6.88 (d, *J* = 8.1 Hz, 1H, H-3), 6.55 (d, *J* = 2.4 Hz, 1H, H-6), 6.47 (dd, *J* = 8.1, 2.5 Hz, 1H, H-4), 3.91 (ddd, *J* = 7.8, 6.2, 3.5 Hz, 1H, H-13), 3.81 – 3.71 (m, 2H, H-12, 14”), 3.68 – 3.59 (m, 2H, H-11, 14’), 3.43 (dd, *J* = 12.8, 3.5 Hz, 1H, H-10”), 3.09 (dd, *J* = 12.8, 7.9 Hz, 1H, H-10’), 2.17 (s, 3H, H-8), 2.12 (s, 3H, H-9). ^{13}C NMR (100 MHz, MeOH-d_4) 148.1 (C-5), 137.9 (C-1), 131.1 (C-3), 126.7 (C-2), 116.7 (C-6), 112.5 (C-4), 74.9 (C-11), 74.4 (C-12), 72.1 (C-13), 64.6 (C-14), 48.1 (C-10), 20.1 (C-8), 18.8 (C-9)

Synthesis of 2,4,6-trichloropyrimidine-5-carbaldehyde (3):

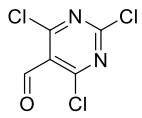

Anhydrous *N*,*N*-dimethylformamide (DMF) (5 mL, 65 mmol) was added dropwise to the stirred solution of barbituric acid (8.45 g, 66 mmol) in phosphorus oxychloride ($POCl_3$) (40 mL, 429 mmol) at 0 °C for 1 h. The reaction mixture was followed by reflux for 16 h at 130 °C. The solvent was removed under reduced pressure, the thick residue was poured into ice-water and stirred to form a solid product, the crude product was collected by filtration and

purified by flash chromatography with an eluent (hexane:ethyl acetate, 9:1) to provide a white solid (9.7 g, 70%).

^{1}H NMR (400 MHz, DMSO-d_6): δ 10.39 (s, 1H).

*Synthesis of 6-chloro-2,4-dioxo-1,2,3,4-tetrahydropyrimidine-5-carbaldehyde (**4**):*

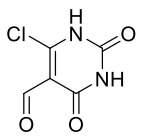

A mixture of 2,4,6-trichloropyrimidine-5-carbaldehyde **3** (1 g, 4.73 mmol) and K_2CO_3 (0.650 g, 4.73 mmol) were added to 40 mL of ethanol:water mixture (2:1) and the solution was stirred for 4 h at room temperature. The reaction mixture was neutralized with acetic acid (4-5 drops), concentrated to 10 mL by rotary evaporation and kept at 4 °C for 2 days. The compound was isolated as a white solid by filtration (0.760 g, 91%).

^{1}H NMR (400 MHz, DMSO-d_6): δ 10.03 (s, 1H).

Synthesis of 5-deazariboflavin:

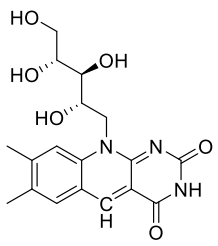

A mixture of 3,4-dimethyl-*N*-D-ribitylaniline **2** (1.02 g, 2.9 mmol) and 6-chloro-2,4-dioxopyrimidine-5-carbaldehyde **4** (0.31 g, 1.8 mmol) were mixed in 10 mL of anhydrous DMF. The reaction mixture was stirred under reflux at 130 °C for 3 h and then cooled to room temperature. Diethyl ether (20 mL) was added with stirring for 1 h and the reaction mixture was kept in the freezer overnight. The compound was collected by filtration and recrystallized from water to form a yellow solid powder (457 mg, 70%).

^{1}H NMR (400 MHz, DMSO-d_6) δ 11.04 (s, 1H), 8.85 (s, 1H), 7.94 (s, 1H), 7.87 (s, 1H), 5.15 (d, J = 5.0 Hz, 1H), 4.99 (s, 1H), 4.90 (d, J = 4.6 Hz, 1H), 4.82 (d, J = 6.2 Hz, 1H), 4.66 (d, J = 14.1 Hz, 1H), 4.50 (t, J = 5.6 Hz, 1H), 4.23 (s, 1H), 3.69- 3.59 (m, 3H), 3.47 (m, J = 6.1 Hz, 2H), 2.46 (s, 3H), 2.34 (s, 3H). ^{13}C NMR (100 MHz, DMSO-d_6) δ 162.6, 141.5, 131.0, 118.3, 74.1, 73.4, 70.0, 63.9, 40.6, 40.4, 40.2, 39.9, 39.7, 39.5, 39.3, 21.4, 19.1.

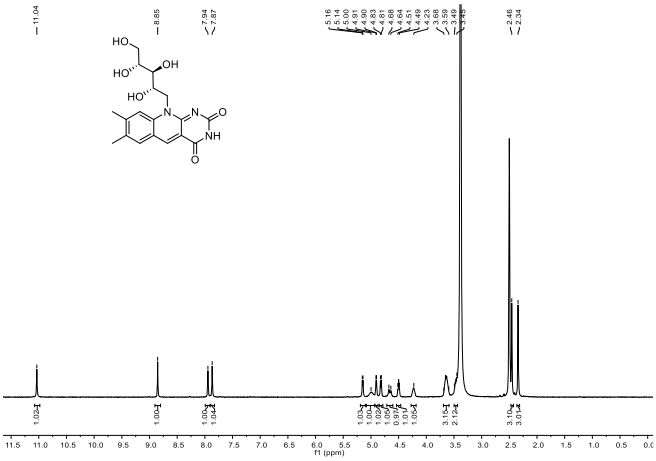

^{1}H NMR spectrum of 5-deazariboflavin.

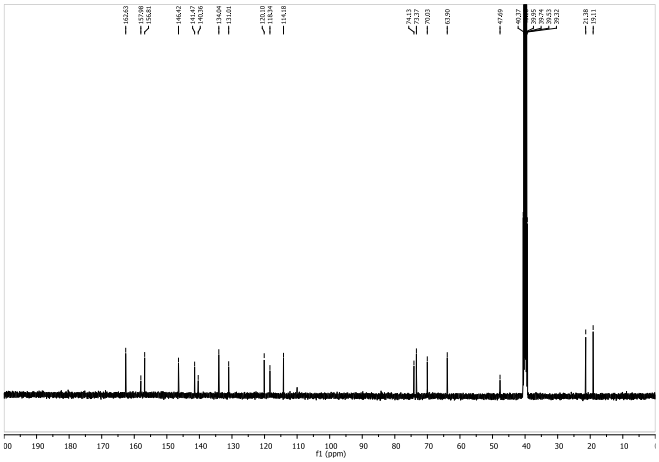

^{13}C NMR spectrum of 5-deazariboflavin.

General procedures

Light-driven NADH recycling

was performed in 25 mL glass reaction tubes containing 5 mL reaction mixture. The reactions were illuminated from all sides by a blue LED light source at a distance of 2 cm. The emission wavelength ranges from 420-500 nm with the maximum intensity

at ~450 nm. The intensity was set to maximum. Reactions were gently stirred using Teflon coated magnetic bars. Temperature was maintained at 30 °C using a jacketed beaker and a thermostat. Anaerobic atmosphere was achieved by bubbling solutions with N_2 for 30 min. Subsequently, the atmosphere was maintained by a N_2 filled balloon *via* needle and septum. Standard reaction conditions for the light-driven regeneration of NADH were 60 µM dRf, 20 mM EDTA, 1-5 µM PDR, and 2 mM NAD^+ in 50 mM Tris-HCl buffer at pH 8.0.

PDR characterisation experiments
were performed in an anaerobic chamber (on average 98% N_2, 2% H_2) with oxygen levels below ppm levels. Reactions were conducted in 1.5 mL glass vials with 1 mL total volume. The reactions were illuminated from all sides by a LED light source at a distance of 10 cm and gently stirred using Teflon coated magnetic bars.

Two pot ketoreductions
were performed to investigate the enzymatic activity of the formed NADH. To do this, the light-driven NADH formation in the first pot was coupled to a subsequent second pot reaction, fuelling the alcohol dehydrogenase ADH-A from *Rhodococcus ruber* DSM 44541 with the formed NADH. To assess the ratio of enzymatically active NADH formed, 400 µL of sample were taken from the first pot. Using 200 µL of the sample the NADH concentration was determined via UV. Additionally, 200 µL of the sample were incubated with 2 µL ADH-A for 15 min to perform the ketoreduction. Product (ethyl 3-hydroxybutyrate) and substrate (ethyl acetoacetate) concentrations of the ADH-A catalysed ketoreduction were determined using gas chromatography.

Simultaneous ketoreduction
was performed in the same manner as the light-driven NADH recycling described above, with the addition of 0.6 U of ADH-A and 10 mM of the appropriate substrate. Reaction time for the substrate comparison reactions was 5 h. Product and substrate concentrations of the ADH-A catalysed ketoreduction were determined using gas chromatography.

Analytical procedures

UV/Vis spectroscopy

For the light-driven NADH recycling experiments 200 µL of sample were diluted 1:5 and the absorbance at 340 nm (ε_{340}= 6.22 mM^{-1} cm^{-1}) was followed to determine the concentration of NADH over time. UV/Vis spectra were recorded using Cary 60 UV-Vis spectrophotometer (equipped with a single cell Peltier accessory) from Agilent technologies.

For PDR characterisation UV/Vis spectra were recorded directly in the reaction vessel using an Avantes DH-2000 UV-VIS-NIR light source and an Avispec 3648 spectrophotometer. PDR reduction was followed at 480 nm to avoid overlap with dRf (ε_{480} = 8.5 mM^{-1} cm^{-1}).[26]

GC-analyses

Samples of 0.2 mL reaction mixture were extracted twice with 0.1 mL ethyl acetate. As internal standard 5 mM dodecane was used, except for analysis of heptanone / heptanol, acetophenone / 1-phenylethanol where 5 mM 1-octanol were applied as internal standard. Analysis were performed with Shimadzu GC-2010 plus gas chromatograph with an AOC-20i Auto injector (injection temperature 250 °C) and flame ionization detection (FID). The carrier gas of the achiral GC was nitrogen with a flow of 31.5 cm × s^{-1}. The chiral GC carrier gas was helium with a flow of 38 cm × s^{-1}.

Table 2. GC analysis specifications for concentration determination

Compounds (retention time)	GC column	GC oven programme
Ethyl acetoacetate (16.8 min)/ ethyl 3-hydroxybutyrate (19.0 min)	CP-wax 52 CB (25 m × 0.25 mm × 1.2 µm)	90 °C for 5 min 5 °C/min to 101 °C hold for 1 min 5 °C/min to 135°C hold for 3 min 10 °C/min to 145 °C hold for 1 min 30 °C/min to 250 °C hold for 1 min.
Heptanone (2.8 min) / heptanol (3.3 min); acetophenone (6.3 min) / 1-phenylethanol (7.5 min); 6-methyl-5-hepten-2-one (3.6 min) / 6-methyl-5-hepten-2-ol (4.2 min)	CP-wax 52 CB (25 m × 0.25 mm × 1.2 µm)	150 °C for 2.2 min 25 °C/min to 210 °C hold for 4.2 min 25 °C/min to 250 °C hold for 1 min.

Table 3. Chiral GC analysis for enantiomeric excess (*ee*)

Compounds (retention time)	GC column	GC oven programme
6-Methyl-5-hepten-2-ol (22.5 min)	CP-Chirasil-Dex CB (25 m × 0.32 mm × 0.25 µm)	50 °C for 5 min 4 °C/min to 90 °C hold for 12 min 20 °C/min to 225 °C hold for 1 min.
2-Phenylethanol (6.3 min)	CP-Chirasil-Dex CB (25 m × 0.32 mm × 0.25 µm)	120 °C for 2.6 min 15 °C/min to 135 °C hold for 3.3 min 25 °C/min to 225 °C hold for 1 min.
Ethyl 3-hydroxybutyrate (13.0 min)	CP-Chirasil-Dex CB (25 m × 0.32 mm × 0.25 µm)	85 °C for 5 min 2 °C/min to 95 °C hold for 5 min 25 °C/min to 115 °C hold for 2 min 25 °C/min to 225 °C hold for 2 min.
Heptanol (14.0 min)	LIPODEX E (50 m × 0.25 m × 0.25 µm)	60 °C for 7 min 4 °C/min to 80 °C 10 °C/min to 160 °C 20 °C/min to 220 °C hold for 1.00 min.

References

[1] U. T. Bornscheuer, G. W. Huisman, R. J. Kazlauskas, S. Lutz, J. C. Moore, K. Robins, *Nature* **2012**, *485*, 185-194.
[2] G. W. Huisman, J. Liang, A. Krebber, *Curr. Opin. Chem. Biol.* **2010**, *14*, 122-129.
[3] W. Kroutil, H. Mang, K. Edegger, K. Faber, *Curr. Opin. Chem. Biol.* **2004**, *8*, 120-126.
[4] A. Weckbecker, H. Groger, W. Hummel, *Adv. Biochem. Eng. Biot.* **2010**, *120*, 195-242.
[5] R. Wichmann, D. Vasic-Racki, in *Technology Transfer in Biotechnology. Adv. Biochem. Engin./Biotechnol., Vol. 92* (Ed.: U. Kragl), Springer, Berlin, Heidelberg, **2005**, pp. 225-260.
[6] H. K. Chenault, G. M. Whitesides, *Appl. Biochem. Biotechnol.* **1987**, *14*, 147-197.
[7] D. Mandler, I. Willner, *J. Chem. Soc. Perk. T. 2* **1986**, 805-811.
[8] S. H. Lee, D. S. Choi, S. K. Kuk, C. B. Park, *Angew. Chem. Int. Edit.* **2018**, *57*, 7958-7985.
[9] E. Steckhan, *Top. Curr. Chem.* **1994**, *170*, 83-111.
[10] H. Asada, T. Itoh, Y. Kodera, A. Matsushima, M. Hiroto, H. Nishimura, Y. Inada, *Biotechnol. Bioeng.* **2001**, *76*, 86-90.
[11] K. A. Brown, M. B. Wilker, M. Boehm, H. Hamby, G. Dukovic, P. W. King, *ACS Catal.* **2016**, *6*, 2201-2204.
[12] J. J. Pueyo, C. Gomezmoreno, *Enzyme Microb. Technol.* **1992**, *14*, 8-12.
[13] L. Wan, C. F. Megarity, B. Siritanaratkul, F. A. Armstrong, *Chem. Commun.* **2018**, *54*, 972-975.
[14] I. F. Sevrioukova, T. L. Poulos, *J. Biol. Chem.* **2002**, *277*, 25831-25839.
[15] W. R. Frisell, C. W. Chung, C. G. Mackenzie, *J. Biol. Chem.* **1959**, *234*, 1297-1302.
[16] W. Y. Zhang, F. Hollmann, *Chem. Commun.* **2018**, *54*, 7281-7289.
[17] M. T. Stankovich, V. Massey, *Biochim. Biophys. Acta.* **1976**, *452*, 335-344.
[18] H. J. Duchstein, H. Fenner, P. Hemmerich, W. R. Knappe, *Eur. J. Biochem.* **1979**, *95*, 167-181.
[19] W. R. Knappe, P. Hemmerich, H. J. Duchstein, H. Fenner, V. Massey, *Biochemistry-Us* **1978**, *17*, 16-17.
[20] B. Kosjek, W. Stampfer, M. Pogorevc, W. Goessler, K. Faber, W. Kroutil, *Biotechnol. Bioeng.* **2004**, *86*, 55-62.
[21] W. Stampfer, B. Kosjek, K. Faber, W. Kroutil, *J. Org. Chem.* **2003**, *68*, 402-406.
[22] W. Stampfer, B. Kosjek, K. Faber, W. Kroutil, *Tetrahedron-Asymmetr.* **2003**, *14*, 275-280.
[23] W. Stampfer, B. Kosjek, W. Kroutil, K. Faber, *Biotechnol. Bioeng.* **2003**, *81*, 865-869.
[24] W. Holzer, J. Shirdel, P. Zirak, A. Penzkofer, P. Hegemann, R. Deutzmann, E. Hochmuth, *Chem. Phys.* **2005**, *308*, 69-78.
[25] M. S. Hossain, C. Q. Le, E. Joseph, T. Q. Nguyen, K. Johnson-Winters, F. W. Foss, *Org. Biomol. Chem.* **2015**, *13*, 5082-5085.
[26] I. C. Gunsalus, G. C. Wagner, *Method. Enzymol.* **1978**, *52*, 166-188.

Chapter 3

Chapter 3: Photocatalytic generation of H_2O_2 to fuel a haloperoxidase

Georg T. Höfler, Morten M. C. H. van Schie, Florian Tieves, Ron Wever, Caroline E. Paul, Isabel W.C.E. Arends, Frank Hollmann

Summary

The photocatalytic generation of hydrogen peroxide to fuel a haloperoxidase was established. One of the main issues when combining photocatalysis with biocatalysis is the enzyme stability. Even application of an extraordinarily stable enzyme such as the thermostable vanadium-dependent chloroperoxidase from *Curvularia inaequalis* (*Ci*VCPO) could not prevent this setback.

To envision a robust system, the separation of photocatalysis from biocatalysis was investigated. As a heterogeneous photocatalyst, graphitic carbon nitride was chosen to allow the separation from the biocatalytic part of the reaction. The photocatalytic formation of hydrogen peroxide was successful using atom efficient sacrificial electron donors, water or formate. The increased hydrogen peroxide formation rate applying formate made it the better choice as electron donor.

Enzyme inactivation and side product formation were successfully circumvented by physical separation of the photocatalyst and biocatalytic reaction. The separation leads to a stable reaction forming solely desired product. In theory, the components are stable enough to perform over an extended period of time, currently the reaction setup is limited by clogging of the filter caused by the small particle size of the g-C_3N_4-25K. In summary, the physical separation of the photocatalyst from the biocatalyst is a promising approach to combine photocatalysis with biocatalysis. Nevertheless, currently the issues in process design and low conversion of hydrogen

peroxide to actual product formation limit this system to non-continuous performance with low concentrations.

Introduction

The halofunctionalisation of aromatic compounds is among the most important reactions in organic chemistry. Introducing halogen atoms in organic compounds influences the biological activity strongly.[1] For instance, chlorothymol has 75 times higher bactericidal potency, while also possessing low human toxicity, compared to thymol.[2] Overall, the pharmaceutical importance of organohalides is undeniable. Furthermore, chlorohydrins are important intermediates in the production of epoxides, which are representing one of the most important compounds in industry.[3] These compounds can be formed by an attack of hypohalites at C=C double bonds or aromatic compounds *via* a halonium ion intermediate. The hypohalite can be efficiently supplied by an enzyme, the vanadium-dependent chloroperoxidase from *Curvularia inaequalis* (*Ci*VCPO).[4] *Ci*VCPO excels by its outstanding activity and stability and is easily produced via heterologous fermentation in *Escherichia coli*. Therefore, this biocatalyst is a good candidate for the replacement of metal catalysts, such as Cu^{II}, commonly used in organic chemistry. These metal catalysts require high catalyst loading compared to chloroperoxidases and often harsher reaction conditions.[2, 5] Although one drawback is the dependence on stoichiometric amounts of H_2O_2 as oxidant.

Nowadays, hydrogen peroxide is produced on an industrial scale by the anthraquinone process. This multistep process requires significant energy input and generates waste, which has a negative effect on its sustainability and production costs.[6] Therefore, alternative ways of forming H_2O_2 are currently investigated, for instance by use of photocatalysis. Recently, the direct combination of biocatalysis and photocatalysis gained increasing interest in the field. The idea is to provide a cost-efficient source of redox equivalents for oxidoreductases compared to their native redox cofactors.

As one of the less complex examples we decided to study the class of peroxidases dependent on the rather simple cosubstrate hydrogen peroxide. The *in situ* formation of H_2O_2 is normally additionally beneficial due to prevention of the suicide inactivation of peroxidases. Due to the outstanding stability of *Ci*VCPO, the primary advantage of *in situ* formation is the minimisation of the oxidation of H_2O_2 by hypohalites, which is considered an undesired electron shunt reaction forming reactive oxygen species like singlet oxygen.[7-8] Herein we propose a light-driven *in situ* formation of H_2O_2 to fuel the *Ci*VCPO applying graphitic carbon nitride doped with potassium (g-C_3N_4-25K) as photocatalyst (Scheme 1). This catalyst efficiently produces H_2O_2, with selective promotion of two-electron reduction of O_2 and suppression of subsequent photodecomposition of the formed H_2O_2. Furthermore, in comparison to the well-known TiO_2 photocatalysts, g-C_3N_4 is more selective and less prone to photodegradation of H_2O_2 induced by UV light due to excitation in the visible light range.[9] The performance of the light-driven system is investigated by the chemoenzymatic bromolactonisation of a γ,δ-unsaturated carboxylic acid, here 4-pentenoic acid (Scheme 1). We provide insight in the performance, limitations and potential of this combination.

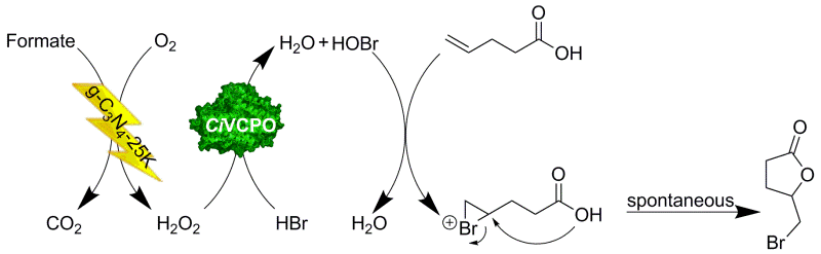

Scheme 1. Photocatalytic generation of H_2O_2 to fuel a haloperoxidase.

Results and Discussion

To demonstrate that *Ci*VCPO reactions can be fuelled by photochemical H_2O_2 generation, we used two model reactions: the chemoenzymatic bromolactonisation of 4-pentenoic acid and the bromination of 4-styrenesulfonate.

H_2O_2 was supplied by the photocatalytic two-electron reduction of O_2 catalysed by g-C_3N_4-25K. This heterogeneous photocatalyst was studied previously investigating different sacrificial electron donors such as water and formate. All studied electron donors are accepted, but use of formate (206 vs 58 µM h^{-1}) as sacrificial electron donor showed the highest formation rate, while having little negative influence on enzyme performance.[10]

In a first set of experiments we validated the g-C_3N_4-25K-catalysed photochemical H_2O_2 generation using formate as sacrificial electron donor (Figure 1).

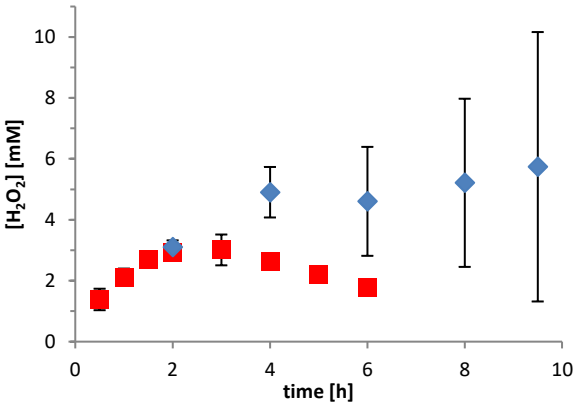

Figure 1. Photochemical hydrogen peroxide formation using g-C_3N_4-25K as photocatalyst in acetate and citrate buffer. General conditions: ■ 200 mM acetate buffer (pH 5); ◆ 200 mM citrate buffer (pH 5); reactions were performed in buffer visible light illumination (λ > 400 nm), T = 25 °C; [formate] = 250 mM; [g-C_3N_4-25K] = 5 mg/mL.

Interestingly, while performing these reactions in acetate buffer, the H_2O_2 concentration culminated after 2 to 3 h, but remained relatively stable in the case of citrate buffer. Possibly, citrate protected H_2O_2 from further oxidation by the photocatalyst through complexation.[11] It is also interesting to note that upon prolonged reaction times very high deviations between individual experiments were observed. Possibly, this may be due to issues in the aeration of the reaction samples due to limited air supply in the experimental setup. The dissolved oxygen in solution

may be insufficient and the supply of aerial oxygen is limited since the experimental setup is mainly a closed system. For all further experiments we used citrate buffer-based reaction media.

In the next step, we added the biocatalyst (*Ci*VCPO) together with the model substrate (4-pentenoic acid) to the reaction medium in order to attain a one-pot-one-step reaction system (Figure 2). Surprisingly, the product formation fell significantly behind our expectations and only about 0.15 mM of the desired product were formed. Furthermore, the formation of product seemed to slow down considerably after 5 h of reaction time. Finally, very much to our disappointment, hardly any difference was found when compared with the negative control (i.e. the reaction performed in the absence of the biocatalyst), giving almost identical product concentrations.

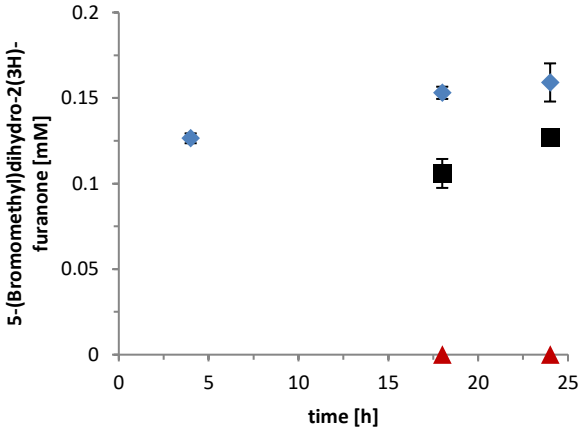

Figure 2. Bromolactone formation with direct light illumination. General conditions: ■ without *Ci*VCPO; ◆ all components; ▲ without KBr and without *Ci*VCPO; reactions were performed in 200 mM citrate buffer (pH 5); visible light illumination (λ > 400 nm); [formate] = 250 mM; [g-C_3N_4-25K] = 5 mg/mL; [KBr] = 40 mM; [*Ci*VCPO] = 180 nM; [4-pentenoic acid] = 10 mM; *T* = 25 °C.

Since the photocatalytic generation of hydrogen peroxide reached concentrations as high as 5 mM, an insufficient supply of hydrogen peroxide can be excluded as the reason for the low product formation. We suspected a poor stability of *Ci*VCPO under the reaction conditions and set out to investigate the inactivation of *Ci*VCPO in more

detail. Therefore, the residual activity of *Ci*VCPO in the presence and absence of g-C_3N_4-25K and under illumination and in the darkness was investigated (Figure 3).

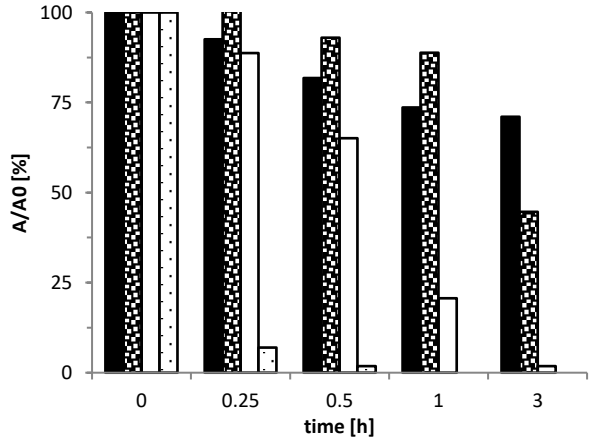

Figure 3. Influence of illumination and g-C_3N_4-25K on the activity of CiVCPO. ■ CiVCPO dark; ▩ g-C_3N_4-25K-CiVCPO dark; □ CiVCPO illuminated; ☐ g-C_3N_4-25K-CiVCPO illuminated; General conditions: incubations were performed in 200 mM citrate buffer (pH 5); visible light illumination (λ > 400 nm); [CiVCPO] = 180 nM, [formate] = 250 mM; [g-C_3N_4-25K] = 5 mg/mL; T = 25 °C. Assay: [Monochlorodimedone (MCD)] = 50 µM; [KBr] = 0.5 mM; [H_2O_2] = 5 mM; [Na_3VO_4] = 0.1 mM in 100 mM citrate buffer (pH 5).

Whereas *Ci*VCPO alone was relatively stable in the absence of external illumination, it was rapidly inactivated upon illumination (loosing 80% of the initial activity within one hour of illumination). This effect was even more pronounced when illuminating *Ci*VCPO in the presence of g-C_3N_4-25K (losing more than 90% of its initial activity within 15 min). In the presence of g-C_3N_4-25K, albeit under dark conditions, *Ci*VCPO also lost some activity, which, however, may also be attributed to adsorption of the biocatalyst to the heterogeneous photocatalyst. Similar observations had been made previously. For example, the rapid inactivation of a peroxygenase in the presence of TiO_2 photocatalysts.[12] These authors ascribed the biocatalyst inactivation to locally high radical concentrations at the photocatalyst surface. Possibly, very similar phenomena account for the observations made here. The inactivation of *Ci*VCPO upon illumination alone is somewhat more difficult to rationalise. Rauch *et al.* reported rapid inactivation of a flavin-dependent enzyme in the presence of blue light.[13] They rationalised this by the photodegradation of the prosthetic flavin group. Whether similar reasons apply for the current system (photochemical degradation of

the vanadate group) remain to be clarified. Nevertheless, it can be asserted that illumination (especially in the presence of g-C_3N_4-25K) is detrimental for *Ci*VCPO stability.

Furthermore, it is worth mentioning that in the case of 4-styrenesulfonate, significant substrate conversion to yet unidentified side products was observed. Again, this may be ascribed to radical species formed at the photocatalyst surface. Therefore, we concluded that one-pot-one-step reaction procedures do not represent a promising approach for photobiocatalytic reactions envisaged in this contribution.

We intended to circumvent these issues by physical separation of the photocatalytic H_2O_2 formation and the *Ci*VCPO catalysed reaction. In order to separate the photocatalysis from the biocatalysis, a two-pot reaction system was designed connected with a continuous flow *via* a filter. The first pot contained g-C_3N_4-25K and was illuminated. The formed H_2O_2 was continuously fed into the second pot containing the substrate, bromide and *Ci*VCPO (Scheme 2).

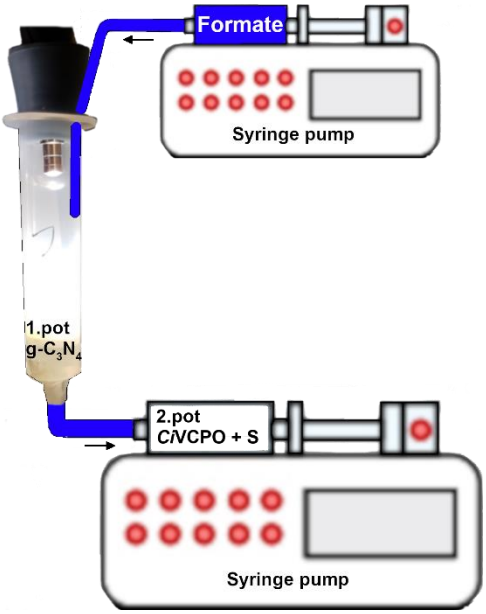

Scheme 2. Physical separation of the photocatalysis from biocatalysis two-pot system.

To characterise this new reaction setup, the formation of hydrogen peroxide in flow was investigated with flow rates of 0.5, 0.75 and 1 mL/h (Figure 4). The flow rate of 0.5 mL/h was chosen showing a linear increase of hydrogen peroxide of 1 mM/h

reaching a maximum concentration of 5 mM in the efflux after 5 h of feeding. In the first 5 h, this corresponds to 2.5 mL with a concentration of 3.75 mM H_2O_2. Subsequently, the actual haloperoxidase product formation was measured in the new designed two-pot system. Initial results applying 4-styrenesulfonate yielded product concentrations up to 1.6 mM (TTN *Ci*VCPO 8888). The separation of substrate and biocatalyst from the photocatalytic reaction resulted in the formation of only one product compared to multiple side products in case of direct contact between the substrate and g-C_3N_4-25K, indicated by NMR comparison (Figure 5).

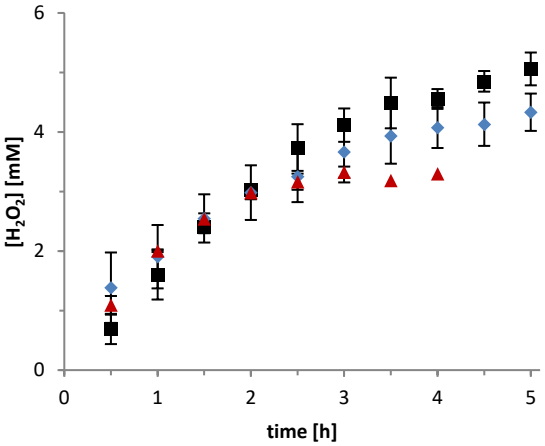

Figure 4. Hydrogen peroxide formation in flow at various flow rates. General conditions: ■ feed rate 0.5 mL/h; ◆ feed rate 0.75 mL/h; ▲ feed rate 1 mL/h reactions were performed in 200 mM citrate buffer (pH 5); visible light illumination (λ > 400 nm); 2 mL reaction volume; [formate] = 250 mM; [g-C_3N_4-25K] = 5 mg/mL.

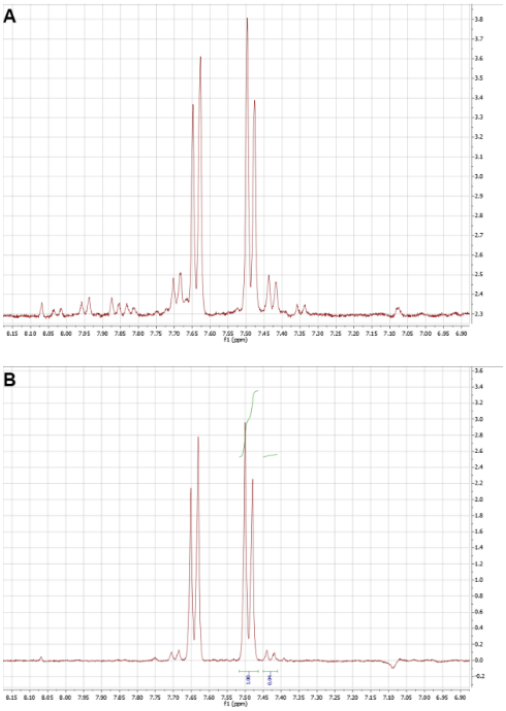

Figure 5. Comparison of NMR spectra of the one-pot and two-pot approach. General conditions: A: reaction performed in 200 mM citrate buffer (pH 5 visible light illumination (λ > 400 nm): [formate] = 250 mM; [g-C_3N_4-25K] = 5 mg/mL; [KBr] = 80 mM; [*Ci*VCPO] = 150 nM; [4-styrenesulfonate] = 40 mM; T = 25 °C; 21 h illumination time. B: reaction performed in 200 mM citrate buffer (pH 5); 1. pot 2 mL visible light illumination (λ > 400 nm): [formate] = 250 mM; [g-C_3N_4-25K] = 5 mg/mL; [KBr] = 80 mM; 2. pot 10 mL: [*Ci*VCPO] = 180 nM; [4-styrenesulfonate] = 40 mM; T = 25 °C; 10 h illumination time; flow rate of 0.5 mL/h.

Derived from Figure 4, the expected concentration of hydrogen peroxide fed over 10 h is 1.875 mM in the final volume of the second pot. With the achieved product concentration, this corresponds to a usage of 85% of the hydrogen peroxide. Duplicates of the reaction conducted with the conditions stated in figure 5 were measured with HPLC and NMR. Both confirm product concentrations of 1.6 mM corresponding to 85% usage of hydrogen peroxide. However, reproduction of this reaction only yielded 0.63 mM ± 0.09 mM product with a resulting TTN of 3488 for *Ci*VCPO and a usage of hydrogen peroxide of 33%.

Due to the inconsistency in the reproduction of the results, an additional model reaction with the substrate 4-pentenoic acid was investigated with a more reliable analysis by gas chromatography. The initial experiment with the 4-pentenoic acid

yielded 1.3 mM bromolactone product with a corresponding TTN of 7222 for *Ci*VCPO and a consumption of 69% of hydrogen peroxide. No side product formation was observed: Again, the reproducibility was low, with repeated concentrations between 0.3-0.5 mM. A last attempt produced 0.26 mM with a TTN of 1444 for *Ci*VCPO.

Since the results of the two-pot system displayed low reproducibility, we proceeded to improve the experimental setup. The *Ci*VCPO was immobilised on IB-COV-3 beads. Substrate and KBr were supplied to the immobilised *Ci*VCPO by an additional feed. The substrate and hydrogen peroxide feed were combined in a T-junction and subsequently flowed over the *Ci*VCPO beads (Scheme 3).

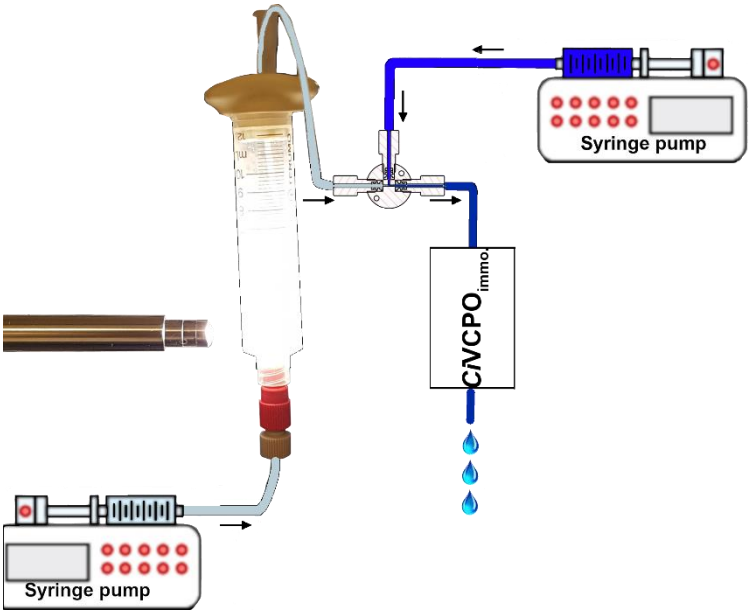

Scheme 3. Continuous flow reactor with immobilised *Ci*VCPO feeding in one feed photocatalytic formed H_2O_2 and *via* a T-junction a second feed with substrate and bromide.

As expected, the product concentration increased initially with increasing hydrogen peroxide concentrations supplied in the efflux of the light reaction. After approximately 7 h, the maximum product concentration of bromolactone in the efflux is expected, 2 h more than with the hydrogen peroxide formation trails, due to the added dead volume of the additional tubing, T-junction and immobilised *Ci*VCPO column in the new experimental setup. The highest product concentration in the

efflux measured was 0.45 mM after 21 h. The continuous reaction was stable with a slight decrease to 0.36 mM product in the efflux after 44 h, and the accumulated amount of bromolactone formed is shown in Figure 6. The reached amount of 165.6 µmol bromolactone accounts for a TTN of immobilised *Ci*VCPO of 1180. In further experiments we hope to achieve higher product formation by optimising the reaction conditions and prolonged reaction performance by preventing the loss of g-C_3N_4-25K in the filter accompanied by decrease of formed hydrogen peroxide.

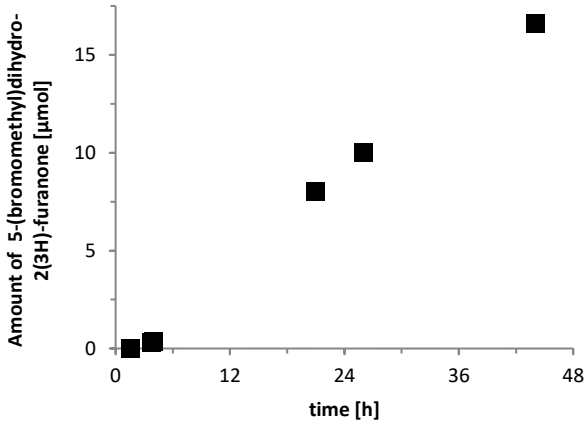

Figure 6. Bromolactone formation with immobilised *Ci*VCPO coupled to g-C_3N_4-25K catalysed H_2O_2 formation. General conditions: reactions were performed in flow. First feed: feed rate 0.5 mL/h; 200 mM citrate buffer (pH 5); [formate] = 250 mM; photoreaction 2 mL; [g-C_3N_4-25K] = 5 mg/mL; visible light illumination (λ > 400 nm); Second feed: feed rate 0.5 mL/h; [KBr] = 80 mM; [4-pentenoic acid] = 40 mM; [*Ci*VCPO immobilised] = 100 mg; T = 25 °C.

Conclusion

With a proof of concept, we addressed the most common issues combining photo and biocatalysis. The photocatalyst shows a high inactivating effect on the enzyme. Additionally, we observed strong side product formation caused by direct contact of photocatalyst substrate, in case of styrenesufonate. These frequent issues were successfully prevented by physical separation of the photocatalytic and enzymatic reaction. The separation let to a stable reaction set up forming solely desired product. In theory the components are stable enough to perform even longer, at the moment the reaction setup is limiting since the system is prone to clogging due to the small particle size of the g-C_3N_4-25K. Further optimisation of the separation setup could possibly lead to continuous production for weeks. The two main issues are resolved. Further improvements of the reaction conditions are likely to improve product formation. In general, the physical separation of photocatalyst and biocatalyst is beneficial in case of incompatibility of substrate, product or enzyme with the photocatalyst.

Material and methods

Materials

Chemicals were purchased from Sigma-Aldrich, Fluka, Acros or Alfa-Aesar with the highest purity available and used as received.

Preparation of the biocatalysts

Vanadium-dependent chloroperoxidase (CiVCPO)

Bacterial strains and plasmids

The plasmid pBADgIIIB containing the gene encoding vanadium-dependent chloroperoxidase (*Ci*VCPO) was transformed into *E. coli* TOP10. Transformed cells were grown for 1 h at 37 °C in LB without antibiotics. 100 µL were plated out on a LB plate containing ampicillin and incubated overnight at 37 °C. A colony was picked and a pre-culture was grown over night at 37 °C. Glycerol stocks TOP10-*Ci*VCPO containing 15% glycerol were prepared from the pre-culture.

Cultivation conditions

A 100 mL pre-cultures of LB medium (100 mL) containing 50 µg/mL of ampicillin was inoculated with *E. coli* TOP10 pBADgIIIB *Ci*VCPO and incubated overnight at 37 °C and 180 rpm. Overexpression was carried out in 5 L flasks with 2 L of TB medium supplemented with 50 µg/mL of ampicillin. Three main-cultures were inoculated with 30 mL of pre-culture (OD_{600} = 3.7) to an OD of approx. 0.05 and grown at 37 °C and 180 rpm.

When an OD_{600} of 0.8-1.0 was reached (approx. 3 h), 2 ml 20% L-arabinose was added to reach a final inducer concentration of 0.02%. After induction, cultures were incubated for additional 24-48 h at 25 °C and 180 rpm.

CiVCPO purification

The bacterial pellets obtained after centrifugation were re-suspended in 50 mM Tris/H_2SO_4 buffer (pH 8.1). The re-suspended bacterial pellets (0.5 g cells per mL) were stored at -20 °C until processed as described below. 0.1 mM PMSF (100 mM stock in isopropanol) was added to the re-suspended cells, which were ruptured by sonication on ice (5 mL sample volume 3 x 1.5 min with 1 min break on ice (output 4, cycle 40%)). Alternatively, a French press (1.5 Bar) for three cycles can be used. The samples were then centrifuged (10 000 × *g* for 20 minutes) and the supernatant was incubated at 70 °C for 1.5 h. The supernatant was again centrifuged for 10 min at 40000 × *g* to remove denaturised protein. Remaining catalase activity was checked with the Quick test: 100 µl enzyme solution (or dilution), 100 µL Triton X 1%, 100 µL H_2O_2 30% in KPi buffer (50 mM pH 7.0). The activity was evaluated based on the amount of bubbles generated.

Then the supernatant was concentrated using Amicon filters (30 kDa cut-off). Next, the solution was desalted with a PD10 against the Tris/H_2SO_4 buffer and 1 mM ortho vanadate added. After centrifugation, the clear supernatant can be used or stored at -20 °C until further purification.

CiVCPO activity

*Ci*VCPO activity can be qualitatively tested using the MCD assay by incubating aliquots of cell extracts or purified enzyme in 50 mM citrate buffer (pH 5) containing monochlorodimedone (MCD), *o*-vanadate, KBr and H_2O_2. Reaction is started by the addition of *Ci*VCPO and absorption is followed at 290 nm.

100 µL	MCD (0.5 mM)	50 µM
5 µL	KBr (1M)	5 mM
100 µL	o-Vanadate (Na_3VO_4, 1 mM)	0.1 mM
100 µL	1 M sodium citrate buffer, pH 5.0	0.1 M
5 µL	H_2O_2 (1 M)	5 mM
20 µL	enzyme solution (diluted)	
670 µL	H_2O	

Preparation of the graphitic carbon nitride

2 g of melamine in 5 mL MilliQ H_2O were sonicated for 30 min. Subsequently, 5 mL of 25 mM KOH were added. The water was evaporated in a rotary evaporator with 150 mbar at 60 °C. The obtained powder was dried at 80 °C. The dry powder was heated to 550 °C with a temperature ramp of 5 °C/min. The temperature of 550 °C was held for 2 h and subsequently cooled down with a rate of 20 °C/min. The obtained solid was ground and always sonicated in solution before use.

General procedures

Hydrogen peroxide formation in one pot
was performed in 4 mL glass reaction tubes containing 2 mL reaction mixture. The reactions were illuminated from the top by lightningcure^{tm} LC8 – L9588 spot light (λ > 400 nm) at a distance of 4 cm. Reactions were stirred using Teflon coated magnetic bars keeping the heterogeneous photocatalyst particles homogeny dispersed in solution. Standard reaction conditions for the light-driven formation of H_2O_2 were 5 mg/mL g-C_3N_4-25K and 250 mM formate in 200 mM citrate buffer at pH 5 and room temperature.

Hydrogen peroxide formation in flow
was performed in a plastic chromatography column containing 2 mL reaction mixture. The reactions were illuminated from the top by a lightningcure^{tm} LC8 – L9588 (λ > 400 nm) at a distance of 4 cm. Reactions were stirred using Teflon coated magnetic bars keeping the heterogeneous photocatalyst particles homogeny dispersed in solution. The reaction mixture contained 5 mg/mL g-C_3N_4-25K, 250 mM formate in 200 mM citrate buffer at pH 5. A solution of 250 mM formate in 200 mM citrate buffer pH 5 was fed with a syringe pump at a flow from 0.5 to 1 mL/h.

CiVCPO activity adsorbed to g-C_3N_4 in dark and illuminated
The *Ci*VCPO activity in the photocatalysis reaction setup was investigated using the standard monochlorodimedone (MCD) assay established for measurement of the

activity of haloperoxidases. The bromination of the MCD is followed by measuring the decline in absorption at 290 nm with a spectrophotometer. Testing the residual *Ci*VCPO activity of the supernatant of a suspension of *Ci*VCPO and g-C_3N_4-25K showed no activity. However, the suspension still containing the g-C_3N_4-25K particles retained the *Ci*VCPO activity. These results indicate the immediate binding of *Ci*VCPO to the g-C_3N_4-25K particles upon mixing. The binding of *Ci*VCPO to g-C_3N_4-25K was further investigated by determination of the protein concentration in the supernatant. The results indicate an immediate binding of 95% *Ci*VCPO to g-C_3N_4-25K upon mixing.

Two-pot reactions

were performed to circumvent VCPO inactivation and side product formation. To do this, the light-driven H_2O_2 formation in the first pot, as in described in the hydrogen peroxide formation in flow, was coupled to second pot reaction, fuelling the *Ci*VCPO with the formed H_2O_2. The flow was 0.5 mL/h maintained by syringe pumps. The second reaction was performed directly in the syringe. With a reaction time of 10 h the total volume was 10 mL with the following composition. Reaction with 4-pentenoic acid: 10 mM 4-pentenoic acid, 20 mM KBr, 180 nM VCPO in 200 mM citrate buffer pH 5. Product (5-(bromomethyl)dihydro-2(3H)-furanone) concentrations were determined using gas chromatography. Reaction with 4-styrenesulfonate: 40 mM 4-styrenesulfonate, 80 mM KBr, 180 nM VCPO in 200 mM citrate buffer pH 5. Product was analysed using NMR and HPLC.

Immobilised setup

Hydrogen peroxide was continuously formed as described in hydrogen peroxide formation in flow with 0.5 mL/h feed rate. *Ci*VCPO was immobilised on IB-COV3 beads by incubating in a rotary shaker overnight. The amount of *Ci*VCPO immobilised was determined with a Bradford assay of the *Ci*VCPO remaining in the aqueous phase (0.94 mg per 100 mg beads). The hydrogen peroxide flow was combined over a T-junction with a second flow of 40 mM 4-pentenoic acid, 80 mM KBr in 200 mM citrate pH 5 with 0.5 mL/h. The combined feeds were pumped over

100 mg of immobilised *Ci*VCPO beads (dead volume 72 µL, residence time 4.3 min). Product concentrations were determined using gas chromatography.

Analytical procedures

GC-analyses

Samples of 0.02 mL reaction mixture were extracted with 0.2 mL ethyl acetate and dried with magnesium sulfate. As internal standard 5 mM acetophenone was used. Analysis were performed with Shimadzu GC-2010 plus gas chromatograph with an AOC-20i Auto injector (injection temperature 250 °C) and flame ionization detection (FID). The carrier gas of the achiral GC was nitrogen with a flow of 31.5 cm × s^{-1}.

Table 1. GC analysis specifications for concentration determination

Compounds (retention time)	GC column	GC oven programme
4-pentenoic acid (5.1 min)/ 5-(hydroxy)dihydro-2(3H)-furanone (9.5 min)/ 5-(bromomethyl)dihydro-2(3H)-furanone (10.5 min)/ acetophenone (8 min)	CP-Sil 5 CB GC column (25 m x 0.25 mm x 1.2 µm)	70 °C for 1 min. 30 °C/min to 140 °C hold for 2 min. 30 °C/min to 195 °C hold for 2 min. 30 °C/min to 225 °C hold for 1 min. 30 °C/min to 345 °C hold for 1 min.

References

[1] K. H. van Pee, S. Unversucht, *Chemosphere* **2003**, *52*, 299-312.
[2] L. Getrey, T. Krieg, F. Hollmann, J. Schrader, D. Holtmann, *Green Chem.* **2014**, *16*, 1104-1108.
[3] E. Santacesaria, R. Vitiello, R. Tesser, V. Russo, R. Turco, M. Di Serio, *Ind. Eng. Chem. Res.* **2014**, *53*, 8939-8962.
[4] R. Renirie, J. M. Charnock, C. D. Garner, R. Wever, *J. Inorg. Biochem.* **2010**, *104*, 657-664.
[5] L. Menini, E. V. Gusevskaya, *Chem. Commun.* **2006**, 209-211.
[6] J. M. Campos-Martin, G. Blanco-Brieva, J. L. G. Fierro, *Angew. Chem. Int. Edit.* **2006**, *45*, 6962-6984.
[7] B. Valderrama, M. Ayala, R. Vazquez-Duhalt, *Chem. Biol.* **2002**, *9*, 555-565.
[8] A. M. Held, D. J. Halko, J. K. Hurst, *J. Am. Chem. Soc.* **1978**, *100*, 5732-5740.
[9] Y. Shiraishi, S. Kanazawa, Y. Sugano, D. Tsukamoto, H. Sakamoto, S. Ichikawa, T. Hirai, *ACS Catal.* **2014**, *4*, 774-780.
[10] M. M. C. H. van Schie, W. Y. Zhang, F. Tieves, D. S. Choi, C. B. Park, B. O. Burek, J. Z. Bloh, I. W. C. E. Arends, C. E. Paul, M. Alcalde, F. Hollmann, *ACS Catal.* **2019**, *9*, 7409-7417.
[11] G. Cronk, Methods of using hydrogen peroxide for in-situ chemical oxidation treatment of soil and groundwater, U.S. Patent Application US9259771B2, **2016-02-16**.
[12] B. O. Burek, S. R. de Boer, F. Tieves, W. Zhang, M. van Schie, S. Bormann, M. Alcalde, D. Holtmann, F. Hollmann, D. W. Bahnemann, J. Z. Bloh, *ChemCatChem* **2019** , *11* , 3093.
[13] M.C.R. Rauch, M.M.E. Huijbers, M. Pabst, C.E. Paul, M. Pešić, I.W.C.E. Arends, F. Hollmann, *BBA-PROTEINS PROTEOM* **2020,** Volume 1868, *1*, 140303.

Chapter 4

Chapter 4: Scaling up an enzymatic bromolactonisation

Georg T. Höfler, Andrada But, Sabry H. H. Younes, Ron Wever, Caroline E. Paul, Isabel W.C.E. Arends and Frank Hollmann

Based on *ACS Sustain. Chem. Eng.* 2020 *8* (7): 2602-2607.

Summary

Lactones are valuable building blocks for further transformations into high added value products, especially in polymer chemistry as starting materials for polyesters.[1] The majority of polyesters, however, are obtained from simple lactones or hydroxyacids leaving little room for further modification and tailoring of the polymer properties. Using more functionalised lactone monomers results in polyesters containing additional handles for modification to tune their hydrophobicity, hydrophilicity, for cross-linking and attachment of functional units. These lactones can be obtained through cyclisation of hydroxyacids. The enzyme vanadium-dependent chloroperoxidase from *Curvularia inaequalis* (*Ci*VCPO) catalyses the formation of hypohalites from H_2O_2 and halides. Due to its outstanding stability, straightforward preparation and easy handling, *Ci*VCPO is a good candidate to replace commonly used chemical catalysts that have a poor atom efficiency and cause a large amount of waste. The scale-up of the chemoenzymatic bromolactonisation to 100 g-scale is presented together with an identification of current limitations. The preparative-scale reaction also allowed for meaningful mass balances identifying current bottlenecks of the chemoenzymatic reaction.

Introduction

Activated, electrophilic halogens are common oxidants in organic synthesis.[2-4] Their high reactivity, however, poses challenges when used as stoichiometric agents. Due to their high instability, their application comes along with considerable safety issues. Furthermore, stoichiometric amounts of salt waste formed during the reaction (or during work-up) pose an environmental issue. Finally, undesired side-reactions are often observed. The latter issue is frequently met using halogen precursors such as *N*-bromosuccinimide (NBS) which gradually release the activated halide species into the reaction. In this case, the problem of waste formation is even more pronounced. An alternative approach is to generate hypohalites *in situ* (i.e. in the reaction mixture) from the corresponding halide and hydrogen peroxide. Common catalysts comprise chalcogens,[5-8] transition metal catalysts[9] and enzymatic methods.[2] The use of haloperoxidases for the *in situ* generation of hypohalites is gaining interest in organic synthesis.[1] Haloperoxidases catalyse the clean, H_2O_2-dependent oxidation of halides to the corresponding hypohalites. Especially the vanadium-dependent chloroperoxidase from *Curvularia inaequalis* (*Ci*VCPO) excels by its extraordinary robustness and its exceptional catalytic activity.[10-17]

The oxidative halolactonisation of γ,δ-unsaturated carboxylic acids is a popular application of activated halides, amongst others in natural product synthesis.[3, 18-20] Very recently, we have demonstrated that *Ci*VCPO is an efficient catalyst to initiate the chemoenzymatic halolactonisation of γ,δ-unsaturated carboxylic acids (Scheme 1).[10] The resulting halo-functionalised lactones may be interesting building blocks for functionalisable polyesters.

Starting from simple 4-pentenoic acid (**1**), for example, (5-(bromomethyl)dihydro-2(3H)-furanone (**2**)) could be obtained in quantitative, yet analytical yield. The aim of this study was two-fold: first, we aimed at identifying the factors influencing the synthesis of **2** and scaling-up the procedure from laboratory scale (1 mL, <50 mM substrate) to preparative scale, and second, to assess the environmental impact (Scheme 1).

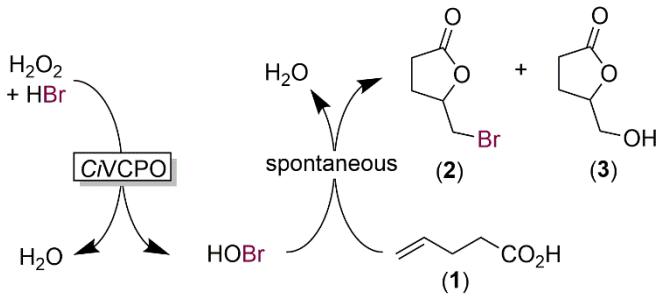

Scheme 1. Vanadium chloroperoxidase (*Ci*VCPO) catalysed bromolactonisation of 4-pentenoic acid.

To determine the environmental impact of the reaction, the E^+-factor,[21] a recent extension of Sheldon's E-factor[22-23] that takes energy-related CO_2 emissions into account, was used.

Results and Discussion

First, the substrate loading was increased, in order to reduce the amount of waste water formed in the reaction.[24] Increasing the substrate concentration from 40 mM to 500 mM, however, resulted in low product formation. Further experiments revealed that the biocatalyst *Ci*VCPO was prone to a pronounced substrate inhibition (Figure 1). In presence of 60 mM 4-pentenoic acid, the biocatalyst's activity was reduced to less than half of its maximal value. At 500 mM, there was almost no enzyme activity detectable. Comparative experiments using 4-pentanoic acid (**1**) gave similar results indicating that high concentrations of carboxylic acids inhibit *Ci*VCPO.

Possibly, this inhibition originates from reversible binding of the carboxylate group to the vanadium prosthetic group.[25-26] Besides the inhibition by 4-pentenoic acid, it is known that bromide inhibits the enzyme.[27] Furthermore, the undesired spontaneous reaction between hypohalites and H_2O_2 yielding $^1O_2$ calls for gradual addition of H_2O_2.[16] We therefore decided to apply a fed-batch strategy adding 4-pentenoic acid together with Br^- and H_2O_2 over time and limit their concentrations (and inhibitory effects).

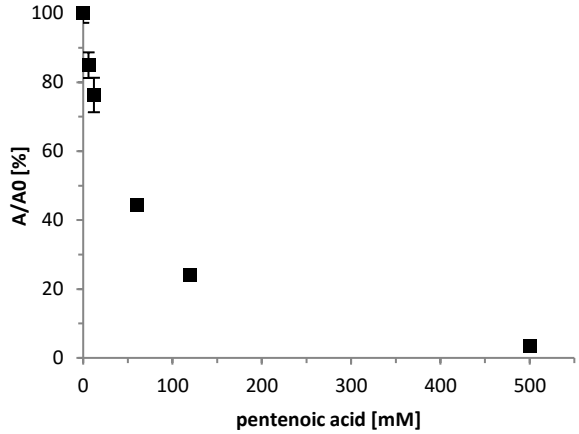

Figure 1. *Ci*VCPO inhibition by pentenoic acid. General conditions: [KBr] = 5 mM; [H_2O_2] = 5 mM; [*Ci*VCPO] = 38 nM; [MCD] = 50 µM; [Na_3VO_4] = 100 µM in 100 mM citrate buffer (pH 5). T = 25 °C; 290 nm; UV-VIS.

Increasing the feed-rate from 0.02 mmol h^{-1} to 0.06 mmol h^{-1} had no obvious effect on the initial reaction rate (Figure 2). Interestingly, also increasing the amount of the biocatalyst (at lower feeding rates) did not affect the product formation. Possibly, the rate of the spontaneous, chemical bromolactonisation was overall rate limiting. High feed rates, however, also yielded a less robust reaction system as the product formation already ceased after approximately 6-10 h. This indicates that also the robust *Ci*VCPO is prone to oxidative inactivation, possibly by the accumulating hypobromite or through singlet oxygen.

In all reactions, the formation of side product was observed. Analysis by GC-MS and NMR identified the side product as 5-(hydroxymethyl)dihydrofuran-2(3H)-one (**3**) (see Figure 9, 10, 11 and 12 for spectra). Possible sources for the side product are a background reaction with H_2O_2 or the hydrolysis of Bromolactone (**2**). The formation of the side product seems to consume hydrogen peroxide and occur without *Ci*VCPO activity over prolonged reaction times (Figure 3.)

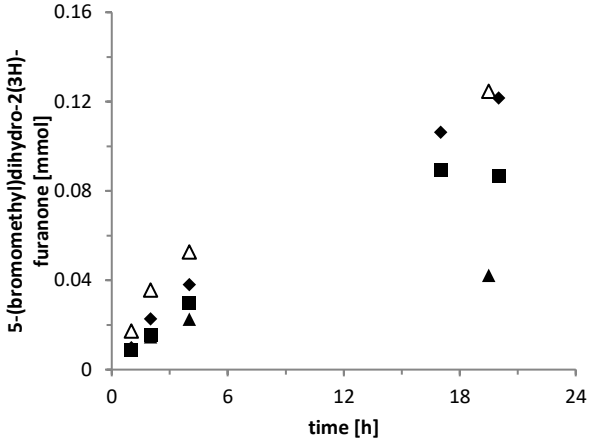

Figure 2. Influence of the reagents feed rate on the formation of (2) in the chemoenzymatic bromolactonisation of (1). ■ 0.02 mmol/h; ◆ 0.03 mmol/h; ▲ 0.06 mmol/h; empty symbols 2x [*Ci*VCPO]; ▲ 0.1 mL/h 0.6 M 4-pentenoic acid, 0.6 M KBr; 0.6 M H_2O_2; ◆ 0.05 mL/h 0.6 M 4-pentenoic acid, 0.6 M KBr; 0.05 mL/h 1 M H_2O_2; ■ 0.033 mL/h 4-pentenoic acid; 0.05 mL/h KBr; 0.067 mL/h H_2O_2; all 0.6 M; start volume: 1 mL, end volume: 4 mL 50 nM *Ci*VCPO, T = 25 °C, in 200 mM acetate buffer (pH 5).

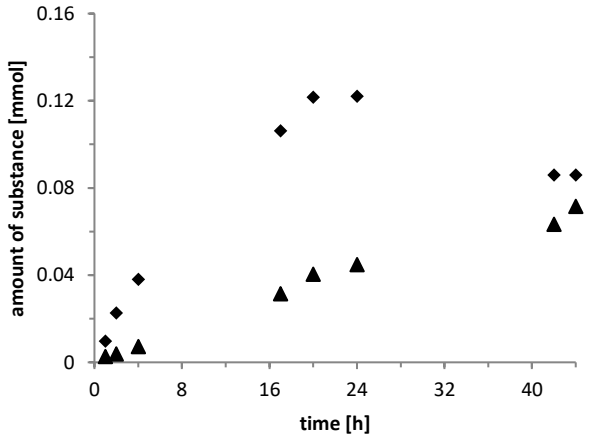

Figure 3. *Ci*VCPO catalysed lactonisation of 4-pentenoic acid successive addition of pentenoic acid, KBr and H_2O_2 with 0.03 mmol/h. Side product formation. General conditions: ◆(5-(bromomethyl)dihydro-2(3H)-furanone); ▲5-(hydroxymethyl)dihydro-2(3H)-furanone); 0.05 mL/h 0.6 M 4-pentenoic acid, 0.6 M KBr, 0.05 mL/h 1 M H_2O_2 for 20 h; Start volume 1 mL; end volume 4 mL 50 nM *Ci*VCPO; T = 25 °C, in 200 mM acetate buffer pH 5.

The most promising conditions of 0.03 mmol/h 4-pentenoic acid (**1**) with a high TTN of 608246 and a linear formation rate were chosen for a 50-fold upscaling to 200 mL (Figure 4). The reaction was performed without buffer, controlling the pH with a pH stat by addition of 1 M acetic acid. We reduced the feeding volume by combining the KBr and 4-pentenoic acid (**1**) feed. After 14.5 h the addition of acetic acid stopped (plateau) indicating the stop of the reaction. At this point 5.72 mmol, corresponding to 36.2 mM, bromolactone (**2**) were formed (measured at 17.5 h). Addition of an aliquot of *Ci*VCPO after 21 h successfully restarted the lactone formation for additional 10 h. The end volume of 200 mL corresponds to 150 mM 4-pentenoic acid (**1**), 150 mM KBr, 250 mM H_2O_2 with 100 nM *Ci*VCPO and 241 mM acetic acid.

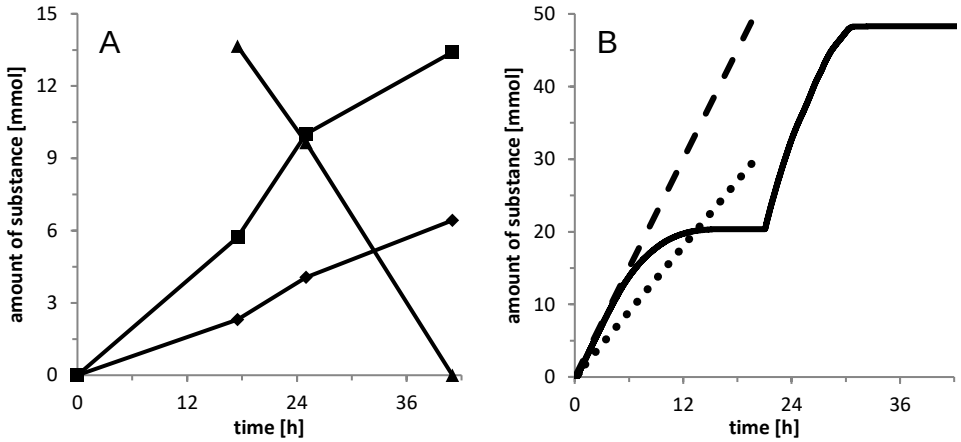

Figure 4. 200 mL scale bromolactonisation with successive addition of pentenoic acid, KBr (1.5 mmol/h) and H_2O_2 (2.5 mmol/h) in pH stat without buffer at pH 5. General conditions: A: ■ 5-(bromomethyl)dihydro-2(3H)-furanone; ◆ 5-(hydroxymethyl)dihydro-2(3H)-furanone; ▲ 4-pentenoic acid; GC analysis; B: solid line 1 M acetic acid added by pH stat, dashed line H_2O_2; dotted line 4-pentenoic acid and KBr added by syringe pump; start volume 50 mL 200 nM *Ci*VCPO; 2.5 mL/h 0.6 M 4-pentenoic acid & 0.6 M KBr pH 5, 2.5 mL/h 1 M H_2O_2 pH 5 for 20 h; Addition of *Ci*VCPO aliquot after 21 h; End volume ~200 mL concentrations end (150 mM 4-pentenoic acid, 150 mM KBr, 250 mM H_2O_2; 100 nM *Ci*VCPO; 241 mM acetic acid; pH 5); T = 25 °C**.**

The highest amount of bromolactone (**2**) measured was 13.4 mmol (67.63 mM) after 41 h (24.5 h of *Ci*VCPO activity according to pH change) correlating to 44.7% conversion of 4-pentenoic acid (**1**) and KBr to the bromolactone (**2**). According to GC measurements, no substrate was present anymore. The formed side product does

not account for the missing 4-pentenoic acid (**1**) (total conversion including side product 66.1%). The strong smell of the substrate and GC analysis of condensate in the headspace of the reaction vessel confirm the evaporation of the substrate to some extent. The isolated yield of **3** was 39.0% regarding **1** and KBr. This corresponds to 2.10 g (2.39 g, 87.7% purity) with a TTN for *Ci*VCPO of 671050. The 12.3% impurity were **3** as observed before. The conversion of the bromolactone regarding H_2O_2 was only 26.8%. Interestingly, the rate of acetic acid added matched the rate of H_2O_2 fed, indicating a rate limitation by H_2O_2. This is unexpected, since the H_2O_2 was fed in 1.66 excess regarding the other substrates. Both observations are indicating a strong side reaction of H_2O_2, probably the shunt reaction with the hypobromite forming singlet oxygen. The amount acetic acid added by the pH stat correlates to 243.6 mM added overall. Within the first 14.5 h, the TOF of *Ci*VCPO was 10.97 s^{-1}, overall 4.55 s^{-1} and excluding the plateaus without *Ci*VCPO activity 6.66 s^{-1}.

In a subsequent experiment, the pH stat was used to adjust the pH by addition of 0.6 M 4-pentenoic acid (**1**) and KBr (Figure 5) to reduce the total volume further and possible further optimise the substrate feeding rate. Furthermore, the H_2O_2 feed was reduced to increase the H_2O_2 conversion and reduce the rate of side reactions, possibly increasing *Ci*VCPO stability due to lower concentrations of H_2O_2 and less singlet oxygen formation. The reaction volume could be decreased by 30 mL, resulting in 170 mL with final concentrations of 175 mM 4-pentenoic acid (**1**), 175 mM KBr, 220 mM H_2O_2 with 129 nM *Ci*VCPO and 124 mM acetic acid.

A higher amount of Bromolactone (**2**) with 13.94 mmol corresponding to a concentration of 81.93 mM was produced within 24 h. The conversion of 4-pentenoic acid (**1**) and KBr increased to 46.5 %, (total including side product 65.3%). The product workup was less efficient, extraction efficiency of 83.3% compared to 87.2%, resulting in a slightly lower isolated yield of 38.8% and a lower purity. Nevertheless, 2.08 g (2.50 g, 83.3% purity) 5-(bromomethyl)dihydro-2(3H)-furanone (**2**) were obtained.

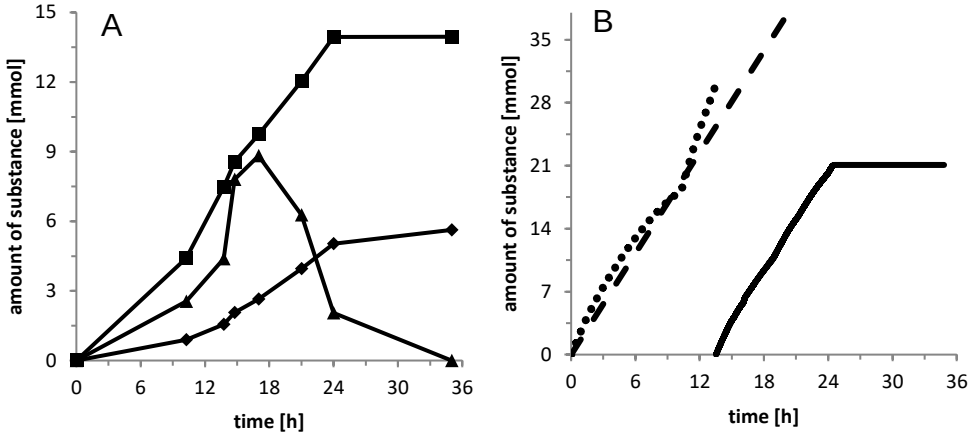

Figure 5: 170 mL scale *Ci*VCPO-catalysed lactonisation of 4-pentenoic acid successive addition of pentenoic acid, KBr by pH stat and H_2O_2. General conditions: A: ■ 5-(bromomethyl)dihydro-2(3H)-furanone; ◆ 5-(hydroxymethyl)dihydro-2(3H)-furanone; ▲ 4-pentenoic acid; GC analysis; B: dotted line 0.6 M 4-pentenoic acid and KBr by pH stat, after 50 mL switched to 1 M acetic acid solid line, dashed line H_2O_2 added by syringe pump; start volume 50 mL 200 nM *Ci*VCPO; pH stat feed 0.6 M 4-pentenoic acid & 0.6 M KBr after 50 mL 1 M acetic acid, 2.5 mL/h 0.75 M H_2O_2 pH 5 for 20 h; Addition of *Ci*VCPO aliquot after 10.25 h and 1/5 aliquot after 19 h) End volume ~170 mL concentrations end (175 mM 4-pentenoic acid, 175 mM KBr, 220 mM H_2O_2; 129 nM *Ci*VCPO; 124 mM acetic acid pH 5); T = 25 °C.

The TOF of *Ci*VCPO could also be increased with 11.96 s^{-1} during the first 10.25 h overall 5.04 s^{-1} and excluding the plateaus without enzyme activity 7.34 s^{-1}. The conversion of H_2O_2 could be increased to 37.2%. Since H_2O_2 was used more efficiently the side shunt reaction was probably decreased, a positive effect of less singlet oxygen on the *Ci*VCPO was not observed though. The TTN of *Ci*VCPO was lower with 634816. A possible explanation is partly inactivation of *Ci*VCPO during the time without stirring, forming a precipitate (see experimental section). At the current optimised conditions, the space time yields for the bromolactone (**2**) are 12 g/L per day bromolactone (0.5 g/L × h) and regarding the applied catalyst amount 58.39 g product/g (*Ci*VCPO × h).

To reduce the (undesired) spontaneous hydrolysis of the bromolactone (**2**) product into the corresponding acid[28], an *in situ* product removal strategy was investigated. For this, we chose the well-known two liquid phase system (2LPS) approach wherein

a water-immiscible organic solvent serves as product sink. Several organic solvents were evaluated with respect to their effect on the stability of the biocatalyst (Figure 6).

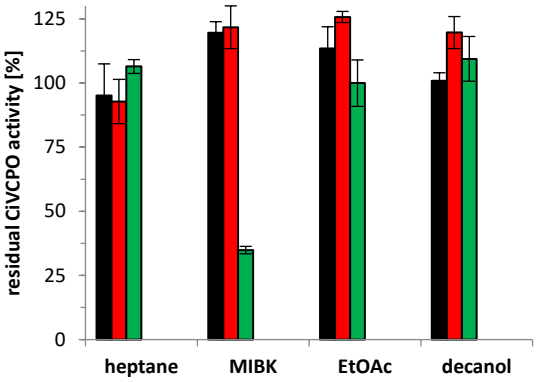

Figure 6. Solvent stability of *Ci*VCPO in biphasic system. Incubation conditions: [*Ci*VCPO] = 700 nM in 100 mM citrate buffer (pH 5), T = 30 °C in the presence of one aliquot of the organic solvent. The mixtures were shaken at 500 rpm in a thermoshaker. Directly after mixing (■) and after 4 h (■) and 24 h (■) samples were taken from the aqueous layer and analysed as described in Figure 1. Values shown represent the ratio of the residual activity of *Ci*VCPO in the presence of solvent to the residual activity of *Ci*VCPO in buffer only under otherwise identical incubation conditions.

Most solvents did not significantly influence the robustness of *Ci*VCPO; only methyl isobutyl ketone (MIBK) seemed to have a negative effect on the enzyme as upon prolonged incubation time (24 h) the activity was reduced by more than 60%. All other solvents tested had no or even a slightly beneficial effect. For further experiments we chose ethyl acetate (EtOAc), since it is generally considered as 'green'[29] and –more importantly for us– showed good solubilisation properties for the product. Ethyl acetate exhibits the lowest boiling point of all solvents tested an important parameter in the recovery process (by distillation) of the product and the recycling of the organic phase.

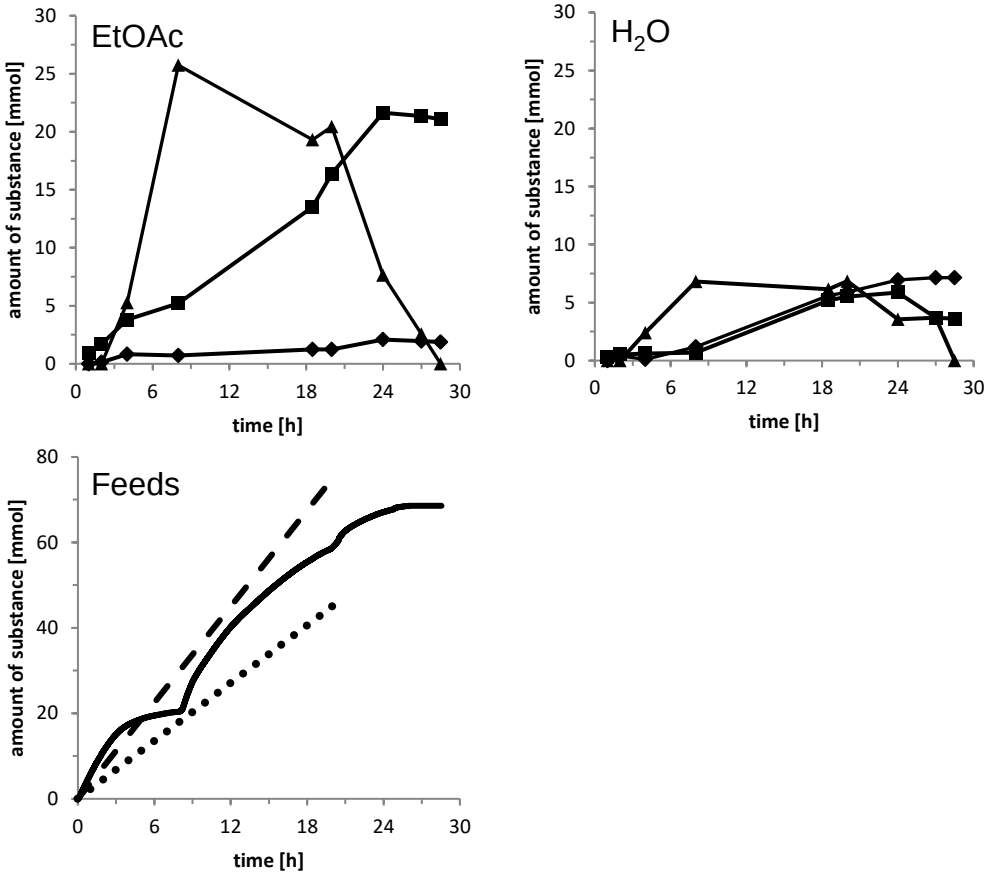

Figure 7. **Biphasic preparative scale bromolactonisation with 200 mL EtOAc and a total end volume 500 mL.** ■ 5-(bromomethyl)dihydro-2(3H)-furanone; ◆ 5-(hydroxymethyl)dihydro-2(3H)-furanone; ▲ 4-pentenoic acid; Feeds:● 4-pentenoic acid 0.6 M and KBr 0.6 M with 3.75 mL/h; H_2O_2 1 M with 3.75 mL/h (dashed line) General conditions: T = 25 °C, pH 5 controlled by pH stat with 1 M acetic acid (solid line), *Ci*VCPO aliquots added (15 nmol) 0 h; 8 h; 25 h; 153 nM *Ci*VCPO.

Further optimisation of some reaction parameters such as feed rates were performed at 500 mL scale (Figure 7). In summary the optimisation resulted in feeds for the 20-fold upscale as following: neat substrate (**1**) (9.8 M) at 4 mL/h together with a feed rate of 37.5 mL/h of KBr (1.2 M) and H_2O_2 (2 M). These feeding conditions turned out to give reasonable productivities of more than 2.3 mM/h corresponding to an average turnover frequency of *Ci*VCPO of more than 10 s^{-1}. The highest amount of bromolactone (**2**) with 21.64 mmol was obtained within 24 h in the EtOAc phase and

only 5.86 mmol of **2** remained in the aqueous phase. The TTN of *Ci*VCPO was 749785 after 28.5 hours at the end of the process. We isolated 4.34 g bromolactone (**2**) from the EtOAc phase with an isolated yield of 46.86% and a purity of 87%.

It is worth mentioning that in these experiments, a significant amount of product **3** (hydroxylactone, only impurity), accounting for approximately one third of the total product, was produced. Comparative experiments showed that the bromolactone (**2**) was stable under the reaction conditions; even upon prolonged incubation in buffer, no conversion of **2** into **3** was observed. We hypothesise that **3** originates from hydrolysis of the intermediate bromonium ion to the corresponding hydroxyl bromide product, the latter is in equilibrium with the corresponding epoxide[12] from which through intramolecular attack by the carboxylate the hydroxylactone may be formed (Scheme 2). Further experiments will clarify the origin of the (seemingly undesired) side reaction.

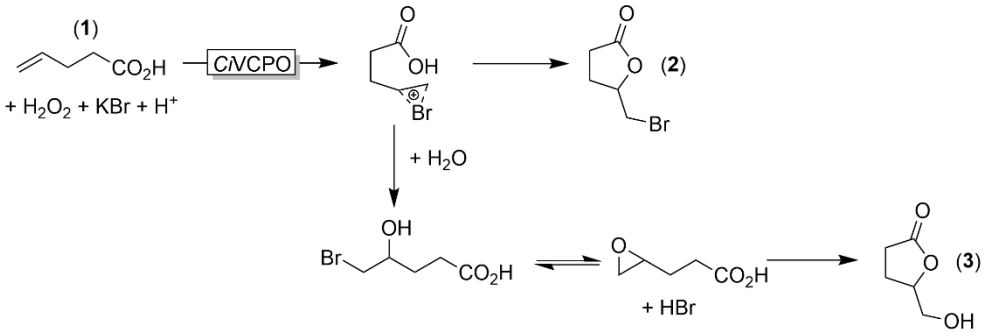

Scheme 2. Hypothesised mechanism for the formation of the hydroxylactone (3).

Also rather unexpectedly, considering the high boiling point temperature of 4-pentenoic acid (**1**) of >180 °C, in these experiments we observed substrate evaporation, which could be solved by using a condenser cooled to approximately 5 °C. Next, we proceeded to a 10 L scale (in a 15 L reactor) reaction using 5 L each of the aqueous reaction mixture (^{dd}water) and of the ethyl acetate organic phase. For safety reasons, to eliminate the possibility of an explosion arising from O_2/ethyl acetate mixtures, the headspace was constantly flushed with a gentle stream of N_2 gas. The time course of this up-scaled reaction is shown in Figure 8. To compensate for the expected pH-increase, we used pH control (acetic acid) to maintain the optimal operational pH of *Ci*VCPO (pH 5).

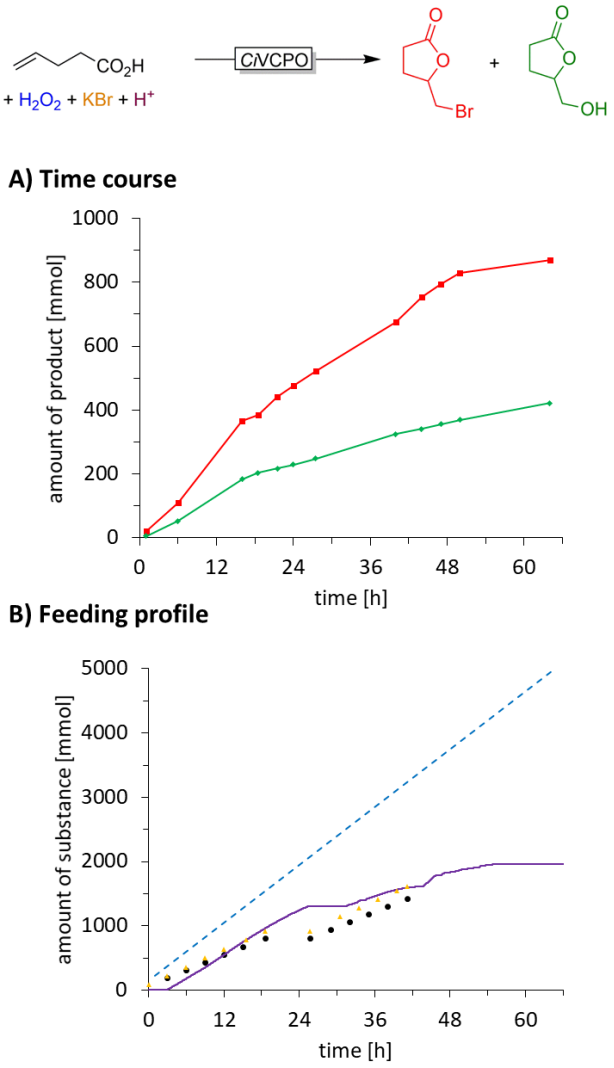

Figure 8. 10 L-scale bromolactonisation of 4-pentenoic acid. A: Time course showing absolute amounts of 2 (■) and 3 (◆); B: Substrate feeding profile (cumulative feed). (●) pure 4-pentenoic acid 9.798 M; 4.04 mL/h; (▲) KBr 1.2 M 37.5 mL/h; (– –) H_2O_2 2M 37.5 mL/h; pH 5 controlled by pH stat with (—) 2 M acetic acid; General conditions: Feeds were started 2h prior to first *Ci*VCPO addition; biphasic system with 5 L EtOAc and a total end volume of 9.84 L; T = 25 °C; 50 rpm after 24 h to 75 rpm; *Ci*VCPO aliquots added (0.3 µmol) 0 h; 6 h; 21.5 h; 27.5 h; 41.5 ; 64 h. Note that the results shown originate from a single experiment. At the start of the reaction, a malfunction of the pH stat lead to hyperacidification of the reaction medium irreversibly inactivating the biocatalyst present at the start of the reaction. Therefore, at t = 2 h, fresh *Ci*VCPO was added (reaction volume = 1.63 L, [4-pentenoic acid] = 49 mM, [KBr] = 55 mM, [H_2O_2] = 92 mM).

In total, 1425 mmol of 4-pentenoic acid (**1**) and equimolar amounts of KBr were fed to the reaction and were converted into 1291 mmol products **2** and **3** (molar ratio approx. 2:1), corresponding to more than 90% yield. The yield in H_2O_2 was less impressive (26%), which we attribute to the undesired reaction of H_2O_2 with hypobromite discussed above. In the course of the reaction, we observed some inactivation of *Ci*VCPO, which was compensated by supplementation with fresh *Ci*VCPO. As *Ci*VCPO generally is a very robust enzyme,[14, 27] we suspect the rigorous stirring as a possible reason for the reduced stability of *Ci*VCPO, but further in-depth studies will be necessary to fully understand the reasons for the reduced *Ci*VCPO stability. Nevertheless, a total turnover number of the enzyme of more than 715000 [$mol_{product} \times mol^{-1}_{CiVCPO}$] was achieved corresponding to the production of more than 770 g of product **2** per gram of *Ci*VCPO.

The product was isolated *via* separation of the organic phase from the reaction phase by centrifugation, drying of $MgSO_4$ and concentration under reduced pressure. The crude product contained acetic acid and the (undesired) hydroxylactone (**3**). Both could be largely removed by treatment with caustic water followed by drying. Overall, 81.4 g of bromolactone (**2**) were obtained with this procedure.

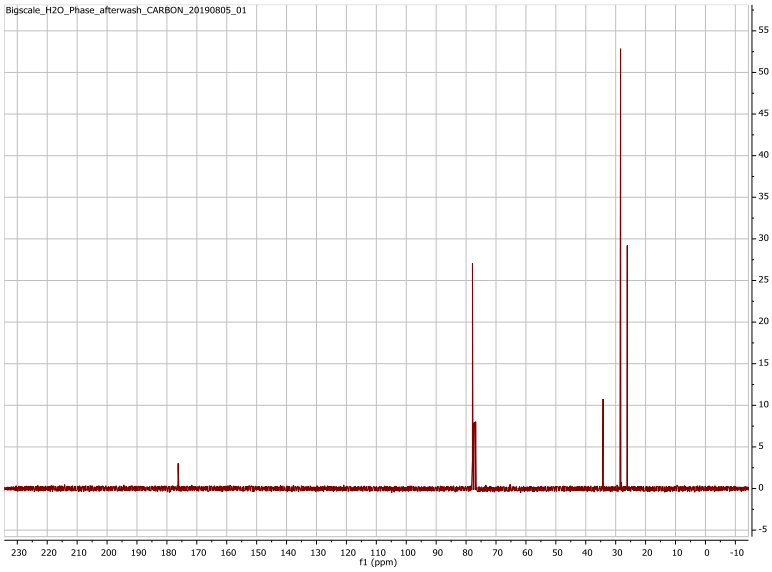

Figure 9. **^{13}C-NMR spectrum of the produced lactones.**

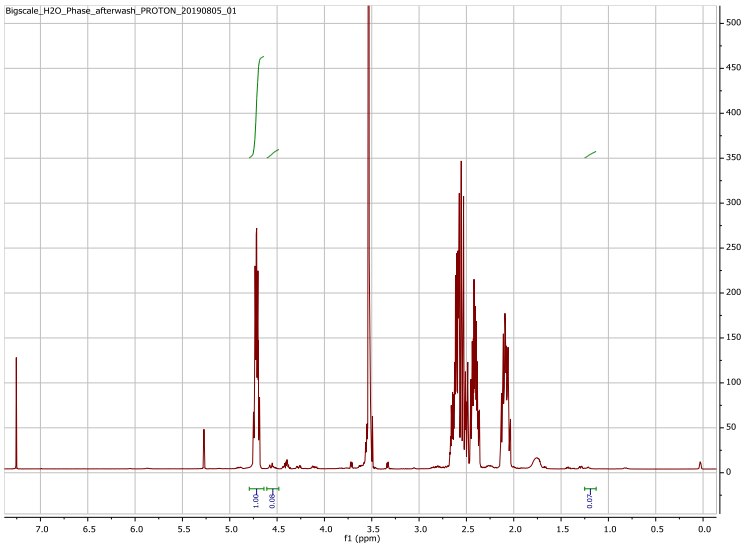

Figure 10. **^{1}H-NMR spectrum of the produced lactones.**

5-(hydroxymethyl)dihydro-2(3H)-furanone): 1H NMR (400 MHz, $CDCl_3$): δ 2.06–2.15 (m, 1 H), 2.18–2.27 (m, 1 H), 2.45–2.63 (m, 2 H), 3.60 (dd, J=4.6, 12.5 Hz, 1 H), 3.85 (dd, *J* = 2.9, 12.5 Hz, 1 H), 4.57–4.62 (m, 1H).

(5-(bromomethyl)dihydro-2(3H)-furanone): 1 H NMR (400 MHz, $CDCl_3$): δ 2.14 (m, 1H: CHHCHO), 2.46 (m, 1H: CHHCHO), 2.53-2.73 (m, 2H, CH_2CO_2), 3.55 (dd, *J* = 5.9, 10.8 Hz, 1H: CHHBr), 3.59 (dd, J = 4.4, 10.8 Hz, 1H: CHHBr), 4.76 (p, J = 6.7, 1H: CHO); ^{13}C NMR (75 Hz, $CDCl_3$): δ 26.6 (CH_2CHO), 28.8 (CH_2Br) 34.5.

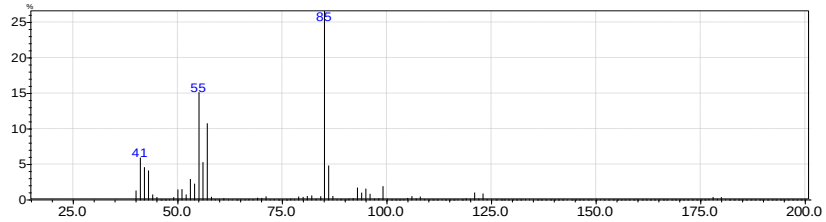

Figure 11. **Mass spectrum 5-(bromomethyl)dihydro-2(3H)-furanone.**

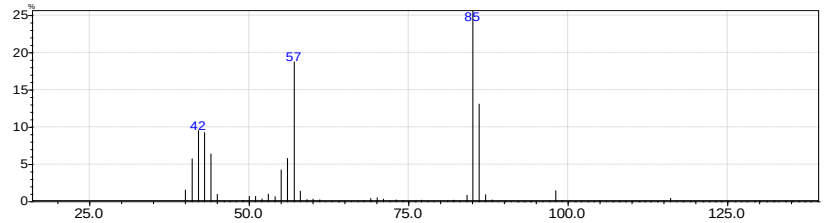

Figure 12. **Mass spectrum 5-(hydroxymethyl)dihydro-2(3H)-furanone.**

Having quantitative data from the 15 L-scale fermentation of *Ci*VCPO as well as the 10 L-scale bromolactonisation at hand, we estimated the environmental impact of the proposed chemoenzymatic production of **2**. Sheldon's E-factor is a very common, simple approach to assess the environmental impact of lab-scale reactions if the data-basis does not allow for a full life cycle assessment.[22-23] The classical E-factor, however, does not take into account CO_2 emissions caused by energy consumed in the process. We therefore used the recently proposed E^+-factor[21] and also measured the electricity used whenever possible. To estimate the electricity-related CO_2-emissions we used the average European CO_2-footprint (i.e. 404 g CO_2 kWh^{-1}).[30] The $E^{(+)}$-factor contributions of the single fermentation and reaction components are listed in Table 1 and Table 2, respectively.

Table 1. Estimation of the E^+-factor for the production of *Ci*VCPO.

Component	Absolute amount	$E^{(+)}$-factor contribution [$g_{waste} \times g^{-1}_{CiVCPO}$]
Fermentation		
Media[a]	805 g	1.188
H_2O	14.000 g	20.650
Cryostat	25.6 kWh (10.3 kg CO_2)	15.278
Stirring and heating	5.68 kWh (2.3 kg CO_2)	3.386
Autoclaving	4.51 kWh (1.8 kg CO_2)	2.689
Centrifugation	16 kWh (6.5 kg CO_2)	9.541
Sum		52.732
Purification		
Buffer components	25 g	37
H_2O	3.320 g	4.900
Total energy[b]	20.87 kWh (8.4 kg CO_2)	12.445
Sum		17.382
Total E^+-factor		70.114

Based on a total yield of 0.678 g of purified *Ci*VCPO; [a] yeast extracts, sugars, buffers, etc.; [b] comprising French press breaking of the cells, centrifuges, FPLC pumps, temperature control.

At first sight, the E^+-factor of *Ci*VCPO is shockingly high as e.g. more than 30 tons of CO_2 per kg of enzyme have been emitted. In addition, the water consumption is very high. Several factors, however, should be considered here. On the one hand, the overexpression of *Ci*VCPO is very low (less than 50 mg L^{-1} fermentation broth); optimised expression systems will certainly yield higher enzyme titers and lower E^+-

factors. Purification also greatly contributed to the overall waste generation, which is why we will consider whole *E. coli* cells in future applications of the enzyme. The environmental impact of enzyme fermentation is also subject to scaling effects and hence may be significantly smaller at industrial scale.[31-32] Finally, it should be kept in mind that *Ci*VCPO is not the final product but rather the catalyst. Hence, due its excellent performance in the bromolactonisation reaction, the immense E^+-factor of *Ci*VCPO is reduced by three orders of magnitude (*vide infra*).

Table 2. Estimation of the E^+-factor for the production of 2.

Component	Absolute amount	E-factor contribution [$g \times g^{-1}_{product}$]
Ethyl acetate	4470 g	55
Water	4839 g	59
*Ci*VCPO	0.1 g	86[a]
Reagents[b]	355 g	4
Cryostat	29.34 kWh (11.9 kg CO_2)	146
Stirring / pump	0.85 kWh (343 g CO_2)	4
Sum		354

Based on a yield of 81.5 g of 2; [a] taking the E^+-factor of *Ci*VCPO (Table 1) into account; [b] (not reacted, by-products, pH control)

Overall, a waste generation of approx. 354 kg per kg of the desired product (**2**) was generated. CO_2 thereby comprised approximately 2/3 of the overall waste generated underlining the importance of taking energy related emissions (wastes) into account!

Conclusion

Overall, in this contribution we demonstrate that the chemoenzymatic bromolactonisation is indeed a practical alternative to the established chemical methods. From a safety point-of-view, we believe that the *in situ* generation of hypobromite is advantageous over its stoichiometric use or the use of elementary bromine. Admittedly, H_2O_2 is not unproblematic but overall easier to handle than HOBr. Furthermore, *in situ* generation of H_2O_2 is principally feasible and may open new avenues for bromolactonisation reactions.[33-34]

The numbers presented here underline the necessity to add energy considerations to the 'classical' E-factor. The CO_2 emissions caused by cooling, stirring and distillation, show that these contributions are in the same order of magnitude as the 'simple' mass balances. We also believe that the E^+-factor can be used as a starting point for further improvements. For example, the contribution of the biocatalyst (its fermentation) underlines the need for better expression systems for *Ci*VCPO as higher enzyme titers will immediately reduce its E^+-factor (contribution). Further process intensification should aim at increasing the product concentrations, which will lead to drastically reduced environmental impacts.

Concerning the product, we envision utilisation as building block for functionalisable polyesters. Lipase-catalysed polymerisation reactions are currently ongoing in our laboratory. The imperfect selectivity of the lactonisation step (yielding bromo- and hydroxylactone) may prove as an advantage form a polymer modification point-of-view as is offers two different functionalities for further modification (Scheme 3).

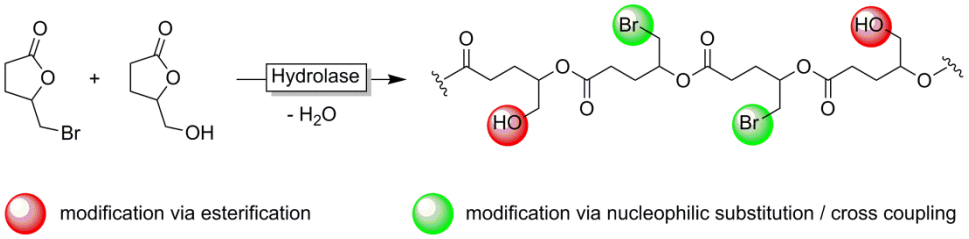

Scheme 3. Envisioned (enzymatic) ring-opening polymerisation of the lactone products obtained in this study to yield polyesters with two different functionalities to synthesise tailored comb-polymers.

Material and methods

Materials

Chemicals were purchased from Sigma-Aldrich, Fluka, Acros or Alfa-Aesar with the highest purity available and used as received.

Preparation of the biocatalysts

Vanadium-dependent chloroperoxidase (CiVCPO)

Bacterial strains and plasmids

The plasmid pBADgIIIB containing the gene encoding vanadium-dependent chloroperoxidase (*Ci*VCPO) was transformed into *E. coli* TOP10 cells. Transformed cells were grown for 1 h at 37 °C in LB without antibiotics. 100 µL were plated out on a LB plate containing ampicillin and incubated overnight at 37 °C. A colony was picked and a pre-culture was grown over night at 37 °C. Glycerol stocks TOP10-*Ci*VCPO containing 15% glycerol were prepared from the pre-culture.

Cultivation conditions

Two 50 mL pre-pre-cultures of LB medium containing 100 µg/mL of ampicillin were inoculated with 5 µL *E. coli* TOP10 pBADgIIIB VCPO glycerol stock and incubated overnight at 37 °C and 180 rpm. Subsequently, two preculture of 200 mL and 500 mL were inoculated with pre-preculture. Overexpression was carried out in 15 L stirred tank reactor with 13 L of TB medium supplemented with 100 µg/mL of ampicillin and cultures were inoculated with 200 mL of pre-culture (OD_{600} = 4.08) to an OD of approx. 0.05 and grown at 37 °C and 180 rpm. When an OD_{600} of 1.0 was reached (approx. 3 h), 15 mL 20% L-arabinose was added to reach a final inducer concentration of 0.02%. After induction, cultures were incubated for additional 24 h at 25 °C and 180 rpm.

CiVCPO purification

The bacterial pellets obtained after centrifugation were re-suspended in 50 mM Tris/H_2SO_4 buffer (pH 8.2). The re-suspended bacterial pellets (0.5 g cells per mL) were stored at -20°C until processed as described below. 0.1 mM PMSF (100 mM stock in isopropanol) was added to the re-suspended cells, which were ruptured with a French press (1.5 Bar) in two cycles. The samples were then centrifuged (10 000 ×g for 20 minutes) and the supernatant was incubated for 0.5 h after reaching 70 °C. The supernatant was again centrifuged for 10 min at 30000 × *g* to remove denaturised protein. Subsequently, the supernatant was concentrated using Amicon membrane filters (30 kDa cut-off). The solution was desalted by exchanging 5 times with 50 mM Tris/H_2SO_4 buffer pH 8.2 and 1 mM ortho vanadate. After centrifugation, the clear supernatant can be used or stored at -20 °C until further purification. Purity of the preparation was accessed by SDS page comparing the band intensities.

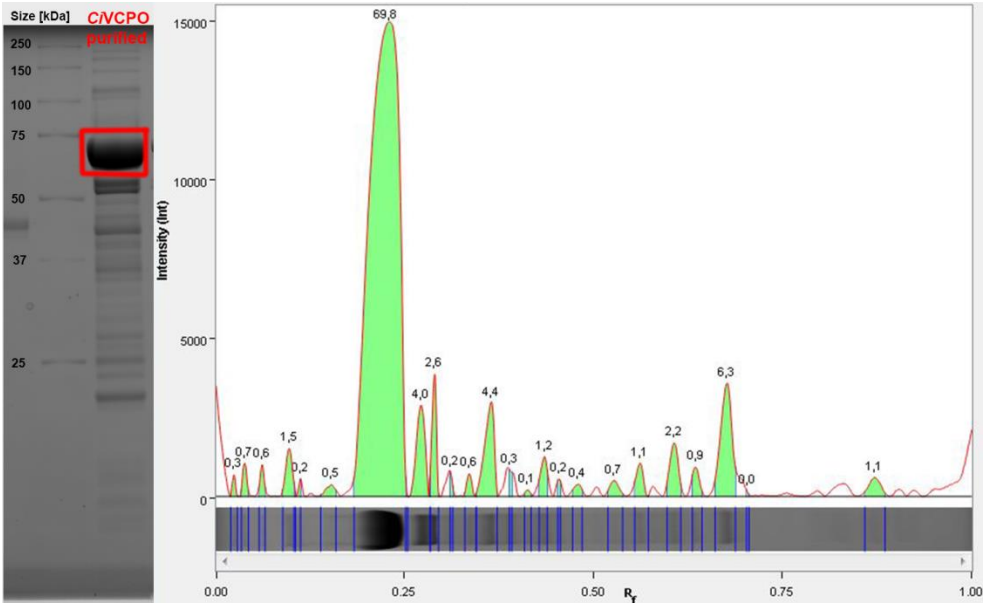

Figure 13. SDS-gel and band intensity of purified *Ci*VCPO.

CiVCPO activity

*Ci*VCPO activity can be qualitatively tested using the MCD assay by incubating aliquots of cell extracts or purified enzyme in 50 mM citrate buffer (pH 5) containing monochlorodimedone (MCD), *o*-vanadate, KBr and H_2O_2. Reaction is started by the addition of *Ci*VCPO and absorption is followed at 290 nm.

100 µL	MCD (0.5 mM)	50 µM
5 µL	KBr (1M)	5 mM
100 µL	o-Vanadate (Na_3VO_4 , 1 mM)	0.1 mM
100 µL	1 M sodium citrate buffer, pH 5.0	0.1 M
5 µL	H_2O_2 (1 M)	5 mM
20 µL	enzyme solution (diluted)	
670 µL	H_2O	

General procedures

4 mL scale reactions

The reactions were performed in 4 mL glass reaction tubes starting with 1 mL reaction mixture containing 200 mM acetate buffer (pH 5) and *Ci*VCPO (200 or 400 nM). The other reaction components were fed separately using a syringe pump at various feed rates (0.033 mL/h – 0.1 mL/h). Stock solutions of 0.6 M 4-pentenoic acid, 1 M H_2O_2, 0.6 mM KBr were used. The feeds were stopped when the end volume of 4 mL was reached. The resulting end concentrations were recalculated. Reactions were followed over time by measuring reactant concentrations via gas chromatography.

pH stat for pH control (200 mL scale)

The scale up reaction was performed in a 500 mL three-neck round bottom flask, containing 200 nM *Ci*VCPO in 50 mL water pH 5 and stirred with a magnetic stirrer (Figure 4). The reaction was fed with 2 separate feeds: 1. 0.6 M 4-pentenoic acid and 0.6 mM KBr (pH 5) and 2.Hydrogen peroxide (1M) (pH 5). Both were fed with a rate of 2.5 mL/h for 20 h. The pH was controlled with a pH STAT titration system (Metrohm pH 5.0, 25 °C) using 1 M acetic acid to adjust the pH. The reaction could

be followed online monitoring the amount of acidic acid added. Substrate and product concentration were measured via gas chromatography. After 21 h an additional aliquot of *Ci*VCPO was added. In total 50 mL acetic acid were added. The end volume of *ca.* 200 mL corresponds to 150 mM 4-pentenoic acid, 150 mM KBr, 250 mM H_2O_2, 100 nM *Ci*VCPO, 250 mM acetic acid.

pH stat for pH control and substrate feed (170 mL scale)

In a subsequent experiment we used the same experimental setup but the pH was adjusted by addition of 0.6 M 4-pentenoic acid and KBr (Figure 5). Only H_2O_2 (0.75 M) was fed with a rate of 2.5 mL/h. After 10.25 h an additional aliquot of *Ci*VCPO was added to keep the reaction rate high and prevent a stop of the reaction as observed before. After 13.5 h the pH stat fed 50 mL 0.6 M pentenoic acid and KBr in total and the pH stat was stopped automatically. This unfortunately also stopped the stirring for approx. 15 min until the pH stat was started again feeding 1 M acetic acid. Without stirring white precipitated formed, probably caused by locally occurring high concentrations of H_2O_2. To compensate for possible *Ci*VCPO activity loss 1/5 of *Ci*VCPO aliquot was added after 19 h. The switch to acetic acid in the pH stat was to convert the accumulated 4-pentenoic acid. To get some of the evaporated substrate back in solution the reaction vessel was inverted.

Preparative scale - 500 mL reaction

The preparative scale reaction was performed in a 500 mL three-neck round bottom flask, containing 200 nM *Ci*VCPO (15 nmol) in 75 mL water pH 5 and stirred with a magnetic stirrer (Figure 7). As a second layer 200 mL ethyl acetate were applied. The reaction was fed with 2 separate feeds: 1) 0.6 M 4-pentenoic acid and 0.6 mM KBr (pH 5) and 2) Hydrogen peroxide (1 M) (pH 4). Both were fed with a rate of 3.75 mL/h for 20 h. The pH was controlled by a pH STAT titration system (Metrohm, pH 5.0, 25 °C) using 1 M acetic acid solution. The reaction was followed online monitoring the amount of acidic acid added. Substrate and product concentration of both phases were measured *via* gas chromatography. An additional aliquot of 15 nmol *Ci*VCPO was added after 8 h and 25 h. In total 68.5 mL 1 M acetic acid were

added. The end volume reached was *ca.* 494 mL. The amount of enzyme applied in the final reaction volume was 45 nmol.

Pilot scale - 10 L reaction

The pilot scale reaction was performed in a 15 L stirred tank reactor (autoclavable bioreactor from Applikon©) equipped with a pH sensor, condenser at 5 °C, stirring 100 rpm. The head space of the reactor was flushed with a soft nitrogen flow. Starting with 5 L of ethyl acetate phase and 1.5 L of aqueous phase. Feeding pure substrate and 2 M acetic acid from the top into the ethyl acetate phase. H_2O_2 (2 M) and KBr (1.2 M) were fed into the aqueous phase through the gas inlet of the reactor with a feeding rate of 37.5 mL/h. The reaction was started with a *Ci*VCPO aliquot of 0.3 µmol. Substrate and product concentration of both phases were measured by gas chromatography. After the reaction the ethyl acetate phase was dried with magnesium sulfate (1 kg) and the solvent was removed by rotary evaporation at 30 °C with 200 mbar pressure. Residual acetic acid was removed by washing with water and potassium carbonate.

Analytical procedures

GC-analyses

Samples of 0.02 mL reaction mixture were extracted with 0.2 mL ethyl acetate and dried with magnesium sulfate. As internal standard 5 mM acetophenone was used. Analysis were performed with Shimadzu GC-2010 plus gas chromatograph with an AOC-20i Auto injector (injection temperature 250 °C) and flame ionization detection (FID). The carrier gas of the GC was nitrogen with a flow of 31.5 cm × s^{-1}.

Table 3. GC analysis specifications for concentration determination

Compounds (retention time)	GC column	GC oven programme
4-pentenoic acid (5.1 min)/ 5-(hydroxy)dihydro-2(3H)-furanone (9.5 min)/ 5-(bromomethyl)dihydro-2(3H)-furanone (10.5 min)/ acetophenone (8 min)	CP-Sil 5 CB GC column (25 m x 0.25 mm x 1.2 µm)	70 °C for 1 min. 30 °C/min to 140 °C hold for 2 min. 30 °C/min to 195 °C hold for 2 min. 30 °C/min to 225 °C hold for 1 min. 30 °C/min to 345 °C hold for 1 min.

GC-MS-analyses

Gas chromatography-mass spectrometry was performed with the Shimadzu GC-2010 system which is connected to the GCMS-QP2010s mass detector from Shimadzu. The carrier gas of the GC was nitrogen with a flow of 31.5 cm × s^{-1}.

Table 4. GC-MS analysis specifications for structure determination

Compounds (retention time)	GC column	GC oven programme
4-pentenoic acid (5.1 min)/ 5-(hydroxy)dihydro-2(3H)-furanone (9.5 min)/ 5-(bromomethyl)dihydro-2(3H)-furanone (10.5 min)/ acetophenone (8 min)	CP-Sil 5 CB GC column (25 m x 0.25 mm x 0.4 µm)	70 °C for 1 min. 30 °C/min to 140 °C hold for 2 min. 30 °C/min to 195 °C hold for 2 min. 30 °C/min to 225 °C hold for 1 min. 30 °C/min to 345 °C hold for 1 min.

References

[1] A. C. Albertsson, I. K. Varma, *Biomacromolecules* **2003**, *4*, 1466-1486.
[2] G. Höfler, A. But, F. Hollmann, *Org. Biomol. Chem.* **2019**.
[3] R. Kristianslund, J. E. Tungen, T. V. Hansen, *Org. Biomol. Chem.* **2019**, *17*, 3079-3092.
[4] M. Grabarczyk, K. Winska, W. Maczka, *Curr. Org. Synth.* **2019**, *16*, 98-111.
[5] E. E. Alberto, L. M. Muller, M. R. Detty, *Organometallics* **2014**, *33*, 5571-5581.
[6] E. E. Alberto, A. L. Braga, M. R. Detty, *Tetrahedron* **2012**, *68*, 10476-10481.
[7] D. E. Higgs, M. I. Nelen, M. R. Detty, *Org. Lett.* **2001**, *3*, 349-352.
[8] S. M. Bennett, Y. Tang, D. McMaster, F. V. Bright, M. R. Detty, *J. Org. Chem.* **2008**, *73*, 6849-6852.
[9] J. P. Ariyarathna, F. Wu, S. K. Colombo, C. M. Hillary, W. Li, *Org. Lett.* **2018**, *20*, 6462-6466.
[10] S. H. H. Younes, F. Tieves, D. M. Lan, Y. H. Wang, P. Suss, H. Brundiek, R. Wever, F. Hollmann, *ChemSusChem* **2020**, *13*, 97-101.
[11] X. Xu, A. But, R. Wever, F. Hollmann, *Chemcatchem* **2020**.
[12] J. J. Dong, E. Fernandez-Fueyo, J. B. Li, Z. Guo, R. Renirie, R. Wever, F. Hollmann, *Chem. Commun.* **2017**, *53*, 6207-6210.
[13] E. Fernandez-Fueyo, S. H. H. Younes, S. van Rootselaar, R. W. M. Aben, R. Renirie, R. Wever, D. Holtmann, F. P. J. T. Rutjes, F. Hollmann, *ACS Catal.* **2016**, *6*, 5904-5907.
[14] E. Fernandez-Fueyo, M. van Wingerden, R. Renirie, R. Wever, Y. Ni, D. Holtmann, F. Hollmann, *ChemCatChem* **2015**, *7*, 4035-4038.
[15] A. But, J. Le Notre, E. L. Scott, R. Wever, J. P. M. Sanders, *ChemSusChem* **2012**, *5*, 1199-1202.
[16] R. Renirie, C. Pierlot, J. M. Aubry, A. F. Hartog, H. E. Schoemaker, P. L. Alsters, R. Wever, *Adv. Synth. Catal.* **2003**, *345*, 849-858.
[17] J. W. P. M. Vanschijndel, E. G. M. Vollenbroek, R. Wever, *Biochim. Biophys. Acta.* **1993**, *1161*, 249-256.
[18] X. J. Jiang, S. H. Liu, S. Yang, M. Jing, L. P. Xu, P. Yu, Y. Q. Wang, Y. Y. Yeung, *Org. Lett.* **2018**, *20*, 3259-3262.
[19] R. Ding, L. Y. Lan, S. H. Li, Y. G. Liu, S. X. Yang, H. Y. Tian, B. G. Sun, *Synthesis* **2018**, *50*, 2555-2566.
[20] J. M. J. Nolsoe, T. V. Hansen, *Eur. J. Org. Chem.* **2014**, *2014*, 3051-3065.
[21] F. Tieves, F. Tonin, E. Fernandez-Fueyo, J. M. Robbins, B. Bommarius, A. S. Bommarius, M. Alcalde, F. Hollmann, *Tetrahedron* **2019**, *75*, 1311-1314.
[22] R. A. Sheldon, *ACS Sustain. Chem. Eng.* **2018**, *6*, 32-48.
[23] R. A. Sheldon, *Green Chem.* **2017**, *19*, 18-43.
[24] Y. Ni, D. Holtmann, F. Hollmann, *ChemCatChem* **2014**, *6*, 930-943.
[25] S. G. Brand, C. J. Hawkins, D. L. Parry, *Inorg. Chem.* **1987**, *26*, 627-629.
[26] A. S. Tracey, M. J. Gresser, K. M. Parkinson, *Inorg. Chem.* **1987**, *26*, 629-638.
[27] J. W. P. M. Vanschijndel, P. Barnett, J. Roelse, E. G. M. Vollenbroek, R. Wever, *Eur. J. Biochem.* **1994**, *225*, 151-157.
[28] S. Kara, D. Spickermann, J. H. Schrittwieser, A. Weckbecker, C. Leggewie, I. W. C. E. Arends, F. Hollmann, *ACS Catal.* **2013**, *3*, 2436-2439.
[29] P. G. Jessop, *Green Chem.* **2011**, *13*, 1391-1398.
[30] I. E. Agency, CO2 emissions from fuel combustion, **2017**.
[31] P. H. Nielsen, K. M. Oxenboll, H. Wenzel, *Int. J. Life Cycle Ass.* **2007**, *12*, 432-438.
[32] K. R. Jegannathan, P. H. Nielsen, *J. Clean Prod.* **2013**, *42*, 228-240.
[33] B. O. Burek, S. Bormann, F. Hollmann, J. Z. Bloh, D. Holtmann, *Green Chem.* **2019**, *21*, 3232-3249.
[34] F. Tieves, S. J. P. Willot, M. M. C. H. van Schie, M. C. R. Rauch, S. H. H. Younes, W. Y. Zhang, J. J. Dong, P. G. de Santos, J. M. Robbins, B. Bommarius, M. Alcalde, A. S. Bommarius, F. Hollmann, *Angew. Chem. Int. Edit.* **2019**, *58*, 7873-7877.

Chapter 5

Chapter 5: Conclusion

Georg T. Höfler, Caroline E. Paul, Isabel W.C.E. Arends and Frank Hollmann

Biocatalysis is a promising research field for more sustainable processes in the chemical industry. In many cases, it enables the valorisation of low value resources through a cost-effective, biodegradable and sustainable alternative with respect to common catalysis. The most applied biocatalysts are hydrolases due to their independence on cofactors and the inherent simplicity of the reaction. However, access to industrially relevant redox chemistry is unattainable with these enzymes. The chemical nature of redox reactions requires a stoichiometric supply of redox equivalents. In classical chemistry, these are often hazardous and environmentally questionable compounds such as chromium oxide for oxidation or sodium borohydride for reduction. Nowadays, however, oxidants such as O_2 and H_2O_2 and reductants such as H_2 are investigated and to some extent already used industrially.

Oxidoreductases are outstanding catalysts for redox reactions and their redox equivalents can be supplied by less hazardous and more environmentally friendly sources, compared to classical methods.[1] As noted, their dependency on specific cofactors as electron mediators for those sources is limiting their applicability. Therefore, the most easily applied oxidoreductases are oxidases due to their simple requirement for molecular oxygen. However, the range of reactions these enzymes can catalyse is limited by substrate specificity and thermodynamics, strongly favouring oxidation. To enlarge the application of various sorts of oxidoreductases in general, the *in situ* supply of redox equivalents is vastly investigated.
Redox equivalents can originate from cost-effective and abundant sacrificial electron donors through the use of photocatalysis. In this case, even water (through catalytic

water splitting) in addition to abundant amines and acids can act as reductant. This research thesis aimed to identify efficient combinations of redox biocatalysis with photocatalysis to supply redox equivalents, thus facilitating the application of oxidoreductases. Different combinations of photo- and biocatalysts were investigated. The cofactors that are required are versatile and differ in their complexity. We focused on one important cofactor and one simpler cosubstrate respectively: NADH for the reduction catalysed by alcohol dehydrogenases (ADH) and H_2O_2 for the oxidation catalysed by peroxidases, in our case a haloperoxidase.

Photoenzymatic regeneration of NADH

The investigations in chapter 2 on a photoenzymatic NADH regeneration system demonstrated that the combination of 5-deazariboflavin (dRf) as photocatalyst and putidaredoxin reductase (PDR) from *Pseudomonas putida* was feasible. The formation of biologically active NADH by PDR was proven *via* a ketoreduction catalysed by the NADH-dependent alcohol dehydrogenase from *Rhodococcus ruber* DSM 44541 (ADH-A) (Scheme 1).

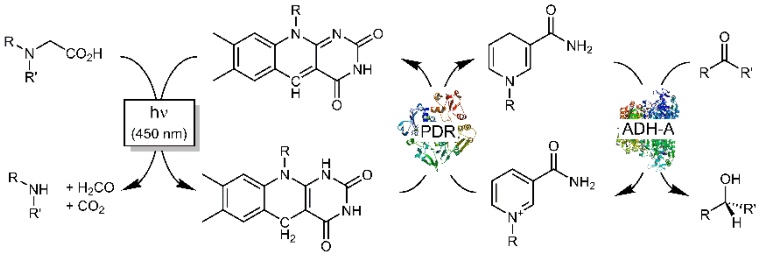

Scheme 1. Photoenzymatic reduction of NAD^+ to promote alcohol dehydrogenase (ADH)-catalysed stereospecific reduction of ketones.

This system proved that PDR, against its natural function, can also be used for the reduction of NAD^+ to NADH. The total turnover number for NAD^+ of 21 is reasonable compared with other light-driven NADH regeneration systems introduced in Chapter 1 performing in a range of single digit to hundred turnovers of NADH. However, this catalytic turnover of NAD^+ is far away from industrial requirements, where a range of 10^3-10^5 turnovers is considered economically sufficient.[2] Furthermore, the

regeneration rate is very low with approximately 9×10^{-4} s^{-1}, whereas applied systems reach turnover rates of 2 s^{-1}.[2-3]

Limitations causing the poor performance, most importantly the low robustness of the system, were identified. The well-known photodegradation of the flavin prosthetic group in PDR is one possible explanation, since renewed addition of PDR can lead to prolonged reaction times.[4-6] Moreover, it turned out to be essential to work under strict anaerobic conditions for the successful regeneration of NADH to prevent oxidative uncoupling of the regeneration reaction from the production reaction, discussed previously. The presence of oxygen causes the reduced photocatalyst to form hydrogen peroxide and reactive oxygen species (ROS) such as superoxide radical anions or singlet oxygen.[7-9] The oxidative uncoupling does not only lead to a loss of redox equivalents, but the ROS are additionally decreasing enzyme activity by protein oxidation.[10]

Moreover, insufficient chemoselectivity of the dRf leads to photochemical side reactions, such as the direct reduction of NAD^+ by dRf that forms the undesired NAD-dimer and enzyme-inactive NAD isomers.[11] To minimise these undesired side reactions the system requires application of PDR in a high enzyme/photocatalyst ratio. Hence, the poor photostability and photocatalytic side reactions result in relatively low total turnovers of the enzyme and respectably the cofactor.

Unexpectedly, photocatalysis is creating rather harsh conditions for biocatalysis frequently leading to the inactivation of enzymes. The application of photocatalysts absorbing light at different wavelengths than that of the prosthetic groups of the enzyme might be beneficial to prevent their photodegradation, for instance in the case of flavin-dependent relay enzymes. Further smart catalyst design, possibly immobilising the enzyme could decrease robustness issues by protecting the enzyme backbone. To make this system environmentally and economically feasible, EDTA as an electron donor is far from practical, especially concerning the atom efficiency, therefore other electron donors should be investigated. Identifying other photocatalysts able to oxidise cheap electron donors like water is a possible next step. However, it is crucial these photocatalysts maintain sufficiently mild conditions

to protect the enzyme from inactivation and possess adequate chemoselectivity to prevent undesired side reactions.

- The photoenzymatic NADH regeneration with this system is possible
- Low regeneration rate and low robustness of the system
- Identify other bio compatible photocatalysts

The photocatalytic generation of H_2O_2 to fuel a haloperoxidase

Noting that one of the main issues when combining photocatalysis with biocatalysis is the enzyme stability, it seems logical to focus on the application of extraordinary stable enzymes. Furthermore, since the formation of hydrogen peroxide in aerobic conditions cannot be prevented in many cases, we decided to use a heterogeneous photocatalyst (graphitic carbon nitride (g-C_3N_4-25K)) to supply hydrogen peroxide instead in combination with peroxidases as catalysts (Scheme 2).
The thermostable vanadium-dependent chloroperoxidase from *Curvularia inaequalis* (*Ci*VCPO), known for its robustness, was chosen to be photocatalytically supplied with hydrogen peroxide. Simultaneously, more atom efficient electron donors like formate or even water are applied to improve environmentally viability. The illumination of g-C_3N_4-25K catalysed the formation of hydrogen peroxide using either water or formate as sacrificial electron donor. The better kinetic performance regarding the hydrogen peroxide formation applying formate as electron donor made it the better choice compared to just water.

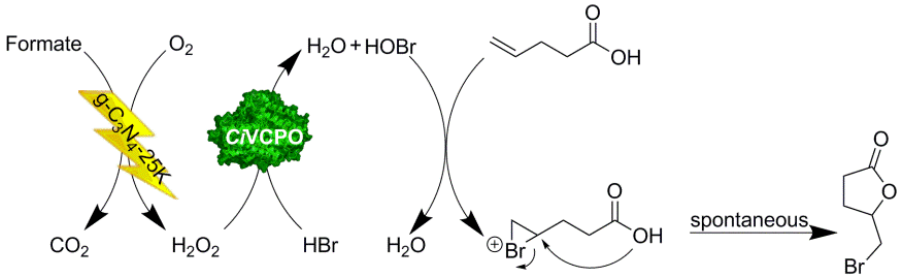

Scheme 2. Photocatalytic generation of H_2O_2 to fuel a haloperoxidase.

Unexpectedly and despite its stability, the *Ci*VCPO was found to be bound to the photocatalyst and was inactivated rapidly. ROS can be formed on the surface of the

photocatalyst and expose *Ci*VCPO locally to very high concentrations of ROS probably causing the strong inactivating effect. Additionally, we observed strong side-product formation caused by direct contact of the substrate with the photocatalyst. These issues of photocatalysis can be prevented by physical separation of the photocatalytic and enzymatic reaction. The separation leads to a stable reaction forming solely desired product.

In summary, the physical separation of the photocatalyst from the biocatalyst is an option for combining photocatalysis with biocatalysis. Nevertheless, the experimental setup needs to be optimised in order to allow for a continuous performance. An interdisciplinary effort from heterogeneous catalysis and biocatalysis could improve the compatibility further, shaping and tuning both catalysts for a better synergy.

- Photocatalytic supply of H_2O_2 to a haloperoxidase is possible
- Physical separation is critical to improve robustness
- Process and catalyst design could improve compatibility

Application of CiVCPO for a scalable and greener halogenation reaction

The results highlighted above indicate that biocatalysts are more strongly influenced by the photocatalysts than initially anticipated. To proof however the high potential of *Ci*VCPO as biocatalyst, photocatalysis aside, an upscaling study was performed. A chemoenzymatic halocyclisation of 4-pentenoic acid at preparative scale was carried out (Scheme 3). The chemoenzymatic bromolactonisation is a practical alternative to established chemical methods. The *in situ* formation of hypobromite by *Ci*VCPO is safer and advantageous over its stoichiometric use or the use of elementary bromine.

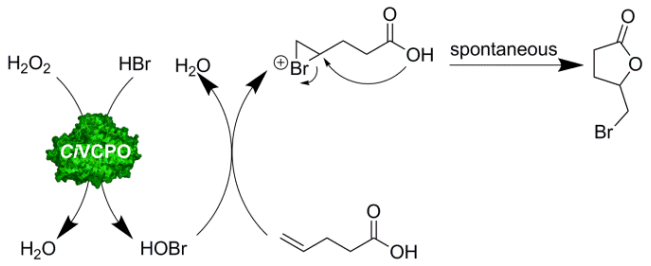

Scheme 3. Vanadium chloroperoxidase (*Ci*VCPO)-catalysed bromolactonisation of 4-pentenoic acid.

In order to upscale a reaction, both volume and concentrations need to be increased. Unexpectedly, the *Ci*VCPO was inhibited by high concentrations of the 4-pentenoic acid. Furthermore, the known competitive inhibition by KBr was strongly pronounced at these high concentrations. The reaction showed a strong increase of pH despite high buffer concentrations. Moreover, high amounts of hydrogen peroxide are wasteful due to the shunt reaction consuming hypobromite as well as hydrogen peroxide.

To enable high product concentrations despite the inhibitions and the strong pH shift a fed-batch strategy with pH control was carried out. In addition, a biphasic system was used, which allowed the use of highly concentrated feeds. The online regulation of the pH indicated inactivation of *Ci*VCPO after several hours despite its high stability under normal conditions. Nevertheless, due to its high activity in optimised feeding conditions even repeated addition does not interfere with an outstanding turnover number.

Overall, 81.4 g of bromolactone were obtained with this procedure. The total turnover number of *Ci*VCPO with 715000 [$mol_{product} \times mol^{-1}_{CiVCPO}$] is reaching the range of 10^6-10^7 required by the fine chemical industry.[12] Furthermore, the obtained 770 $g_{product} \times g^{-1}_{CiVCPO}$ also comply to the desired productivity of free enzymes in the biocatalytic production of fine chemicals with the reported range of 670-1700 $g_{product} \times g^{-1}_{enzyme}$. [13]

Whereas it might be debateable if the bromolactone itself qualifies as fine chemical with further valorisation of the monomer by polymerisation, we are confident the resulting polymer would classify as fine chemical. The E^+-factor of the overall process (reaction and downstream processing) was 354 $kg_{Waste} \times kg^{-1}_{product}$. For an

environmentally-friendly application this value is still too high, but the calculation of the single parameters contributing to the E^+-factor is crucial to improve the system further and reduce the environmental impact. For example, the addition of hydrogen peroxide is of no concern from an environmental point of view. On the other hand, a more environmentally friendly purification step would be very beneficial. The heat-purification is an easy to perform purification step, but the heating is an immense energy drain. As an alternative the precipitation of undesired protein by solvent treatment is imaginable. Arguably, the environmental benefit is strongly dependent on the choice of solvent. Positively, the removal of solvent would not require any additional steps, since in the following desalting step, necessary to prevent undesired halogenations, would also serve this purpose thereby not complicating the easy procedure. Furthermore, the relatively low expression levels should be increased by finding better expression system for instance *Pichia pastoris*.

The main disadvantage of *Ci*VCPO from a biocatalytic point of view is its apparent lack of selectivity. Substrates specificity and regioselectivity for certain haloperoxidases has been reported but is still not well understood and investigations should be intensified.[14] Adding the major advantage of enzymes, superb selectivity, to *Ci*VCPO would certainly make it one of the most remarkable biocatalysts developed.

We could show that this biocatalytic reaction is well scalable, maintaining the magnitude of key parameters like TTN, product concentrations and $g_{product} \times g^{-1}_{enzyme}$ consistent during the scale-up. The pursuit of higher-turnover-number catalysts represents an important research direction and might be more important than recyclable catalysts.[15] Further optimised process engineering could enable application of even higher concentrated feeds like 50% H_2O_2 thereby further reducing dilution by feeding and possibly reach even higher concentrations. A better choice of solvent could further improve the downstream processing. The substitution of acetic acid for pH adjustment with an inorganic acid to prevent problems in the downstream process is highly recommended.

The application of *Ci*VCPO can contribute to sustainable solutions for industrial oxidations. One example is the synthesis of profitable halogenated compounds by means of mild *in-situ* generation of hypohalites.

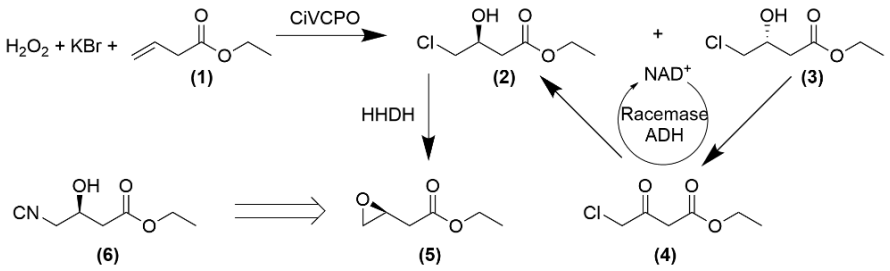

Scheme 4. Envisioned dynamic kinetic resolution of an atorvastatin intermediate.

As described in Chapter 1, a two-step, three-enzyme process for the synthesis of a key intermediate of atorvastatin could be envisioned as a process including *Ci*VCPO.[16] The biocatalytic cascade shown in Scheme 4 proposes an alternative process applying *Ci*VCPO, ADH-Racemase and halohydrin dehalogenase (HHDH) and includes an alternative starting material.[17] *Ci*VCPO catalyses the formation of the ethyl 4-chloro-3-hydroxybutyrate (2+3) in mild conditions *via* the hypochlorite. The obtained ethyl (*S*)-4-chloro-3-hydroxybutyrate (**2**) will be converted by the HHDH to enantiopure epoxide (**5**). As recently reported in several studies, enantio-unselective ADHs can be used for the racemisation of chiral alcohols.[17] The combination of the racemase-ADH and HHDH can be applied for the dynamic kinetic resolution of the epoxide (**6**). This is only one possible example how *Ci*VCPO could be relevant for important industrial processes.

In addition, apart from the production of chemicals, *Ci*VCPO can contribute to sustainable solutions for oxidative treatments or cleaning. Using nature as a role model one could envision the application of *Ci*VCPO in its natural capacity providing hypohalites as antimicrobial detergents. The use of this incredibly stable enzyme as additive in anti-fouling coatings for ships has been close to application.[18-19] Furthermore, the development of dry sanitation bags to provide sterile alternatives for people without sanitation is an interesting possible application.[20] For this, the inside of a biodegradable plastic bag could be coated with a mixture of enzymes, including *Ci*VCPO as catalyst for antimicrobial production. Human faeces with a median pH of 6.64, composed of mainly water and bacterial biomass containing also undigested carbohydrates, fibres, proteins, and fats, provides possible substrates to produce the necessary hydrogen peroxide.[21] This would probably allow for a more

local production and solution of the sanitary problem. The company Exoxemis already develops haloperoxidase products for prevention and treatment of serious infections, to address the growing problem of microbial drug resistance. However, their chosen heme haloperoxidase could possibly be outperformed by *Ci*VCPO in terms of stability and catalytic activity since the *Ci*VCPO is an outstanding member of this enzyme class.

- Scalability of a biocatalytic process has been demonstrated
- Performance relevant for industrial application could be achieved
- *Ci*VCPO is a viable alternative for the *in situ* generation of hypohalites and "can even be handled by a chemists" [22]

As a general conclusion, the combination of biocatalysis with photocatalysis is in principle possible, but is accompanied by many challenges. Interdisciplinary efforts could help paving the road towards a more robust and applicable photo-biocatalysis in the future.

For this purpose, the field of biocatalysis could investigate how nature is coping with oxidative and radical stress in phototroph organisms forming more robust systems. Microorganisms that are exposed to high light intensities have evolved specific mechanisms to prevent photooxidative stress. These mechanisms include the use of quenchers, such as carotenoids, which interact either with excited photosensitiser molecules or singlet oxygen itself to prevent damage of cellular molecules. In contrast to radical scavengers like glutathione, which react with singlet oxygen irreversible, the quenchers can in theory be regenerated.

However, these *in vivo* mechanisms are rather complex and might be to inconvenient to use *in vitro*. Moreover, they might increase robustness of the system, but do not prevent the loss of redox equivalents through the undesired ROS side reactions. The use of antibodies on the other hand could be a more elegant solution. A universal ability of antibodies to generate H_2O_2 from $^1O_2$ and water has been reported. This could solve the problem of ROS at the root, improving the robustness and redox equivalent efficiency of light-driven peroxidase systems simultaneously.[23]

Additionally, starting the thorough investigation of already photo active enzymes from phototroph organisms seems promising. These enzymes have been optimised by nature to work together with light over millennia and the reasons for their synergy has to be understood more profoundly to facilitate photo-biocatalysis. Even if we cannot explain the reasons for the improved synergy, from the field of protein engineering we know it is easier to improve an already present, even if very weak, activity compared to introducing a completely new activity into a protein. Therefore, starting with an enzyme that already possesses weak photo-biocatalytic activity and evolving the enzyme for the desired process could be beneficial.
From an industrial point of view, the current approaches are magnitudes away from being applicable. Performance regarding total turnover numbers, turnover frequencies, product concentrations and process stability need to be improved. The key issue being the radical nature of photocatalysis impairing the robustness of biocatalytic reactions.

Biocatalysis itself provides a viable alternative to common catalysis. In order to further develop this field and promote its application, the focus should be on reporting honest and comparable numbers. We need to catch the attention of classic chemists to the competitiveness and advantages of biocatalysis by demonstrating the ability to reach high total turnover numbers, high turnover frequencies, product concentrations relevant for industry purposes and extraordinary selectivity. Further process intensification should aim at increasing the product concentrations, which will lead to drastically reduced environmental impacts. The investigation of sustainability should be further intensified. The determination of the E^+-factor is a start, using a simple tool to assess environmental impact. A life-cycle assessment would shine light on the real impact of processes.[24] Unfortunately, its complexity makes it difficult to assess for a single scientists and more specialised analysts for the life-cycle assessment will be required.
The tuneable and thereby adaptable nature of enzymes makes them the most promising future for catalysis. At the foundation of outstanding advances in humanity is the written word and the understanding of it. Highly comparable to the binary code forming the basis of the computer science era, also the centre of biocatalysis, an

enzyme, is based on the quaternary code of the DNA. The decipherment and use of this language will bring on the era of biocatalysis and biotechnology for a hopefully sustainably future.

References

[1] F. Hollmann, I. W. C. E. Arends, K. Buehler, *ChemCatChem* **2010**, *2*, 762-782.
[2] W. A. van der Donk, H. M. Zhao, *Curr. Opin. Biotechnol.* **2003**, *14*, 421-426.
[3] V. I. Tishkov, V. O. Popov, *Biochemistry-Moscow+* **2004**, *69*, 1252.
[4] W. Holzer, J. Shirdel, P. Zirak, A. Penzkofer, P. Hegemann, R. Deutzmann, E. Hochmuth, *Chem. Phys.* **2005**, *308*, 69-78.
[5] P. S. Song, D. E. Metzler, *Photochem. Photobiol.* **1967**, *6*, 691-709.
[6] W. M. Moore, S. D. Colson, J. T. Spence, F. A. Raymond, *J. Am. Chem. Soc.* **1963**, *85*, 3367-3372.
[7] D. Holtmann, F. Hollmann, *ChemBioChem* **2016**, *17*, 1391-1398.
[8] A. Fujishima, X. T. Zhang, D. A. Tryk, *Surf. Sci. Rep.* **2008**, *63*, 515-582.
[9] T. Daimon, T. Hirakawa, M. Kitazawa, J. Suetake, Y. Nosaka, *Appl Catal a-Gen* **2008**, *340*, 169-175.
[10] M. J. Davies, *Biochem. Bioph. Res. Co.* **2003**, *305*, 761-770.
[11] F. Hollmann, A. Schmid, *Biocatal. Biotransfor.* **2004**, *22*, 63-88.
[12] J. Hagen, *Industrial catalysis: a practical approach*, John Wiley & Sons, Hoboken, United States, **2015**.
[13] P. Tufvesson, J. Lima-Ramos, M. Nordblad, J. M. Woodley, *Org. Process. Res. Dev.* **2011**, *15*, 266-274.
[14] A. Butler, J. N. Carter-Franklin, *Nat. Prod. Rep.* **2004**, *21*, 180-188.
[15] J. A. Gladysz, *Pure Appl. Chem.* **2001**, *73*, 1319-1324.
[16] S. K. Ma, J. Gruber, C. Davis, L. Newman, D. Gray, A. Wang, J. Grate, G. W. Huisman, R. A. Sheldon, *Green Chem.* **2010**, *12*, 81-86.
[17] M. M. Musa, J. M. Patel, C. M. Nealon, C. S. Kim, R. S. Phillips, I. Karume, *J. Mol. Catal. B-Enzym* **2015**, *115*, 155-159.
[18] R. W. a. W. Hemrika, *Handbook of Metalloproteins - Vanadium haloperoxidases*, John Wiley & Sons, Ltd,, Chichester, England, **2001**.
[19] G. W. Gribble, *J. Nat. Prod.* **1992**, *55*, 1353-1395.
[20] I. F. Persoon, M. A. Hoogenkamp, A. Bury, P. R. Wesselink, A. F. Hartog, R. Wever, W. Crielaard, *J Endodont* **2012**, *38*, 72-74.
[21] C. Rose, A. Parker, B. Jefferson, E. Cartmell, *Crit. Rev. Env. Sci. Tec.* **2015**, *45*, 1827-1879.
[22] F. Arnold, *Chains conference speech*, The Netherlands, **2019**.
[23] A. D. Wentworth, L. H. Jones, P. Wentworth, K. D. Janda, R. A. Lerner, *P Natl Acad Sci USA* **2000**, *97*, 10930-10935.
[24] J. B. Guinee, R. Heijungs, G. Huppes, A. Zamagni, P. Masoni, R. Buonamici, T. Ekvall, T. Rydberg, *Environ. Sci. Technol.* **2011**, *45*, 90-96.

Curriculum Vitae

Georg Theo Höfler was born on the 7th of July 1988 in Friedrichshafen, Deutschland, and grew up in Immenstaad am Bodensee. He discovered his love for biotechnology early on and obtained his abitur at the biotechnological gymnasium (Droste-Hülshoff-Schule) in Friedrichshafen. At 19 years old he moved to Cologne serving his time as a civil servant at St. Vinzenz-Hospital. Following his passion for biotechnology he obtained his bachelor degree in molecular biotechnology at the TU Munich. His bachelor thesis was on crystallisation of technical enzymes in mL- and L-scale using additives at the Institute of Biochemical Engineering (TUM BioVT) under Prof. Dr.-Ing. Dirk Weuster-Botz. After finishing his bachelor, he moved to Aachen to further obtain his master degree in molecular and applied biotechnology at the RWTH Aachen. His main focus during his master was enzymology and industrial biotechnology. His master thesis was on characterisation of commercial laccase preparations regarding suitable reaction conditions for the enzymatic depolymerization of lignin at the chair of Enzyme Process Technology (AVT.EPT) under the supervision of Prof. Dr.-Ing. habil. Antje Spieß. After finishing his studies, he moved on to become a PhD student at the TU Delft in the biocatalysis group under the supervision of Prof. Dr. Frank Hollmann.

List of publications

N. Ihling, N. Bittner, S. Diederichs, M. Schelden, A. Korona, G. T. Höfler, A. Fulton, K.-E. Jaeger, K Honda., H. Ohtake and J. Büchs, *Biotechnol. Prog.* **2018**, 34: 315-327.

G. T. Höfler, E. Fernández-Fueyo, M. Pesic, S. H. Younes, E.-G. Choi, Y. H. Kim, V. B. Urlacher, I. W. C. E. Arends, F. Hollmann, *ChemBioChem.* **2018**, 19: 2344.
L. Josa-Culleré, A.S.K. Lahdenperä, A. Ribaucourt, G. T. Höfler, S. Gargiulo, Y.-Y. Liu, J.-H. Xu, J. Cassidy, F. Paradisi, D. J. Opperman, F. Hollmann, C. E. Paul, *Catalysts.* **2019**, *9*: 207.

G. T. Höfler, A. But, and F. Hollmann *Org. Biomol. Chem.***2019** 17.42: 9267-9274.

G. T. Höfler, A. But, S. H. H. Younes, R. Wever, C. E. Paul, I. W. C. E. Arends, and F. Hollmann, *ACS Sustain. Chem. Eng.* **2020** *8* (7): 2602-2607.

Acknowledgements

I consider myself a fairly adventurous person, always curious to gain new experiences. I did not expect the PhD to be one of the toughest and thrilling adventures of my life. In this journey many extraordinary people took part.

First of all, I want to thank my Promotor Frank Hollmann. I am very happy that you chose to believe in me and took me on this adventure. You gave me many opportunities to evolve, travel, network and expand my horizon in the scientific world. Just to name some of the amazing opportunities: conferences in Budapest and Boston, as well as working in South Korea with Professor Kim at UNIST. I am thankful for all your ideas and your relentless optimism, always finding a way to tackle challenges. I learned from you and I hope I can preserve parts of your remarkable attitude.

Further I have to thank Caroline. Without you this thesis would not be. I quickly realised that in you I had a fellow scientist with common core values. Accuracy is a virtue. After leaving us shortly for Wageningen, even though you already had imprinted on my development as a PhD, you came back at a crucial time during my PhD to support me as my copromotor. In you I had a supervisor that I could identify with completely. You are an amazing teacher. I hope you keep your empathic, open and respectful attitude towards your students.

Fortunately, I had the privilege to have a second promotor in you, Isabel. Even though we didn't have many opportunities to meet in person, I am very grateful for the part you took in writing this thesis. Your much-appreciated feedback made this thesis what it is.

To my three musketeers, I don't know how to put this in the correct order. Hence, we use the scientific approach, alphabetically:

Marine, in you I had a companion with whom I could share my struggle like no other. Sharing these challenging times with you helped me to carry on and push through the rough parts. You are one of the kindest and most helpful people I have the pleasure of knowing. I am sure that without your help in the bureaucratic parts of the PhD we all would have finished with some more grey hair.

Morten, my eternal conference roomie. You are without a doubt the most positive, relentless person I know. Thank you for your optimism and help. I wish you all the best for your academic future. I am sure you will keep working hard towards your goals and reach them.

Seb. I have no words. You made the at times stale lab work worthwhile with your presence. Be it with your jokes, music or attitude. In you I found another child in a man's body I could share laughter and mischief with. Thank you for sharing this insane adventure.

I will remember our great times together be it at conferences, in France for holidays, at German "Volksfesten", crying over games during group weekends or lying on the floor laughing in agony.

Hanna, in dir hatte ich eine unglaubliche Mitstreiterin oder auch Chauffeurin. Danke für alle emotionale Unterstüztung und dein ansteckendes Durchhaltevermögen während Motivationstiefs. Deine norddeutsche Seele war immer sehr erfrischend, vorallem morgens beim pendeln.
Fabio - fratello italiano per sempre – thank you for being my emotional pillar during the darker times, always keeping me moving forward, helping me to find energy and balance in my life.

I was lucky enough to have many Post-Docs guiding me during my time as a PhD student. Thank you, Elena, Milja, JiaJia, Wuyuan, Jonathan, Florian, Sandy, Sabry and Andrada. I always felt mutual respect and you were all kind and patient teachers.

Furthermore, without our amazing visitors, just to name some: Andrés, Carmen, Sumanth, Elia, Tiago and Laura this journey would have not been the same. Furthermore, I would like to thank all the technicians for always lending me a helping hand and advice when needed. You are all your own characters. I like and respect you for it. My thanks also to our secretary Mieke for being always helpful and caring with organisation, refunds and presents. A thank you to every single BOC member for the nice atmosphere.

Furthermore, I want to thank my little Indian family, Teju and Sami, for giving me a great first home in the Netherlands. I will never forget the beginning of the PhD with you in Jan Campertlaan.

I also want to thank my good friends, I might have been in a foreign land, but that didn't stop you from keeping me company with many reenergising visits.

Last but not least, I want to thank my family: My mother Ursula, my father Hans and my sisters Katharina and Cornelia. You are a constant in my life that I can always count on. It gives me strength to know I always have a home I can come back to. Thank you for all your support during my long adventure as a "student". I would not be who I am today without you.